PSI-1356

RECOVERY AND SEQUESTRATION OF CO_2 FROM STATIONARY COMBUSTION SYSTEMS BY PHOTOSYNTHESIS OF MICROALGAE

Quarterly Technical Progress Report for the Period Ending 30 September 2001

(Quarterly Report #4: Year 1 Summary Report)

Reporting Period Start Date: 1 October 2000
Reporting Period End Date: 30 September 2001

Prepared by

Dr. T. Nakamura
Physical Sciences Inc.
20 New England Business Center
Andover, MA 01810-1077

in collaboration with

Dr. Miguel Olaizola
Aquasearch Inc.
73-4460 Queen Kaahamanu Highway
Suite 110, Kailua-Kona, HI 96740

and

Dr. Stephen M. Masutani
Hawaii Natural Energy Institute
School of Ocean & Earth Science and Technology
University of Hawaii at Manoa
2540 Dole Street, Holmes Hall 246
Honolulu, HI 96822

DOE Contract No. DE-FC26-00NT40934
U.S. DEPARTMENT OF ENERGY
National Energy Technology Laboratory
P.O. Box 10940
Pittsburgh, PA 15236

January 2002

ABSTRACT

Most of the anthropogenic emissions of carbon dioxide result from the combustion of fossil fuels for energy production. Photosynthesis has long been recognized as a means, at least in theory, to sequester anthropogenic carbon dioxide. Aquatic microalgae have been identified as fast growing species whose carbon fixing rates are higher than those of land-based plants by one order of magnitude. Physical Sciences Inc. (PSI), Aquasearch, and the Hawaii Natural Energy Institute at the University of Hawaii are jointly developing technologies for recovery and sequestration of CO_2 from stationary combustion systems by photosynthesis of microalgae. The research is aimed primarily at demonstrating the ability of selected species of microalgae to effectively fix carbon from typical power plant exhaust gases. This report is the summary first year report covering the reporting period 1 October 2000 to 30 September 2001 in which PSI, Aquasearch and University of Hawaii conducted their tasks. Based on the work conducted during the previous reporting period, PSI initiated work on the component optimization work. Aquasearch continued their effort on selection of microalgae suitable for CO_2 sequestration. University of Hawaii initiated effort on system optimization of the CO_2 sequestration system.

TABLE OF CONTENTS

LIST OF FIGURES

LIST OF FIGURES (Continued)

LIST OF FIGURES (Continued)

LIST OF FIGURES (Continued)

LIST OF FIGURES (Continued)

LIST OF TABLES

1. INTRODUCTION

Emissions of carbon dioxide are predicted to increase in this century (McCabe and Smith, 1976) leading to increased concentrations of carbon dioxide in the atmosphere. While there is still much debate on the effects of increased CO_2 levels on global climate, many scientists agree that the projected increases could have a profound effect on the environment. Most of the anthropogenic emissions of carbon dioxide result from the combustion of fossil fuels for energy production. It is the increased demand for energy, particularly in the developing world, which underlies the projected increase in CO_2 emissions. Meeting this demand without huge increases in CO_2 emissions requires more than merely increasing the efficiency of energy production. Carbon sequestration, capturing and storing carbon emitted from the global energy system, could be a major tool for reducing atmospheric CO_2 emissions from fossil fuel usage.

The costs of removing CO_2 from a conventional coal-fired power plant with flue gas desulfurization were estimated to be in the range of $35 to $264 per ton of CO_2 (Perry and Chilton, 1973). The cost of power was projected to increase by anywhere from 25 to 130 mills/kWh. DOE's goal is to reduce the cost of carbon sequestration to below $10/ton of avoided net cost.

Photosynthesis has long been recognized as a means, at least in theory, to sequester anthropogenic carbon dioxide. There has been relatively little research aimed at developing the technology to produce a gaseous combustion effluent that can be used for photosynthetic carbon sequestration. However, the photosynthetic reaction process by plants is too slow to significantly offset the point source emissions of CO_2 within a localized area. Aquatic microalgae have been identified as fast growing species whose carbon fixing rates are higher than those of land-based plants by one order of magnitude.

The Department of Energy has been sponsoring development of large-scale photovoltaic power systems for electricity generation. By this analogy, a large-scale microalgae plantation may be viewed as one form of renewable energy utilization. While the PV array converts solar energy to electricity, the microalgae plant converts CO_2 from fossil combustion systems to stable carbon compounds for sequestration and high commercial value products to offset the carbon sequestration cost. The solar utilization efficiency of some microalgae is ~ 5%, as compared to ~ 0.2% for typical land based plants. Furthermore, a dedicated photobioreactor for growth of microalgae may be optimized for high efficiency utilization of solar energy, comparable to those of some photovoltaic cells. It is logical, therefore, that photosynthetic reaction of microalgae be considered as a mean for recovery and sequestration of CO_2 emitted from fossil fuel combustion systems.

Stationary combustion sources, particularly electric utility plants, represent 35% of the carbon dioxide emissions from end-use of energy in the United States (McCabe and Smith, 1976). The proposed process addresses this goal through the production of high value products from carbon dioxide emissions. Microalgae can produce high-value pharmaceuticals, fine chemicals, and commodities. In these markets, microalgal carbon can produce revenues of order $100,000 per kg C. These markets are currently estimated at >$5 billion per year, and projected to grow to >$50 billion per year within the next 10 to 15 years. Revenues can offset carbon sequestration costs.

An ideal methodology for photosynthetic sequestration of anthropogenic carbon dioxide has the following attributes:

1. Highest possible rates of CO_2 uptake
2. Mineralization of CO_2, resulting in permanently sequestered carbon
3. Revenues from substances of high economic value
4. Use of concentrated, anthropogenic CO_2 before it is allowed to enter the atmosphere.

In this research program, Physical Sciences Inc. (PSI), Aquasearch, and the Hawaii Natural Energy Institute at the University of Hawaii are jointly developing technologies for recovery and sequestration of CO_2 from stationary combustion systems by photosynthesis of microalgae. The research we propose is aimed primarily at quantifying the efficacy of microalgae-based carbon sequestration at industrial scale. Our principal research activities will be focused on demonstrating the ability of selected species of microalgae to effectively fix carbon from typical power plant exhaust gases. Our final results will be used as the basis to evaluate the technical efficacy and associated economic performance of large-scale carbon sequestration facilities.

Our vision of a viable strategy for carbon sequestration based on photosynthetic micro-algae is shown conceptually in Figure 1. In this figure, CO_2 from the fossil fuel combustion system and nutrients are added to a photobioreactor where microalgae photosynthetically convert the CO_2 into compounds for high commercial values or mineralized carbon for sequestration. The advantages of the proposed process include the following.

1. High purity CO_2 gas is not required for algae culture. It is possible that flue gas containing 2~5% CO_2 can be fed directly to the photobioreactor. This will simplify CO_2 separation from flue gas significantly.

2. Some combustion products such as NO_x or SO_x can be effectively used as nutrients for micoralgae. This could simplify flue gas scrubbing for the combustion system.

3. Microalgae culturing yields high value commercial products that could offset the capital and the operation costs of the process. Products of the proposed process are: (a) mineralized carbon for stable sequestration; and (b) compounds of high commercial value. By selecting algae species, either one or combination or two can be produced.

4. The proposed process is a renewable cycle with minimal negative impacts on environment.

The research and experimentation we propose will examine and quantify the critical underlying processes. To our knowledge, the research we propose represents a radical departure from the large body of science and engineering in the area of gas separation. We believe the proposed research has significant potential to create scientific and engineering breakthroughs in controlled, high-throughput, photosynthetic carbon sequestration systems.

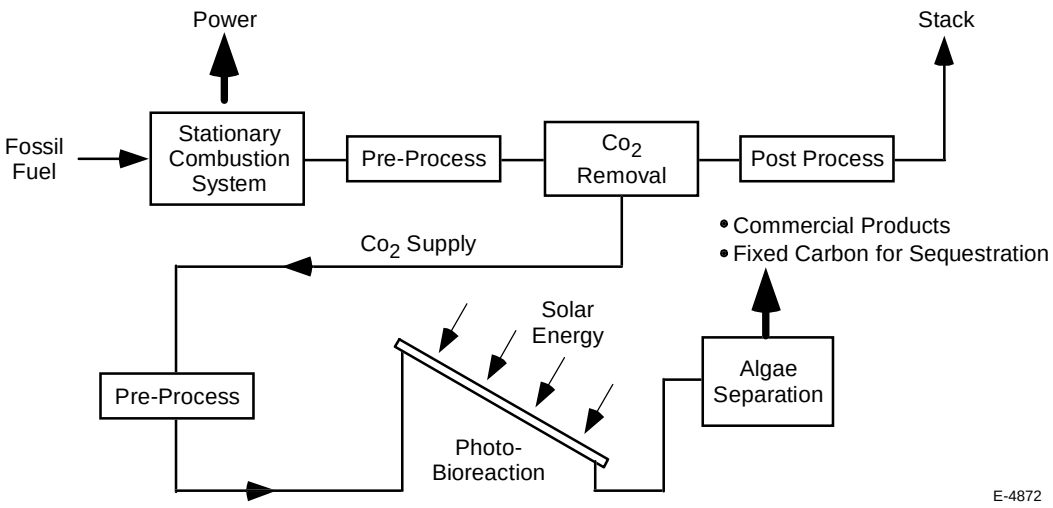

Figure 1. Recovery and sequestration of CO_2 from stationary combustion systems by photosynthesis of microalgae.

2. EXECUTIVE SUMMARY

The present program calls for development of key technologies pertaining to: (1) treatment of effluent gases from the fossil fuel combustion systems; (2) transferring the recovered CO_2 into aquatic media; and (3) converting CO_2 efficiently by photosynthetic reactions to materials to be re-used or sequestered.

The work discussed in this report covers the reporting period from 1 July to 30 September 2001. This report is also meant to be a summary of the work conducted in the first year period (1 October 1, 2000 through 30 September, 2001). Up to this point in time we have

- Characterized power plant exhaust gas
- Identified suitable CO_2 separation method and clean-up technologies
- Conducted analysis of carbon dissolution methods
- Tested 50 different strains of microalgae for growth at five different temperatures (15, 20, 25, 30 and 35°C) and 4 strains at three temperatures (15, 20, and 25°C)
- Tested 10 different strains for pH shift tolerance in chemostat cultures
- Analyzed 34 different strains for high value pigments
- Tested 17 strains at the chemostat level for growth and carbon uptake rate
- Tested 3 different strains for carbon sequestration potential into carbonates for long-term storage of carbon and we have
- Designed and built a gas distribution and control system to test the tolerance of microalgae to mixtures of gases representing different flue gases
- Started testing the tolerance of microalgae to simulated flue gases
- Began intitial work on designing key components including: CO_2 removal process; CO_2 injection device; photobioreactor; product algae separation process; and process control devices
- Demonstrated separation of PAR from the entire solar spectra and converted spectra outside of the PAR to electrical power an efficiency about 15.5%
- Demonstrated that full utilizations of solar spectra is possible for two distinct purposes: CO_2 sequestration; and electric power generation
- Preliminary process model for CO_2 supply, separation, and biological uptake using microalgae has been laid-out
- The ASPEN model has been shared with PSI and Aquasearch for their review and comment.

3. WORK ACOMMPLISHED

The schedule for the program submitted at the kick off meeting held at 6 November 2000 is given in Figure 2. This report covers the period ending 30 September 2001.

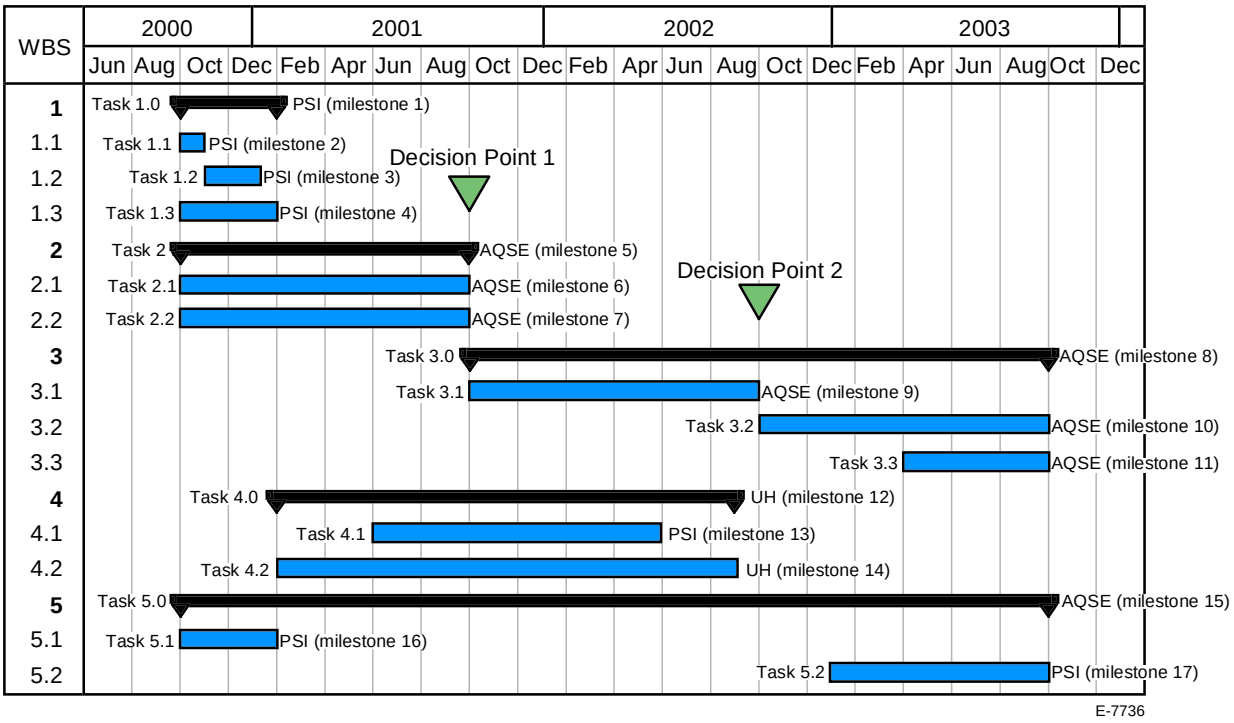

Figure 2. Project schedule submitted at the kick-off meeting.

3.1 Task 1: Supply of CO_2 from Power Plant Gas to Photobioreactor

3.1.1 Task 1.1: Power Plant Exhaust Characterization

In the United States about two-thirds of the capacity in the utility power generation sector is based on fossil fuel combustion (Table 1). Coal and natural gas are the primary fuels for power generation; fuel oil is important in specific regions. All fossil fuels amount to 71% of the electricity generating capacity. Fossil fuels represent an even larger segment of the non-utility power generation market (approximately 90%, if the use of biomass is included).

To be effective, sequestration of CO_2 using the photobioreactor needs to be located in an area with higher solar flux and warmer temperatures. If we consider only the sunnier and more southern regions of the US, as shown in Table 2, the capacity represents about half of the total US capacity. Generalizations have been made about climate in this exercise, which is intended to show only that a significant amount of fossil fuel combustion sources exist in places with climates most conducive to the photobioreactor.

Table 1. Electricity Production (Nameplate capacity) for 1999, by Sector and Energy Source

Sector/Fuel	Megawatts	
Utility		
Coal-Fired	296,883	
Petroleum-Fired	54,444	
Gas-Fired	129,510	
Nuclear-Powered	102,291	
Hydroelectric	89,800	
Other	4,883	
Total Utility		677,811
Non-Utility		
Coal-Fired	48,501	
Petroleum-Fired	40,508	
Gas-Fired	49,353	
Nuclear-Powered	1,542	
Hydroelectric	5,662	
Other	21,791	
Total Non-Utility		167,357
Total		**845,168**

Source: Energy Information Agency

Table 2. Electricity Production for 1999, by Sector and Region

Region	Utility		Non-Utility	
	Number of Units	**Nameplate Capacity (MW)**	**Number of Units**	**Nameplate Capacity (MW)**
*Other**	*4,372*	*235,165*	*2,974*	*88,908*
South Atlantic	1,345	152,463	726	14,416
East South Central	490	66,150	185	6,009
West South Central	795	109,473	576	17,929
Mountain	783	52,265	376	6,842
Pacific	1,708	62,296	1,167	33,254
Total	**9,493**	**677,812**	**6,004**	**167,358**

*Northeast, Middle Atlantic, and North Central Regions

Source: Energy Information Administration

Based on the information in Table 2, non-utility electricity generators using fossil fuels may be attractive for application of a photobioreactor because the average size of such plants is smaller than that of utility plants (28 MW versus 71 MW). Implementation of the concept may be easier on a smaller scale, particularly initially.

As shown in Table 3, the CO_2 content of flue gas from boilers (as opposed to gas turbine combustors) has low amounts of excess oxygen (typically 6 vol%) and CO_2 concentrations on the order of 12-15 vol%. Gas turbine combustors have much lower CO_2 and higher excess oxygen.

Table 3. Typical Flue Gas Compositions for Different Fuels and Combustion Systems

	Utility Boilers						
Volume %	**Bituminous Coal**	**Sub-bituminous Coal**	**Fuel Oil**	**Biomass**	**Natural Gas**	**GTCC Natural Gas**	**Diesel Fuel Oil**
CO_2	12.7%	15.1%	12.1%	19.0%	7.4%	3.4%	3.8%
H_2O	5.0%	12.2%	7.5%	13.0%	14.8%	6.9%	3.4%
O_2	6.0%	6.0%	6.0%	6.0%	6.0%	13.8%	15.0%
N_2	76.9%	71.0%	76.0%	62.0%	71.8%	75.0%	77.7%
SO_2 [ppm]	50-500	300-500	300-1300	100-200	0	0	10-100
NO_x [ppm]	50-500	50-500	300-500	200-400	100-300	25	150

Concentrations of trace acid gas species such as NO_x and SO_2 depend on the composition of the fuel and on the air pollution control system employed. Natural gas-fired combustors have virtually no SO_2 in the flue gas, while coal-fired systems have hundred of parts per millions. The range of NO_x emissions given in Table 3 reflects the use of low NO_x burners and/or post-combustion NO_x control to remove some of the NO_x from the flue gas.

Future efforts to aid CO_2 capture from combustion sources may include modifications to the combustion system that result in much higher concentrations of CO_2 in the exhaust. Oxygen-enriched combustion and recycle of flue gas back into the boiler are currently being investigated at the laboratory- and pilot-scale in the US and in other countries. Since the photobioreactors currently use a pure CO_2 stream, using a very CO_2-rich flue gas stream would require less modifications to existing commercial practice for growth of microalgae.

3.1.2 Task 1.2: Selection of CO_2 Separation and Clean-Up Technologies

According to recent reports (Perry and Chilton, 1973) the most likely options currently available for CO_2 separation from combustion flue gas include: gas adsorption (both physical and chemical), cryogenic separation, and membrane separation. Some of the major commercial applications of these processes are given in Table 4.

In gas adsorption systems, CO_2 reacts with a liquid solvent in which it is soluble. Both physical and chemical solvents have been used. Physical solvents take up CO_2, but do not react with it, whereas chemical solvents cause the formation of an intermediate compound with CO_2.

Table 4. Examples of Commercial Applications of CO_2 Removal by Gas Adsorption

Process	Owner	Uses	Comments
Sulfinol	Shell Oil Company	Natural gas, refinery gas, and synthesis gas	180 commercial units in operation or under construction in 1996
Selexol	UOP	Natural gas, refinery gas, and synthesis gas	53 commercial units installed by 1992
Rectisol	Lurgi GmbH and Linde AG	Heavy oil partial oxidation process of Shell and Texaco, also Lurgi gasification	More than 100 commercial units in operation or under construction in 1996
Purisol	Lurgi GmbH	Natural gas, hydrogen, and synthesis gas	Seven commercial units in operation or under construction in 1996
Catacarb	Eickmeyer & Associates	Any gaseous stream	
Benfield	UOP	Synthesis gas, hydrogen, natural gas, town gas	600 commercial plants had been installed by 1992
Alkanolamines	No specific owner	Any gaseous stream	Chemicals produced and supplied by Dow, DuPont, Union Carbide; they do not supply process equipment

Physical adsorption processes are more suitable for mixed gas streams that are under high pressure because the solubility of CO_2 increases with increasing gas pressure. Physical adsorption can be carried out in a solvent according to Henry's law; regeneration is accomplished using heat or pressure reduction. Solvents used for physical adsorption include dimethylether of polyethylene glycol (Selecol process) or cold methanol (Rectisol process). Physical adsorption processes are more economical if the CO_2 partial pressure is above 200 psia. At low CO_2 partial pressure, chemical adsorption processes are favored.

Chemical solvents (for example, monoethanolamine (MEA), dimethanolamine (DEA), ammonia, or hot potassium carbonate) form an intermediate compound that can be broken down by heating to give the original solvent and CO_2. These processes can be used at low partial pressure of CO_2, but the flue gas must be free of SO_2, hydrocarbons, and particulate matter. In particular, SO_2 must be reduced to below 5 to 10 ppmv for MEA adsorption.

Pressure-swing adsorption (PSA) or temperature-swing adsorption (TSA) are used in chemical process streams and have also been proposed for removal of CO_2 from flue gas. A combination of chemical and physical adsorption is used with beds of solid sorbents, for example, of alumina, zeolite, or activated carbon.

Gas adsorption or gas separation membranes have the potential to remove CO_2 from flue gas. Gas separation membranes employ a membrane that is selective for transport of CO_2 and high pressure on the flue gas side to concentrate CO_2 on the low pressure side of the membrane.

Gas adsorption membranes employ a liquid on the other side of the membrane instead of a gas stream.

Application of these carbon dioxide separation processes to flue gas depends on the concentration of CO_2 in the stream, on the presence of impurities in the gas, and on the pressure of the flue gas stream. Chemical adsorption may be preferred for cases in which the concentration of CO_2 is low and the pressure is near atmospheric. Physical adsorption is favored for higher total pressure and concentration of CO_2.

Chemical adsorption using MEA is the most mature technology and looks to be the most economically viable in the near future. An example of an MEA system applied to flue gas is given here, taken from a DOE report (United Technologies Research Center, 1999).

Figure 3 shows a process flow diagram for an MEA absorption process as applied to flue gas from a coal-fired power plant. In this implementation, gas leaves the flue gas desulfurization (FGD) unit at 56°C and is drawn into a fan and the pressure is boosted to 19.7 psia. The gas stream is cooled slightly and then enters the absorber where it contacts the lean MEA stream flowing countercurrently. The lean MEA stream contains 30 wt% MEA and absorbs more than 90% of the CO_2 in the flue gas (which can now be discharged to the atmosphere). The rich MEA solution is pumped from the bottom of the absorber to a stripper in which water vapor (produced in the reboiler) is used to strip CO_2 from the solution. The CO_2 and water vapor go to a condenser and gas/liquid separator. The condensed water is recovered and the CO_2 can be further processed downstream.

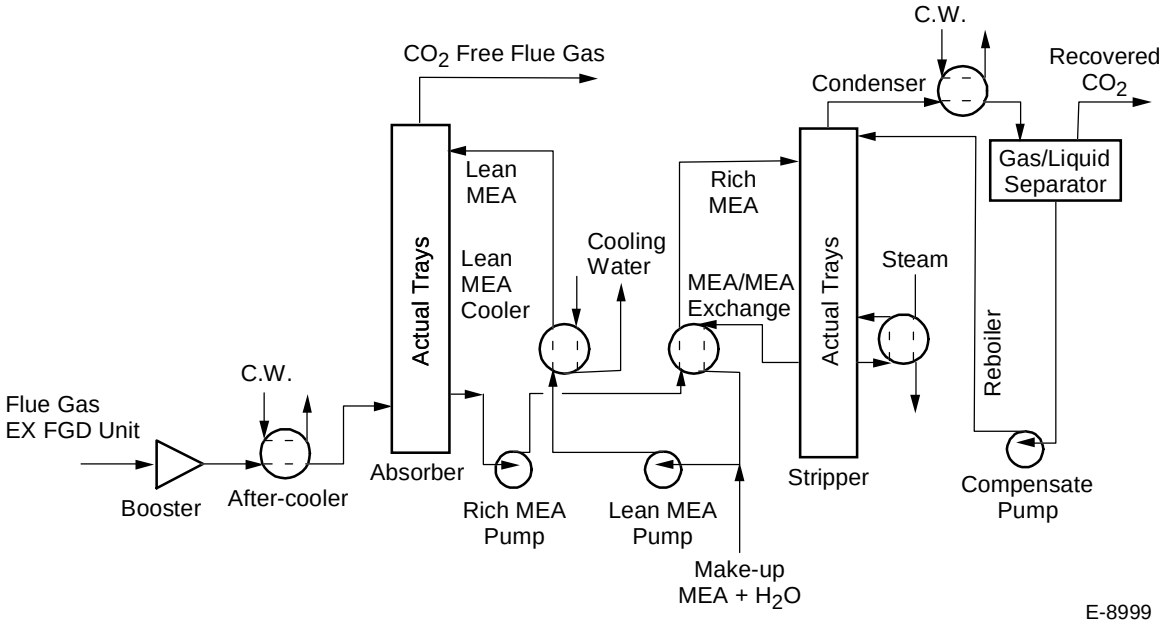

Figure 3. Process flow diagram for MEA absorber unit for removal of CO_2 from coal-fired flue gas (United Technologies Research Center, 1999).

A unit sized for a 25 MWe plant burning a bituminous coal would process 235,000 lb/hr of flue gas and produce 42,000 lb/hr of CO_2. Table 5 lists the major equipment and costs. The total major equipment cost is approximately $5M (1999 dollars). The total capital cost is on the order of $11M.

Table 5. Cost for Major Equipment in MEA Absorber
(United Technologies Research Center, 1999)

Equipment		Cost, in 1999 Dollars
Absorber	1	210,000
Stripper	1	17,000
MEA Make Up Tank	1	29,000
After Cooler	1	127,000
MEA Cooler	1	344,000
MEA/MEA Exchanger	1	481,000
Condenser	1	1,921,000
Reboiler	1	1,324,000
Booster	1	601,000
Rich-MEA Pump	2	34,000
Lean-MEA Pump	2	31,000
Condensate Pump	2	6,000
Total		5,125,00

The processes discussed above are currently demonstrated on a commercial scale, but for the production of CO_2 (from chemical plants or natural gas processing plants, for example). The cost of these technologies is too high for the reduction of greenhouse gases. Research into less expensive processes that are aimed at carbon emissions reductions is still in the early stages. The hope is that in the near future, less costly options will be available for fossil fuel-fired combustion sources. Some of the technologies now being developed include membranes, novel gas-liquid contactors, solid sorbents, and the formation of CO_2/water hydrates.

3.1.3 Task 1.3: Carbon Dioxide Dissolution Method

In this task, we will undertake theoretical and experimental investigations of the optimum method for dissolving carbon dioxide from the flue gas mixtures into the aqueous environment of the bioreactors. In the current Aquasearch commercial reactor, there are two gas streams added to the photobioreactor. A large stream of transport air is added using multiple injectors arranged radially near the walls of the photobioreactor. Large (~1.25 cm (~ ½ in.)) diameter nozzles are used. This air is used to add momentum to the liquid and promote liquid circulation in the long tube that comprises the photobioreactor. In the current design, a high-volume, low-pressure flow of filtered ambient atmosphere is introduced in a 2-m vertical airlift section of the reactor in which fluid rises, creating the head pressure necessary for recirculation.

Slightly upstream of the air injection location, pure CO_2 is added through a small pipe with a sparger on the end to produce small bubbles. The CO_2 is introduced in a 2-m "down-flowing" section, where it rises against the fluid flow. This procedure dramatically improves the

dissolution of CO_2. CO_2 is not added continuously, but rather is added when the pH of the liquid rises to a certain level. CO_2 is used both to provide carbon for growth of microalgae and to keep the pH in an optimum regime for growth.

In the commercial-scale photobioreactors, air is needed for circulating the liquid. In the smaller chemostats that are used to grow microalgae in the laboratory, CO_2 is sometimes used by itself, without adding any air to promote mixing. This can result in much higher carbon conversion (or efficiency of CO_2 utilization) than in the larger scale system. As far as the growth rate of microalgae is concerned, air has both advantages and disadvantages.

The chief advantage of the transport air is that it removes some of the dissolved oxygen in the water. Photosynthesis results in the production of O_2 by the microalgae. Under some conditions, the water can be supersaturated with oxygen. When this occurs, the rate of photo-synthesis (and growth) falls rapidly. The relatively large flow of air through the photobio-reactors strips out some of the dissolved oxygen and prevents high levels of supersaturation.

The chief disadvantage of the transport air addition is that is strips CO_2 as well as O_2 from the water. The removal of CO_2 lowers the efficiency of carbon utilization by 50% to 80%. Thus, in the commercial photobioreactors, the efficiency of CO_2 utilization (based on carbon production and CO_2 usage) is only 12.5%.

What determines the efficiency of CO_2 utilization by the microalgae: the rate of incorporation of CO_2 into the liquid or the rate of uptake of CO_2 by the microalgae? In the former situation, the microalgal growth is limited by the rate that CO_2 is dissolved into the liquid. In the latter, there is adequate CO_2 in the water and the rate is limited by the available sunlight. We would like to find a balance in which as much of the CO_2 added as possible is incorporated into biomass.

In the First Year, we began a theoretical investigation to explore the limits of the mass transfer and the dependence of mass transfer on operating parameters, in preparation for a more detailed experimental and theoretical investigation. The mass transfer rate to bubbles is controlled by:

- The concentration driving force between the interface and the bulk liquid;
- The interfacial area for mass transport, a;
- The mass transfer coefficient in the liquid, k_x.

The resistance on the gas-side in the bubble is usually negligible unless the gas in question is very soluble in the liquid; therefore, mass transfer in the gas will be neglected. The overall mass transfer rate, in moles per sec per volume of liquid is (McCabe and Smith, 1976):

$$N_A / V = k_x a(x_i - x) \tag{1}$$

where x and x_i are the mole fractions of component A in the liquid at the bulk and interface, respectively. Once again, a is the interfacial area per unit volume and k_x is the mass transfer coefficient in the liquid.

For small bubbles (diameters less than 0.5 mm), the liquid mass transfer coefficient is calculated from the following relationship (McCabe and Smith, 1976):

$$\frac{k_x D_P M_\ell}{\rho \mathscr{D}_v} \tag{2}$$

where D_p is the bubble diameter
M_l is the mean molecular weight of the liquid
ρ is the liquid density
$\mathscr{D}_v$ is the diffusivity of the dissolved gas in the liquid
μ is the liquid viscosity
$\Delta\rho$ is the difference between the liquid and gas density ($\sim\rho$)
g is the gravitational acceleration

For large bubbles (diameters greater than 2.5 mm), the following should be used (McCabe and Smith, 1976):

$$\frac{k_x D_P M_\ell}{\rho \mathscr{D}_v} = 2.0 + 0.31\left(\frac{\mu}{\rho \mathscr{D}_v}\right)^{1/3}\left(\frac{D_p^3\, \rho \Delta\rho g}{\mu^2}\right)^{1/3} \tag{3}$$

In order to use Eq. (1), we need to have the mean diameter of the bubbles and the interfacial area. The interfacial area can be calculated from (McCabe and Smith, 1976):

$$a = \frac{6\varepsilon}{D_p} \tag{4}$$

where ϵ is the gas hold-up (the relative volume of the dispersed phase, i.e., the gas). Equation 4 was used to calculate the interfacial area using values for ϵ taken from Figure 18-129 in Perry and Chilton, 1973.

Using Eq. (1), the maximum rate of mass transfer can be estimated by setting the bulk concentration of the gas species A to zero and by using the saturated value for the interfacial concentration. Thus

$$N_A / V \approx k_x a x_i \tag{5}$$

There will be two regimes: the small bubble regime is probably more typical of the CO_2 injection sparger, which is designed to produce fine bubbles; the large bubble regime is more like the air injectors which are one-half inch pipes. For formation of single bubbles from a submerged orifice of diameter D_o , the bubble diameter is given by (McCabe and Smith, 1976):

$$D_p = \left[\frac{6 D_o \sigma}{g \Delta\rho}\right]^{1/3} \tag{6}$$

where σ is the interfacial tension. Using this equation, the diameter of the bubbles from the air nozzles in the Aquasearch photobioreactors is estimated to be 8 mm.

In Figure 4, this maximum mass transfer rate is plotted as a function of diameter using the"small" bubble relationship (Eq. (2)), which applies to the conditions under which the CO_2-containing gas is added, and the "large" bubble relationship (Eq. (3)), which applies to the conditions under which the transport air is added. The calculations were carried out for pure water at 20°C. One set of curves applies to O_2 and the other, to CO_2. The differences in solubilities between the two molecules account for the differences in maximum amount of mass transfer.

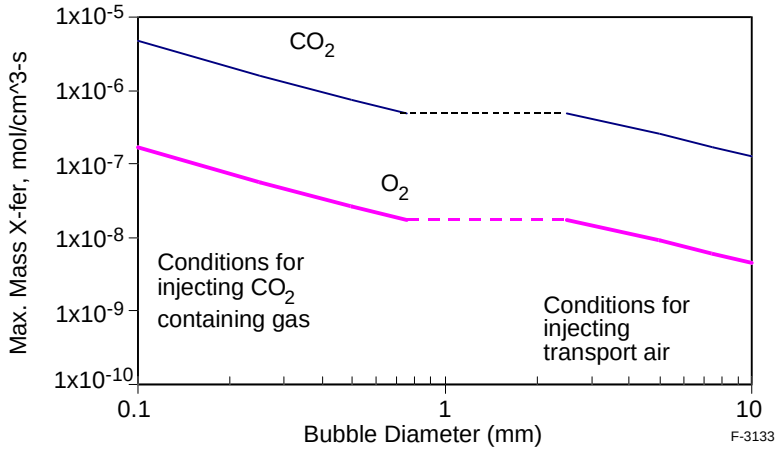

Figure 4. Maximum mass transfer rate from bubbles in water at 20°C as a function of bubble diameter.

In the photobioreactor, we would like to maximize the transfer of CO_2 to the water, while minimizing the amount of CO_2-stripping by the air that is being injected. At the level of this analysis, it is obvious that if the CO_2 is to be injected separately from the air, then the size of the bubbles from the air injectors should be large to produce the largest possible bubbles. This will reduce CO_2-stripping. At the same time, the bubble size for the CO_2 inlet stream should be as small as possible. This is what one would expect, of course, but Figure 4 shows how strong the dependence is on diameter.

If we introduce a flue gas containing 5 to 10% CO_2 in the down-flowing section where pure CO_2 is currently introduced, the 10 to 20-fold increase in flow rate could create a substantial back-pressure on the airlift-driven circulation. We may be able to solve this problem by simply increasing the flow rate of the airlift supply to overcome the flow rate of the flue gas. However, the solution may not be so simple. The flue gas supply will be pulsed (because it is used to regulate pH), whereas the airlift is continuous. Thus, we might create a strongly modulated fluid flow rate that is not favorable to the microalgae cultures. Other solutions could involve (a) decreasing bubble size of the flue gas to provide for higher dissolution rates, or (b) automatic modulation of the airlift flow rate to offset the counter-flow of flue gas.

A more detailed theoretical investigation in the Second Year will provide guidance for these activities. Specific questions to be answered are as follows:

1. Given the circulation rate of the liquid in the AGM and the flow rate of the flue gas being injected, what is the increase in dissolved CO_2 as a result of injection?

2. Complete dissolution of the flue gas bubbles would not be expected; how much oxygen is stripped from the liquid by the flue gas?

3. Some of the trace acid gases (SO_2, HCl, NO_2) are soluble in water; what are the dissolution rates of these species and how does this affect the pH of the liquid?

4. How much CO_2 and O_2 are removed from the liquid by injection of the transport air?

These questions will be considered by carrying out analyses of transient mass transfer from bubbles coupled with a simple models for the overall reactor: a continuously stirred reactor for the chemostat experiments and a plug flow reactor for the AGM.

3.2 Task 2: Selection of Microalgae

3.2.1. Task 2.1: Characterization of Physiology, Metabolism and Requirements of Microalgae

3.2.1.1 Microalgae Culture Collection

The Aquasearch Culture Collection consists at the present time of 78 different strains of microalgae representing an estimated 68 species (Figure 5). Sixty strains have been isolated locally (i.e., in Hawaii) by the staff at Aquasearch and are maintained as unialgal cultures. It is expected that strains isolated in Hawaii are adapted to relatively high temperatures. Furthermore, 18 strains have been imported from established culture collections (chosen either for their ability to produce high value products or to mineralize CO_2 into carbonates). The strains are maintained on an agar-based nutrient medium. When needed for an experiment, cells from the agar cultures are transferred to test tubes containing liquid growth medium. After a few days of growth (may vary depending on the strain) the cultures are transferred to larger containers such as 250 ml Erlenmeyer flasks. Further scale up is performed according to the type of experiment planned.

In February ’01 scale up of the microalgal cultures was started. Up to this point the cultures had been maintained in Petri dishes on a solid nutrient medium (agar based). The cultures were started in liquid nutrient medium in small test tubes (5 ml). The cultures were grown under a 14:10 hr light:dark cycle in a temperature-controlled room (24°C ±2°C) until enough biomass was produced to inoculate Erlenmeyer flasks (250 ml flasks with 100-150 ml of nutrient medium).

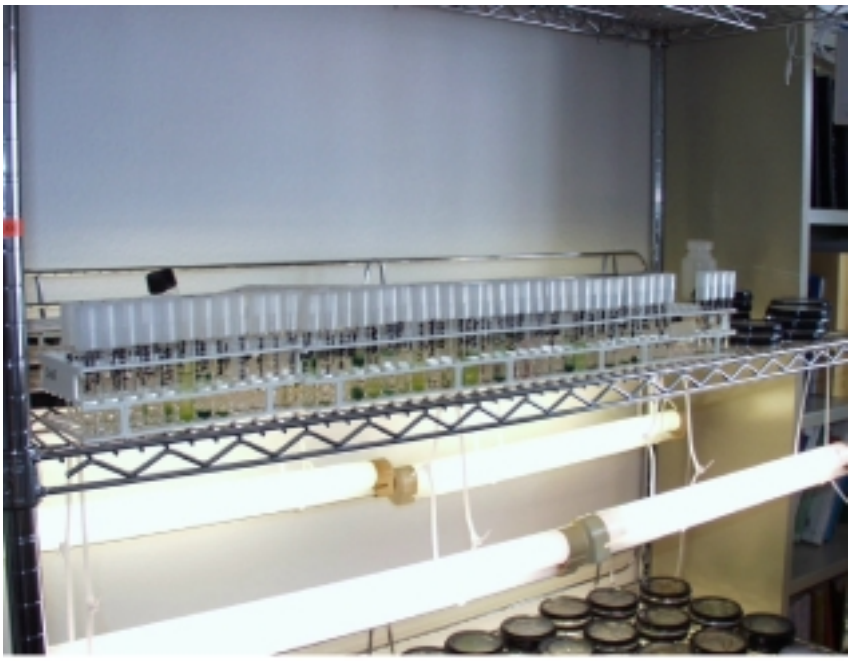

Figure 5. The Aquasearch Culture Collection. At the present time over 60 strains of microalgae are maintained. Ten more strains will be added over the next 2 months.

Table 6 lists the strains that have already been grown on liquid medium as well as the largest cultivation container to which they have been scaled. For proprietary considerations the strains are only identified by their culture collection identifier.

3.2.1.2 Culture Growth

Culture Growth in Batch Cultures

Batch cultures are defined as those cultures where a container with a fixed volume of nutrient medium is inoculated with microalgal cells. The cells grow until a nutrient becomes limiting (or light, as in our case). While the cells are not limited, the growth rate is high. As the cells encounter limiting conditions, the growth rate slows down and finally growth ceases. Estimates of culture growth are calculated from changes in culture biomass estimated once daily. Culture biomass is estimated from *in vivo* fluorescence. A Pulse Amplitude Modulated (MINI PAM, Walz, Germany) fluorometer is used to measure culture *in vivo* fluorescence. The fluorescence measured is proportional to the amount of chlorophyll, and thus biomass, of the culture. The following formula is then used to estimate growth rates:

$$\mu = \mathrm{Ln}\left(\frac{F_2 / F_1}{\Delta T}\right) \qquad (7)$$

where μ is the growth rate (d^{-1}), F_2 is the fluorescence at time 2, F_1 is the fluorescence at time 1 and ΔT is the difference between time 2 and time 1 in days. The temperature tolerance experiments were conducted on cultures grown in batch mode.

Table 6. List of Strains That Have Been Grown on Liquid Medium (60 Strains) as Well as The Largest Cultivation Container to Which They Have Been Scaled (Tt = test tube, E2 = 250 ml Erlenmeyer Flask, CH = 3.3 liter chemostat).

For proprietary considerations the strains are only identified by their culture collection identifier. The dates indicate when the different growth experiments were started (15°C, 20°C, 25°C, 30°C, 35°C indicate temperature tolerance experiments; "chemostats" indicates pH tolerance experiment).

	Largest scale	**15°C Growth**	**20°C Growth**	**25°C Growth**	**25°C B Growth**	**30°C Growth**	**35°C Growth**	**Chemostats**
AQ0001	E2	5/15/2001	5/15/2001	5/15/2001				
AQ0002	E2	5/15/2001	5/15/2001	5/15/2001				
AQ0003	E2	5/15/2001	5/15/2001	5/15/2001				
AQ0008	E2	5/15/2001	5/15/2001	5/15/2001				
AQ0009	E2	5/15/2001	5/15/2001	5/15/2001	9/26/2001	9/26/2001	9/26/2001	
AQ0011	CH	3/24/2001	3/24/2001	3/24/2001	9/15/2001	9/15/2001	9/15/2001	6/11/01
AQ0012	CH	3/17/2001	3/17/2001	3/17/2001	9/15/2001	9/15/2001	9/15/2001	4/17/01, 6/12/01
AQ0013	E2	3/24/2001	3/24/2001	3/24/2001	9/15/2001	9/15/2001	9/15/2001	11/22/01
AQ0016	E2	4/18/2001	4/18/2001	4/18/2001	9/26/01, 10/20/01	9/26/01, 10/20/01	9/26/01, 10/20/01	
AQ0017	E2	4/18/2001	4/18/2001	4/18/2001	10/20/01	10/20/01	10/20/01	
AQ0018	E2	3/17/2001	3/17/2001	3/17/2001	10/14/01	10/14/01	10/14/01	
AQ0019	E2	4/18/2001	4/18/2001	4/18/2001	10/20/01	10/20/01	10/20/01	
AQ0020	E2	4/18/2001	4/18/2001	4/18/2001	10/20/01	10/20/01	10/20/01	
AQ0021	E2	4/18/2001	4/18/2001	4/18/2001	10/20/01	10/20/01	10/20/01	
AQ0022	CH	3/24/2001	3/24/2001	3/24/2001	9/15/2001	9/15/2001	9/15/2001	7/30/01
AQ0023	E2	3/17/2001	3/17/2001	3/17/2001	10/20/01	10/20/01	10/20/01	
AQ0024	CH	3/24/2001	3/24/2001	3/24/2001	9/15/2001	9/15/2001	9/15/2001	7/31/01
AQ0025	CH	3/24/2001	3/24/2001	3/24/2001	9/15/2001	9/15/2001	9/15/2001	8/01/01
AQ0027	E2	4/18/2001	4/18/2001	4/18/2001	10/20/01	10/20/01	10/20/01	
AQ0028	E2	3/24/2001	3/24/2001	3/24/2001	10/14/01	10/14/01	10/14/01	11/21/01
AQ0029	E2	3/24/2001	3/24/2001	3/24/2001	10/14/01	10/14/01	10/14/01	11/21/01
AQ0030	E2	4/18/2001	4/18/2001	4/18/2001	10/20/01	10/20/01	10/20/01	
AQ0031	E2	4/18/2001	4/18/2001	4/18/2001	11/04/01	11/04/01	11/04/01	
AQ0032	E2	3/17/2001	3/17/2001	3/17/2001	11/04/01	11/04/01	11/04/01	
AQ0033	CH	4/29/2001	4/29/2001	4/29/2001	9/26/2001	9/26/2001	9/26/2001	6/24/01
AQ0034	E2	4/29/2001	4/29/2001	4/29/2001	9/26/2001	9/26/2001	9/26/2001	
AQ0035	E2	4/29/2001	4/29/2001	4/29/2001	9/26/2001	9/26/2001	9/26/2001	
AQ0036	CH	4/29/2001	4/29/2001	4/29/2001	9/26/2001	9/26/2001	9/26/2001	6/24/01
AQ0037	E2	4/18/2001	4/18/2001	4/18/2001	11/04/01	11/04/01	11/04/01	
AQ0038	E2	4/24/2001	4/24/2001	4/24/2001	9/15/2001	9/15/2001	9/15/2001	8/16/01, 7/27/01

Table 6 (Continued). List of Strains That Have Been Grown on Liquid Medium as Well as The Largest Cultivation Container to Which They Have Been Scaled

(Tt = test tube, E2 = 250 ml Erlenmeyer Flask, CH = 3.3 liter chemostat).

	Largest scale	**15°C Growth**	**20°C Growth**	**25°C Growth**	**25°C B Growth**	**30°C Growth**	**35°C Growth**	**Chemostats**
AQ0039	E2	4/18/2001	4/18/2001	4/18/2001	11/04/01	11/04/01	11/04/01	
AQ0040	E2	3/24/2001	3/24/2001	3/24/2001	9/15/2001	9/15/2001	9/15/2001	8/16/01
AQ0041	E2	3/24/2001	3/24/2001	3/24/2001	10/7/2001	10/7/2001	10/7/2001	11/22/01
AQ0042	E2	3/24/2001	3/24/2001	3/24/2001	10/7/2001	10/7/2001	10/7/2001	9/13/01
AQ0043	E2	3/24/2001	3/24/2001	3/24/2001	10/14/01	10/14/01	10/14/01	
AQ0044	E2	5/29/2001	5/29/2001	5/29/2001	10/7/2001	10/7/2001	10/7/2001	9/13/01
AQ0045	E2	5/29/2001	5/29/2001	5/29/2001	10/14/01	10/14/01	10/14/01	
AQ0046	E2	5/29/2001	5/29/2001	5/29/2001	10/7/2001	10/7/2001	10/7/2001	
AQ0048	E2	12/3/01	12/3/01	12/3/01	10/14/01	10/14/01	10/14/01	
AQ0050	E2	5/29/2001	5/29/2001	5/29/2001	11/04/01	11/04/01	11/04/01	
AQ0051	E2	5/29/2001	5/29/2001	5/29/2001	11/04/01	11/04/01	11/04/01	
AQ0052	CH	5/15/2001	5/15/2001	5/15/2001	11/22/01	11/22/01	11/22/01	6/19/01
AQ0053	CH	5/15/2001	5/15/2001	5/15/2001	11/22/01	11/22/01	11/22/01	6/19/01, 7/19/01
AQ0054	E2	12/3/01	12/3/01	12/3/01	11/22/01	11/22/01	11/22/01	
AQ0055	E2	12/3/01	12/3/01	12/3/01	11/22/01	11/22/01	11/22/01	
AQ0056	E2	12/3/01	12/3/01	12/3/01	11/22/01	11/22/01	11/22/01	
AQ0058	E2	12/3/01	12/3/01	12/3/01	11/22/01	11/22/01	11/22/01	
AQ0059	E2	12/3/01	12/3/01	12/3/01	11/22/01	11/22/01	11/22/01	
AQ0060	Tt							
AQ0062	E2	12/3/01	12/3/01	12/3/01	11/22/01	11/22/01	11/22/01	
AQ0063	Tt							
AQ0064	E2	12/3/01	12/3/01	12/3/01	11/22/01	11/22/01	11/22/01	
AQ0067	E2							
AQ0068	E2							
AQ0072	E2							
AQ0073	E2	12/3/01	12/3/01	12/3/01	11/22/01	11/22/01	11/22/01	
AQ0074	E2	12/3/01	12/3/01	12/3/01	11/22/01	11/22/01	11/22/01	
AQ0077	E2	12/3/01	12/3/01	12/3/01	11/22/01	11/22/01	11/22/01	
AQ0078	E2							
AQ0079	E2	12/3/01	12/3/01	12/3/01	11/22/01	11/22/01	11/22/01	

Culture Growth in Chemostat Cultures

Chemostat cultures, as opposed to batch cultures, receive a continuous supply of nutrient medium. Our cultures are grown under light limitation. As the cells are diluted by the continuous medium addition more light/cell is available, permitting cell growth. Thus, the growth rate is dependent on the rate of medium addition. At steady state (no change in cell

concentration in the chemostat culture) the growth rate is equivalent to the dilution rate. Also, at steady state, the growth conditions stay constant, allowing for better characterization of the physiological state of the cells. The physiological state of the cells was determined daily using fluorescence techniques based on the techniques developed by Schreiber et al (1986). Briefly, fluorescence measurements were carried out on the experimental cultures using the MiniPAM system (Walz, Germany). The MiniPAM can be used to estimate the so-called F_v/F_m, an estimate of the fraction of open reaction centers in photosystem II of photosynthetic organisms. The fraction of open reaction centers is directly proportional to the probability that the energy of an absorbed photon will participate in photosynthesis. Thus, it is a measure of the photosynthetic efficiency of the cells and of their physiological state.

While at steady state the dilution rate (or rate of nutrient addition to the culture) determines the growth rate, during the initial ramp up phase the chemostat culture is managed as a batch culture. A 3.3 liter chemostat vessel is inoculated with a starter culture and allow to grow. Once the culture reaches a sufficiently high biomass (the culture starts to reach light limitation), nutrients are continuously added using a pump. Over the first few days, then, we can estimate a maximal growth rate can be estimated from changes in daily biomass estimated from fluorescence measurements. This estimated growth rate is considered 'maximal' under since during that period in the cultures life light is not yet limiting (i.e., the culture is sufficiently dilute still). The pH tolerance experiments were conducted on cultures grown in chemostats.

Temperature Tolerance Experiments

To determine the growth rates of microalgae at different temperatures, cultures were incubated submerged in temperature-controlled water baths at 60 $\mu E\ m^{-2}\ s^{-1}$ of PAR. The cultures were batch grown in 250 ml Erlenmeyer flasks. The flasks were agitated three times daily. Changes in biomass were estimated from changes in fluorescence measured once daily. For each strain two separate experiments were conducted. On the one hand, flasks at 25, 30 and 35ºC were grown. A second run was conducted at 25, 20, and 15ºC.

Figure 6 summarizes the results of culture growth for 54 strains at up to five different temperatures. The data indicate there is a large degree of uncertainty about the mean growth rate of each culture (standard deviation > mean in all cases, not shown). This is the case for two reasons. First, these experiments were designed to quickly provide information on temperature tolerances for the different strains. As such the cultures were grown in batch mode. Cultures in batch mode show different growth rates at different stages of the cultures' growth curve. Second, a number of these cultures are of a filamentous and clumping nature. Thus, the cells are not uniformly distributed throughout the growth medium. This translates into inherently noisy data. However, from the point of view of the objective of the experiment (to determine the temperature tolerances of the different microalgal strains), the results are valid. The results show that for the tested strains two did not grow at 15ºC, one did not grow at 15 and 20ºC, nine did not grow at 35ºC, and one did not grow at 30 and 35ºC.

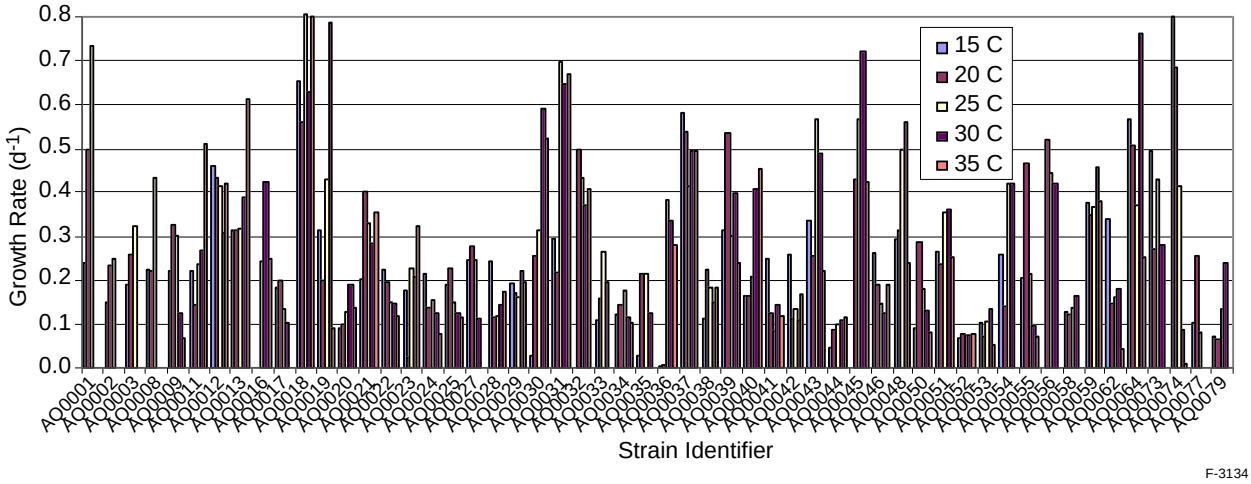

Figure 6. Results of growth rate measurements on 54 species of microalgae at up to five different temperatures.

pH Tolerance Experiments

To test the pH tolerance of the different microalgal strains, the cultures were grown in chemostats and exposed to different pH conditions. Initially, the cultures were grown in chemostats at a pH range of 7.4-7.6. The pH of the cultures was automatically controlled by CO_2 injections into the growth medium in response to raises in pH. Fluorescence-based biomass estimates during the initial growth phase of the chemostat cultures (i.e., before nutrient additions were started and steady state was reached) were used to estimate a maximal growth rate of the culture. These growth rates represent a near-maximum attainable since both nutrients and light are not limiting during this period of culture growth. The growth rates achieved range between 0.39 and 0.87 d^{-1} (Figure 7).

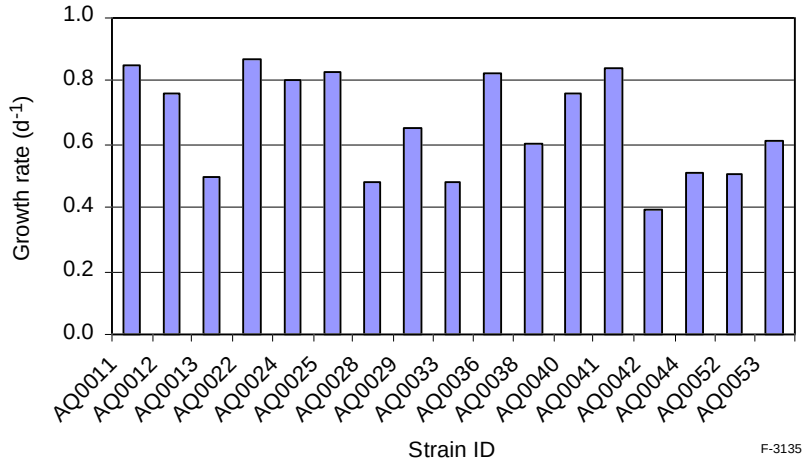

Figure 7. Growth rate of different microalgal strains during the initial phase (the ramp-up phase) of the chemostat cultures.

Once the chemostats were at steady state (no change in biomass from day to day) the pH set points were changed to either 6.4-6.5 or 8.4-8.6. A decrease in biomass in response to the pH manipulations would indicate that the culture was being washed out, that the growth rate did not keep up with the dilution rate. An increase in biomass in response to pH manipulations would indicate the growth rate of the culture was higher following changes in pH.

We have attempted to grow 13 different strains at the chemostat scale. Of those, three strains (AQ0025, AQ0052 and AQ0053) were not successfully grown for a long enough period of time to test the different pH levels. We report here results obtained from the other ten strains. Table 7 summarizes the results of the pH experiments. The table lists the fluorescence based biomass values measured in the chemostats following adjustments in the pH set points. A lower biomass level versus that at pH 7.5 indicates that the culture's growth is not keeping up with the chemostat's dilution rate and, thus, the growth rate is lower than under the standard condition (pH = 7.5). Lower biomass levels at high pH (8.5) could be interpreted as CO_2 limitation of the cultures. Lower biomass levels at low pH (7.5) could be interpreted as a detrimental effect on the cells due to the acidity of the medium.

Table 7. Summary Table Listing the Fluorescence-Based Biomass Values Measured in the Chemostats Following Adjustments in the pH Set Points

For growth at pH = 6.5, the pH set points were 6.4 and 6.6.
For growth at pH = 7.5, the pH set points were 7.4 and 7.6.
For growth at pH = 8.5, the pH set points were 8.4 and 8.6.

Strain/Culture ID	pH 6.5	pH 7.5	pH 8.5
AQ0011-010611	83	144	42
AQ0012-010612	35	41	36
AQ0022-010730	118	79	74
AQ0024-010731	74	78	72
AQ0033-010624	15	15	17
AQ0036-010624	61	61	55
AQ0038-010927	9	8	7
AQ0040-010816	45	43	37
AQ0042-010913	74	75	61
AQ0044-010913	79	83	57

Of the 10 strains so far characterized 4 maintained a higher biomass level at pH 6.5 than 7.5 possibly indicating carbon limitation at 7.5 pH. Similarly, 9 strains maintained higher biomass level at pH 7.5 than 8.5 indicating carbon limitation at 8.5 pH. This will become important in the final phase of this project, during the design of a microalgal facility to sequester smoke stack CO_2. An oversized facility would translate into lower CO_2 available for the cultures, decreasing its efficiency.

Figure 8 shows the results of the fluorescence measurements, averaged over several days, for the chemostat cultures grown at different pH. The highest F_v/F_m values are those of AQ0011, AQ0022, AQ0024, AQ0040, AQ0042, and AQ0044. These strains belong to the Chlorophyceae

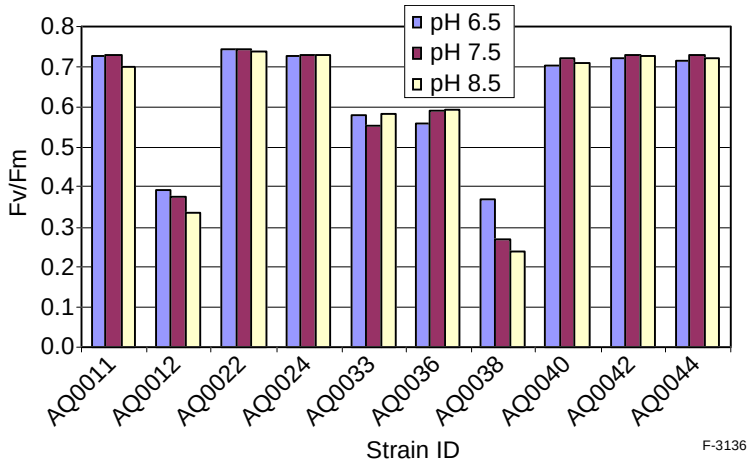

Figure 8. The average F_v/F_m value (a measure of the photosynthetic efficiency) measured in steady-state chemostat cultures grown at different pH.

or green algae. AQ0033 and AQ0036 belong to the Rhodophyceae, or red algae. These strains show a lower F_v/F_m than the green algae due to the difference in photosystem architecture. However, note that there are no discernible changes in Fv/Fm among all these strains in response to changes in culture pH. AQ0012 and AQ0028 are representatives of the Cyanophyceae, or blue-green algae. In this case there appears to be a reduction if photosystem efficiency at the higher pH values (equivalent to lower levels of dissolved CO_2 in the culture medium).

Flue Gas Tolerance Experiments

These experiments are getting underway at the present time. To test the flue gas tolerance of the different microalgal strains, the cultures are grown in chemostats and exposed to different gas mixtures selected to mimic the flue gas from power plants utilizing different fuels (Table 8). Initially, the cultures are grown in chemostats at a pH range of 7.4-7.6. The pH of the cultures is automatically controlled by pure CO_2 injections into the growth medium in response to raises in pH. Once the cultures have reached steady state, the stream of pure CO_2 for pH

Table 8. Typical Composition of Industrial Flue Gases as per the Type of Fuel Combusted

% Composition	Utility Boilers Bituminous Coal	Utility Boilers Sub-Bituminous Coal	Utility Boilers Natural gas	GTCC Natural Gas	Diesel Fuel oil
CO_2	12	15	7.5	3.5	4
H_2O	7	12	15	7	3.5
O_2	6	6	6	13.5	15
N_2	74.8	66.94	71.49	76	77.475
SO_2	0.16	0.04	0	0	0.005
NO	0.036	0.018	0.009	0.00225	0.018
NO_2	0.004	0.002	0.001	0.00025	0.002

control is substituted for the mixtures of gases specific to mimic different flue gas compositions (Table 8). As in the pH tolerance experiments (above) changes in the fluorescence-based estimates of biomass and photosynthetic efficiency in response to exposure to different gas mixtures will indicate whether the cells are negatively affected.

To carry out these experiments we have constructed a unique, computer controlled, pH control and gas distribution system. The apparatus uses a data acquisition and control system to control, monitor and acquire data through a multi-channel Ethernet, I/O modules, sensors and electrodes. The system provides intelligent signal conditioning, analog I/O,digital I/O, RS-232 and RS-485 communication. The systems communicate with their controlling host computer over a multi-drop RS-485 network. The data is analyzed and converted to usable information through applications software. This software must be written to query the I/O modules for the raw data and send control commands to the proper channels. The I/O modules must be configured for output and input of the proper data formats.

In the application of pH monitoring and control, a pH electrode is immersed into a live algal culture. The pH electrode sends an electronic message through a signal amplifier to the respective I/O control point (Figure 9). The host computer queries the I/O module; when the pH signal passes above the alarm setting, a command is sent to a separate relay module control point, which opens a solenoid valve allowing CO_2 gas to flow though a rotameter into the chemostat, thereby controlling the pH in the growth module. This process is repeated in reverse when the pH in the growth module reaches the low threshold and the solenoid is switched to the off position. By adding an RTD or thermocouple and the proper I/O module, this system also supports the monitoring and control of temperature in the growth module. A system of three solenoid valves, controlled by simple on/off switches, is used to distribute up to three different gases to each growth module (Figure 9 and 10). When the channel is switched on, the gas passes through a rotameter for flow control and flow rate measurement before entering into the growth module (Figure 11).

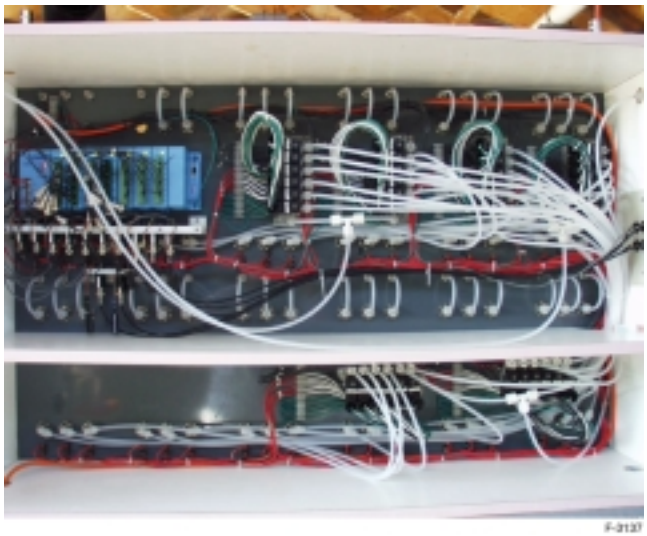

Figure 9. Rear view of the pH control and gas distribution system showing the I/O modules as well as tubes and solenoids that distribute and feed the gas mixtures to the chemostat cultures.

Figure 10. Rear and side view of the pH control and gas distribution system showing two ports (top) to accept gas mixtures for distribution to 12 different channels and 6 ports to accept input from 6 different pH probes. Six more probe ports are found on the opposite side (out of view).

Figure 11. Partial front view of the pH control and gas distribution system showing the rotameters and outlets that distribute the gas mixtures into the chemostats. Each channel controls gas flow through three rotameters. The mix of three different gas streams results in the desired composition to mimic different industrial flue gases.

In order to facilitate the accurate measurement of carbon uptake in the algae during the process of photosynthesis, a time base and flow measuring system has been added to this control system. This consists of two pulse generators combined with the appropriate frequency counting I/O modules. The first pulse generator generates a frequency, which is used to increase the accuracy of the rotameters. A pulsing current is sent to the solenoid valves, reducing the mass flow rate as the gas passes through the valves and respective rotameters. The naturally low flow rate of the different gases into the growth module necessitates this increase in accuracy of flow measurement. The frequency generated by the second generator creates a time base, which is used to measure the time the solenoid valves are open. The pulse generators give the system the capability to accurately measure the amount of gas (and carbon) entering the individual growth modules and a historic record of the data.

At this time we have started flue gas experiments on three microalgal strains (AQ0008, AQ0012, and AQ0038). Preliminary data indicates no detrimental effect by the flue gasses on the organisms' ability to photosynthesize. We expect to report more extensively on these experiments on our next quarterly report.

3.2.2 Task 2.2: Achievable Photosynthetic Rates, High Value Product Potential and Sequestration of Carbon into Carbonates

3.2.2.1 CO_2 Utilization Efficiency

CO_2 Utilization Efficiency of a Commercial Microalgal Facility

We have estimated the CO_2 utilization efficiency of Aquasearch's commercial facility which produces a high value pigment (astaxanthin) from the microalga *Haematococcus pluvialis*. The efficiency was calculated as the ratio of the amount of carbon contained in the biomass of *H. pluvialis* produced by Aquasearch to the amount of CO_2 that Aquasearch purchases for biomass production.

The calculated CO_2 utilization efficiency for Aquasearch's commercial facility for the production of astaxanthin from *H. pluvialis* is about 12.5 %. This means that 12.5% of the CO_2 purchased by Aquasearch to control the pH of, and provide carbon nutrition to, its cultures is captured in the biomass harvested.

CO_2 Utilization Efficiency of Experimental Chemostat Cultures

The CO_2 utilization efficiency of the experimental chemostat cultures was calculated as the ratio of the amount of carbon taken up by the experimental culture per unit time to the amount of CO_2 that is fed into the chemostat per unit time. The uptake of CO_2 by the culture is estimated from changes in the concentration of CO_2 in the growth medium as indicated by changes in pH and from changes in the biomass. The amount of CO_2 that is fed into the chemostat is estimated from the flow rate of the CO_2 gas times the period of time during the CO_2 is flowing into the chemostat.

The chemostat cultures are temperature and pH regulated. A pH probe immersed in the growth medium automatically logs the pH of the culture at a resolution of 15 seconds. A computer is programmed with the high and low pH set points. When the pH of the culture rises, caused by CO_2 uptake by the microalgal cells, above the high set point, a stream of CO_2 is automatically injected into the culture causing a drop in pH. When the pH `becomes lower than the low set point, the CO_2 stream is automatically shut off. The flow rate of the CO_2 stream multiplied by the duration of the injection results in the total amount of CO_2 injected. The amount of carbon actually taken up by the cells in the culture is estimated from the biomass of the culture and its growth rate.

We estimate the amount of dissolved carbon species in the medium using a standard titration method (Clesceri et al., 1995). Following an injection of CO_2 into the medium (see above), the pH of the medium decreases, reflecting an increase in the concentration of CO_2. After the injection period, the pH increases caused by photosynthetic uptake of CO_2 by the algae. The slope of this increase results from the rate of uptake of CO_2 by the culture.

Figure 12 is made up of two photographs of the same chemostat containing a culture of microalgal strain AQ0012 but at different times (April 20 and April 27, 2001, respectively) and it shows the potential for carbon sequestration of microalgal cultures. Figure 13 shows the changes of pH in this chemostat over a two day and one night period (39 hr). The upward changes in pH are produced by photosynthetic uptake of CO_2 from the culture medium, the drops are produced by automatic injection of CO_2 into the culture medium. The data is collected by our automatic monitoring and control system and is used to estimate the amount of CO_2 injected into the culture.

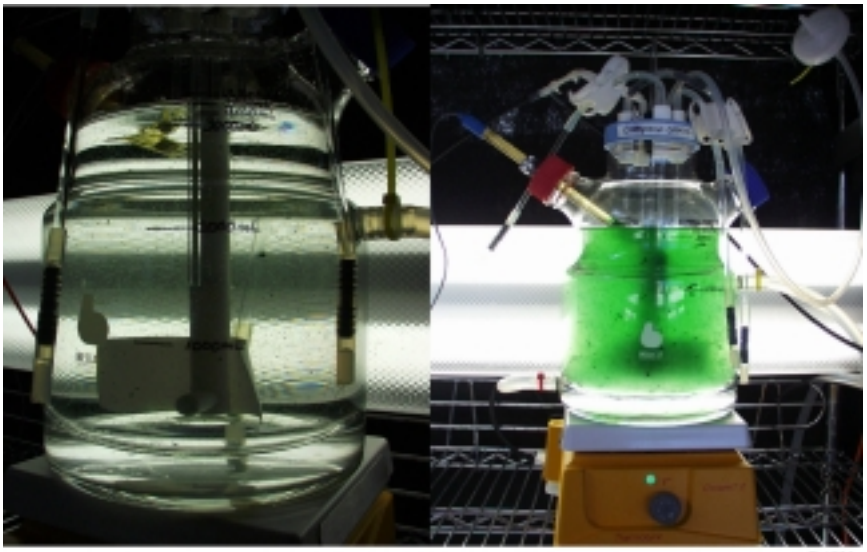

Figure 12. Photographs of the same chemostat culture (AQ0012) seven days apart showing the large capacity for carbon sequestration of microalgal cultures. The panel on the left shows little biomass, mostly concentrated in 3-4 mm clumps. The panel on the right is the same culture after seven days of photosynthetic growth.

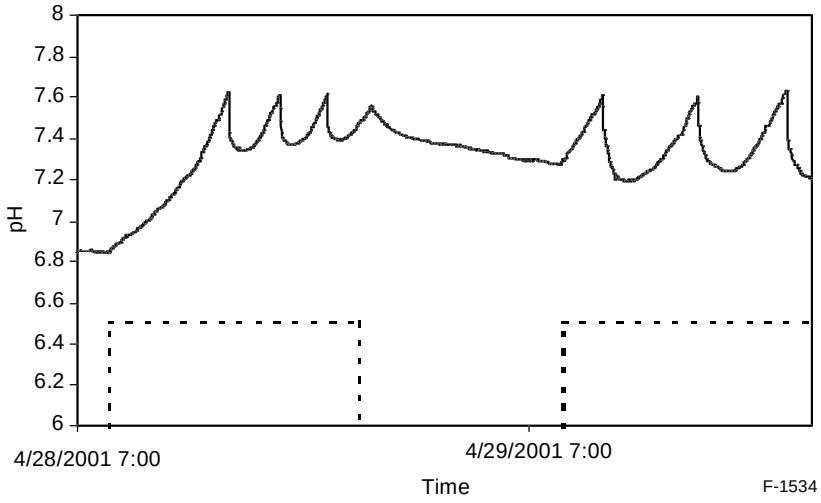

Figure 13. Computer generated trace of culture pH measured in the chemostat photographed in Figure 12. Rises in pH are caused by photosynthetic uptake of CO_2 by the algal cells. When the pH reaches the high set point (7.6 pH in this case), CO_2 is automatically injected into the culture medium and the pH drops. The broken line represents the periods during which the culture received light. The slope of the rise in pH, driven by photosynthesis, indicates carbon uptake be the culture.

The average growth rate of this chemostat culture was about 0.65 d^{-1}, which is equivalent to about 1 doubling of the biomass per day. At a typical biomass concentration of 0.4 g/l, in a 3 l chemostat, this is equivalent to 1.2 g of biomass produced per chemostat per day. As a first approximation we will assume that 50% of the biomass weight is carbon. Thus, the chemostat culture fixes about 0.6 g of carbon per day. This is equivalent to 2.2 g of CO_2 per day or about 1.1 l of CO_2 per day. Typical amounts of CO_2 injected into the chemostat culture are about 1.25 l of CO_2 per day. The efficiency of carbon transfer from gaseous CO_2 to algal biomass carbon is, thus, about 88% at this point. While this is well above our benchmark (12.5%), it should be noted that this is a preliminary result from our first chemostat culture and will need to be corroborated.

CO_2 Utilization Capacity of Microalgal Cultures Grown in Chemostats

The automated pH monitoring and control system allows us to closely follow changes in pH in all the chemostat cultures. As an example, Figure 14 shows the changes in pH over the life history of a chemostat culture of strain AQ0022. Changes in pH reflect changes in the concentration of dissolved CO_2 and the total dissolved inorganic carbon (DIC = CO_2 + HCO_3^- + CO_3^{2-}). We make the assumption that increases in DIC in the medium are produced either by respiration by the algae or by the injection of CO_2. We also make the assumption that decreases in DIC are produced by photosynthetic uptake of carbon and degassing from the culture medium. Figure 15 shows an example of such changes. The figure shows two traces. The first trace is the pH of the culture medium over 4 days and nights for a culture of strain AQ0036. Decreases in pH correspond to increases in DIC produced by CO_2 injections and algal respiration. Increases in pH correspond to decreases in DIC caused by photosynthetic uptake of CO_2 by the algae or degassing.

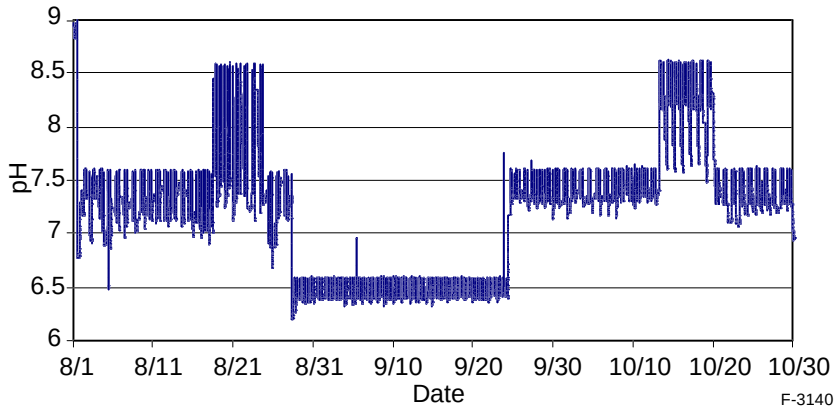

Figure 14. This figure shows an example of a computer generated trace of culture pH measured in a chemostat culture of strain AQ0022. This chemostat was maintained for 3 months and it clearly shows the periods of time during which the culture's pH was maintained at 6.5, 7.5, and 8.5. Chemostat cultures were used for the determination of differences in steady state biomass levels in response to changes in culture pH.

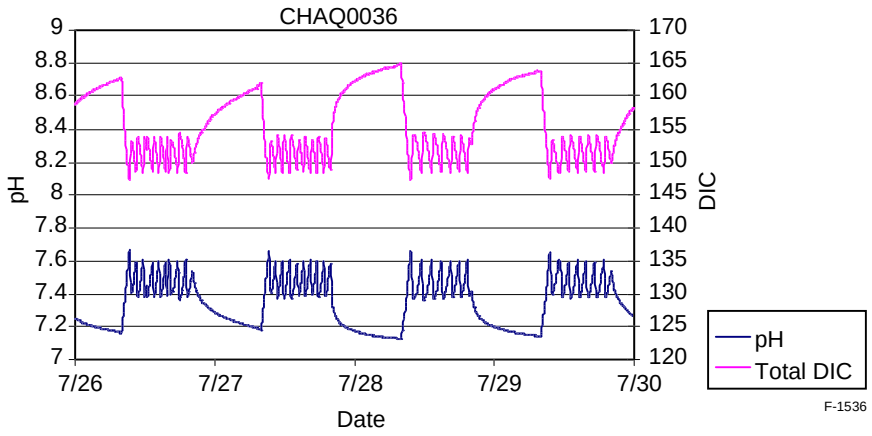

Figure 15. Changes in pH and total DIC over a four day period for a chemostat culture of strain AQ0036.

Using the changing concentrations of DIC over time we can calculate the net rate of carbon uptake (mg CO_2 l^{-1} min^{-1}). The results of this calculation, with a resolution of 5 min, are shown in Figure 16. Positive values indicate net uptake of CO_2 by the culture and degassing of CO_2 from the culture medium while negative values indicate injection of CO_2 into the medium and cellular respiration. Note that, in this case, degassing during the night periods (which would be evidenced by a rise in pH) is negligible. If we calculate an average net CO_2 uptake rate, using the values when no CO_2 is being injected, we obtain an average net rate of 0.094 mg CO_2 l^{-1} min^{-1}. For a 14 hr day this is equivalent to 79 mg CO_2 l^{-1} d^{-1} or 21.5 mg C l^{-1} d^{-1}.

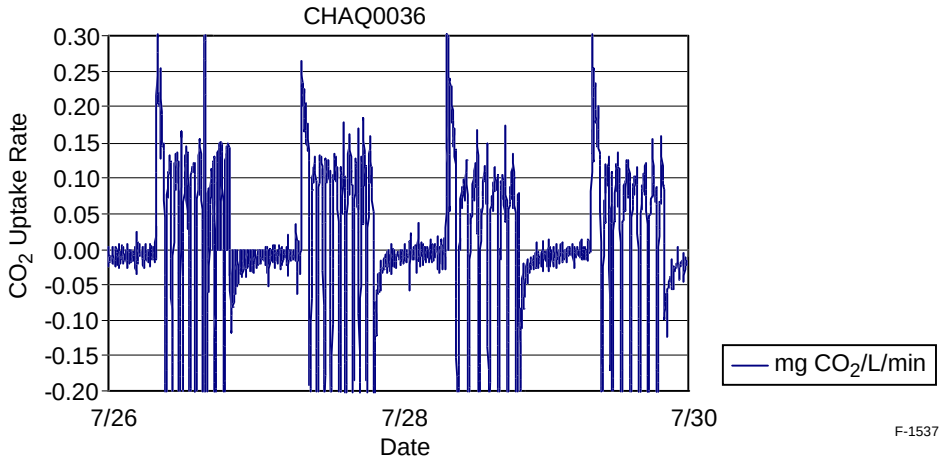

Figure 16. Changes in carbon uptake rate over a four day period for a chemostat culture of strain AQ0036. Positive values indicate net uptake rate of carbon. Negative values represent injection of CO_2 into the culture and respiration by the cells.

We have now started to analyze the data obtained in these experiments to understand not only how the physiology and the growth of the microalgal cells may change when grown at different pH but also how the different medium pH affects the degassing of CO_2 from the medium and the uptake of CO_2 by the microalgae. For example, if we consider the changes in pH during the light and dark period (i.e., no photosynthetic carbon uptake) for the AQ0011 grown at different pH, both the rate of uptake and the rate of degassing are inversely proportional to the medium pH (Figure 17). At lower pH the concentration of CO_2 is higher in the medium so diffusion of CO_2 out of the medium is expected to be faster. If we compare the calculated rates between the light and dark periods the difference should be that due to photosynthetic uptake of CO_2. The result indicates that the photosynthetic uptake of CO_2 is also pH dependent.

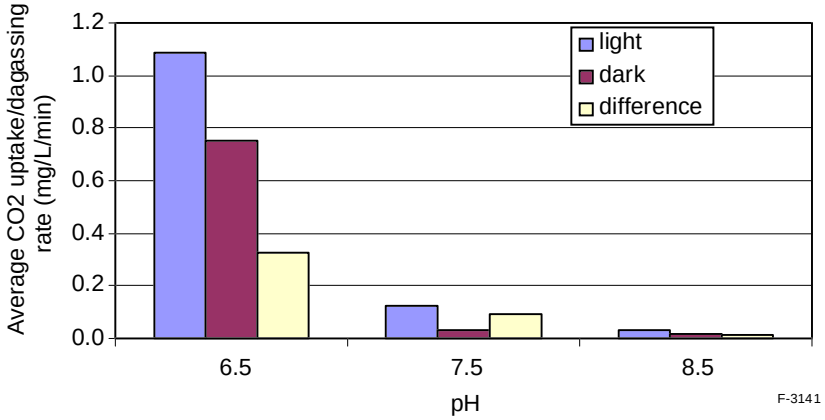

Figure 17. Rates of CO_2 uptake and/or degassing from the culture medium averaged over several days following injections of CO_2 to control the culture's pH either during the light and dark periods. In the light, both photosynthesis and degassing are taking place. In the dark we assume no photosynthesis. The difference between the light and dark rates is attributed to photosynthesis.

While scale up of these systems will not occur until Year 2 and 3 of this project we can compare these values with the productivity of existing commercial scale outdoor photobio-reactors. Olaizola (2000) showed the productivity of such systems to be on the order of 40 to 50 mg l^{-1} d^{-1} of dry weight biomass for *Haematococcus* cultures. If we assume that about 50% percent of *Haematococcus* biomass is made up of carbon this is equivalent to about 20 to 25 mg C l^{-1} d^{-1}. Comparing this value with that obtained for AQ0036 grown in chemostats (21.5 mg C l^{-1} d^{-1}) we can expect that results obtained in our chemostat experiments are applicable to outdoor conditions and can be used to predict the behavior of our strains at full scale outdoor conditions.

We expect to report further on the chemostat-based pH data as data analysis is completed over the next few months.

3.2.2.2 Production of High Value Products from Microalgae to Offset the Cost of Carbon Sequestration

High Value Pigment Analysis

Microalgae are a diverse group of over 30,000 species of microscopic plants that have a wide range of physiological and biochemical characteristics. Microalgae produce many different substances and bioactive compounds that have existing and potential applications in a variety of commercial areas, including human nutrition, pharmaceuticals, and high value commodities. Algal pigments (carotenoids and phycobiliproteins) are one such group of molecules. Examples of natural algal pigments that already been commercialized include B-carotene (food additive grade worth about $1,400 per kg, market size estimated >$500 million per year), astaxanthin (feed additive grade worth about $2,500 per kg-market size about $200 million- but up to >$100,000 per kg for nutraceutical grade-market size not know at this point).

Phycobiliprotein Pigments

Presence/absence of phycobiliproteins is determined by visual inspection of microalgal biomass after extraction of chlorophylls and carotenoids using an organic solvent. Microalgal biomass is centrifuged and the overlying medium is decanted. The remaining pellet is mixed with an appropriate amount of solvent (e.g., acetone, methanol) and centrifuged a second time. The solvent is decanted removing the chlorophyll and carotenoids. The pellet is then visually inspected for color. A blue colored pellet is indicative of phycocyanin while a pink colored pellet is indicative of phycoerythrin.

Carotenoid Pigments

Carotenoids are analyzed via High Performance Liquid Chromatography (HPLC). The carotenoid pigments are extracted from the algal biomass with a mixture of methanol, ammonium acetate and dimethyl sulfoxide. The extract is then injected into the HPLC system. Our system consists of a Beckman System Gold with a model 126 programmable solvent module, a model 168 diode-array detector, and a model 508 injector with a 100 µL loop. The

column is a Supelco Discovery C8 column 150 × 4.6 mm, 5 µm particle size. The solvent system consisted of:

A	MeOH: Acetonitrile: Acetone at 20:60:80
B	MeOH: Ammonium Acetate 0.25M: Acetonitrile at 50:25:25
	using the following time program:
%B	100 → 60 over 22 min
%B	60 → 5 over 6 min
%B	5 for 10 min
%B	5 → 100 over 2 min.

The total run time is 40 min at a flow rate of 1.5 ml/min.

Pigment Concentrations of Microalgal Strains Grown Under Standard Conditions

So far we have analyzed the pigment content of 34 different microalgal strains. First we will report on results of pigment analysis carried out on microalgal cultures grown under standard conditions (temperature: 25°C; irradiance: 60 µE m^{-2} s^{-1}; light/dark: 14 hr/10 hr). The first group of strains for which we report pigment content was made up of 11 cyanobacterial strains grown in batch cultures. This group was tested first since the Cyanobacteria are good potential candidates as sources of high value pigments. Two different cultures were analyzed from each strain; a relatively young culture and a relatively older culture (Figure 18). The most abundant carotenoids present in these strains are zeaxanthin and B-carotene and are reported as the mass ratios to chlorophyll-a, an indicator of algal biomass. B-carotene is used widely as a

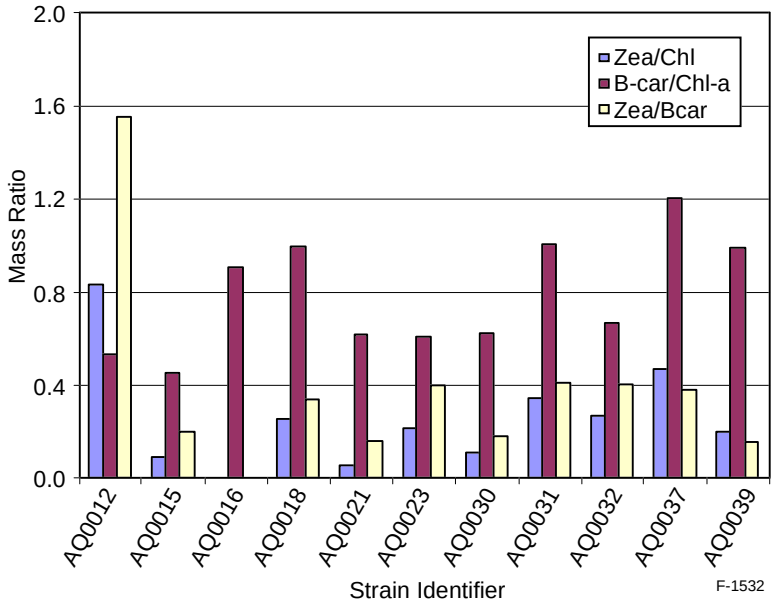

Figure 18. Summary of carotenoid pigment analysis of 11 strains of Cyanobacteria. Zea/Chl: mass ratio of zeaxanthin to chlorophyll-a, B-car/Chl: mass ratio of B-carotene to chlorophyll-a, Zea/Bcar: mass ratio of zeaxanthin to B-carotene. The values reported are the average of measured concentrations in two different cultures of each strain.

food coloring in margarine, butter, drinks, cakes and candies. It is also sold as a nutritional supplement or nutraceutical. Zeaxanthin is a carotenoid believed to be important in human nutrition and, specially, eye health. Of the 11 strains tested, AQ0012 showed potential as a source of zeaxanthin. Five other strains may be considered potential sources of B-carotene, also a high value pigment. All strains had phycobiliproteins as part of their pigment complement (characteristic of the Cyanobacteria). Of those, seven strains contained phycocyanin and four contained phycoerythrin. The phycobiliproteins are also high value molecules used to produce fluorescent probes useful in diagnostic biochemistry.

A second group of pigment analysis was carried out on strains grown at the flask scale (150 ml cultures) also grown under standard conditions. These strains represent the microalgal Classes Chlorophyceae, Bacillariophyceae, Eustigmatophyceae and Prymnesiophyceae. The results of that analysis are summarized in Figure 19. Based on the results obtained we consider strain AQ0056 (a diatom, Bacillariophyceae) a possible good source of fucoxanthin. Recent reports in the literature indicate that fucoxanthin may have anticancer activities (Kim et al., 1998). Our results also indicate that strain AQ0059 can be considered a good source of lutein. Lutein, as zeaxanthin, has been identified as a carotenoid with application in human eye health.

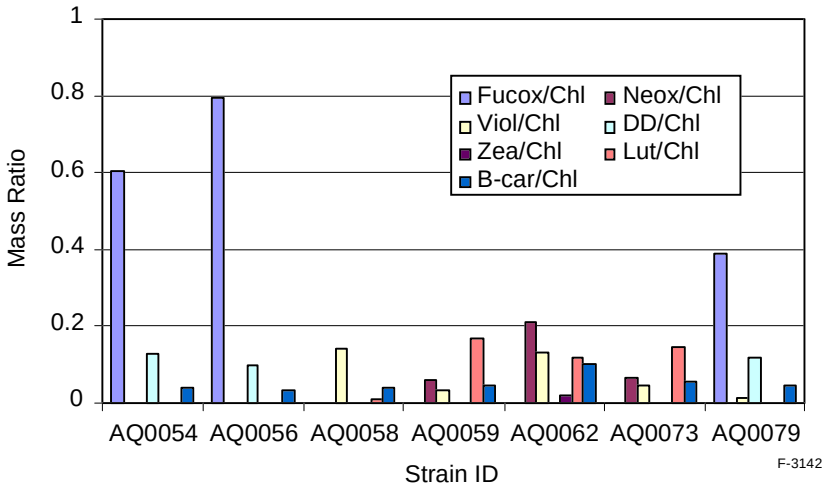

Figure 19. Summary of carotenoid pigment analysis of 6 microalgal strains grown at flask scale (150 ml). Fucox: fucoxanthin; Neox: neoxanthin; Viol: violaxanthin; DD: diadinoxanthin; Lut: lutein; Zea: zeaxanthin; B-car: B-carotene; Chl: chlorophyll-a.

A third group of pigment analysis was carried out on strains grown at the chemostat scale (3.3 liters) under standard conditions. In this group we have representatives of the Chlorophyceae, Bacillariophyceae and Cyanophyceae. The results of that analysis are summarized in Figure 20. Based on those results we can consider strain AQ0038 a very good source of lutein (even better than strain AQ0059, Figure 19). Strain AQ0042 can also be considered a good source of the high value carotenoids lutein and B-carotene. Finally, strain AQ0044 can be considered a good source of carotenoid complex or mixture since it contains high levels of B-carotene, lutein and violaxanthin. Although violaxanthin has not yet been identified as a high value carotenoid it can be considered a precursor of zeaxanthin (via the xanthophylls cycle, Yamamoto and Kamite, 1972).

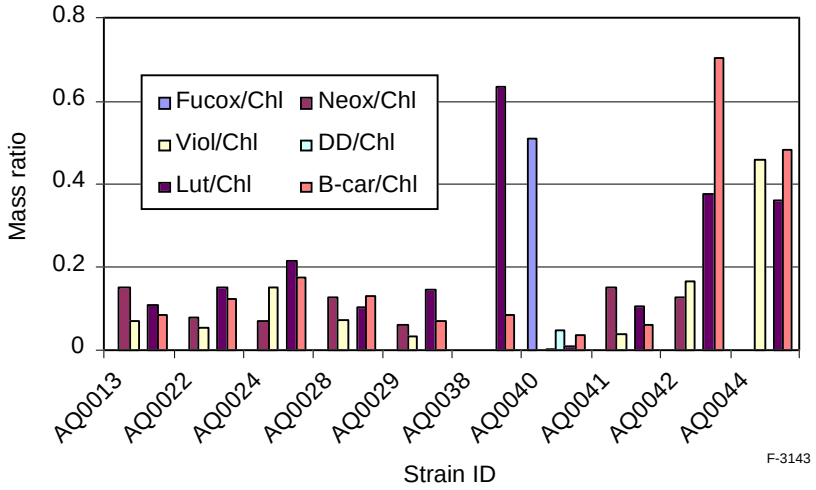

Figure 20. Summary of carotenoid pigment analysis of 10 microalgal strains grown at chemostat scale (3.3 l). Fucox: fucoxanthin; Neox: neoxanthin; Viol: violaxanthin; DD: diadinoxanthin; Lut: lutein; B-car: B-carotene; Chl: chlorophyll-a.

Pigment Concentrations of Microalgal Strains Grown Under Non-Standard Conditions

It is well known that microalgal pigment content may vary depending on the growth conditions (e.g., light, nutrients). Here, we report results of analysis carried out on cultures grown continuously in chemostats as well as analysis of cultures grown under stress conditions believed to be conducive to carotenogenesis.

Methods and Data Analysis

Six species of microalgae were selected for the pigmentation experiments. The chlorophyte strain AQ0011 and cyanobacterium strain AQ0012 were isolated locally in Kona, Hawaii. The Porphyridium strains AQ0033 and AQ0036 represent Rhodophyta, obtained from the University of Texas at Austin, while AQ0052 and AQ0053 are *Dunaliella* species of the division Chlorophyta, obtained from the Hawaii Culture Collection.

The cultures were grown in 3.3 L chemostats, using a 10:14 light:dark cycle, with temperature (25ºC)and pH control (7.4-7.6). The chemostats provided the culture material for the experimental treatments. Daily fluorescence readings with a Pulse Amplitude Modulator Fluorometer (PAM) monitored the biomass indirectly. PAM measures minimal (F_o) and maximal fluorescence (F_m) of the culture in a dark adapted state. The difference between F_o and F_m was F_v. The ratio F_v/F_m was used to estimate the photosynthetic efficiency of the cells. Initially, the chemostats were grown in batch mode. When a certain cell density was reached, the cultures were switched to continuous mode, which allowed the cells to attain a well-defined physiological state (Nyholm and Peterson, 1997).

PAM data measured in darkness was utilized to determine the percent functional reaction centers in the photosystem of the algal cells. The dark PAM reading of each hour was divided by the initial PAM reading to determine this value for the light intensity experiments. For the

nitrate deprivation and salt/sodium acetate experiments, daily PAM readings helped to monitor the health of the cells. A decline in these Fv/Fm values indicated that the cells were experiencing stress. The Fv/Fm value from each flask was plotted each day and a linear regression analysis was performed to measure the trends.

The spectrophotometric data was normalized to 750 nm, by subtracting the absorption at 750 nm from the absorption at each wavelength within a sample to eliminate the contribution of light scattering to absorption readings. The spectra were also analyzed on a volumetric basis by multiplying the normalized absorbance by the volume extracted with DMSO divided by the culture volume. In addition, differences spectra were calculated by subtracting the spectrum of each hour from the initial spectrum to show how the pigments changed and absorbed light differently through time.

The HPLC chromatograms were analyzed by identifying the peaks of zeaxanthin, lutein, β-carotene, and chlorophyll according to published spectral data (Jeffrey et al., 1997). The concentration of the biomass was determined by centrifuging a known volume of culture and transferring the pellet to a preweighed 15 ml tube, which was placed in a 65°C drying oven for 24 hours. After drying, the tube was re-weighed and the concentration of biomass per ml of culture was calculated. Pigments were quantified based on the areas of the peaks, which were multiplied by previously determined response factors of standard pigment samples. The amount of pigment (ng) injected was divided by the volume injected into the HPLC to determine the concentration of the extract (ng/ml), and then multiplied by the volume of DMSO used for the extraction. This determined the total amount of pigment in the extract, which was divided by the original volume of culture used for extraction. Averages were taken of duplicate samples. Percent lutein, zeaxanthin, and β-carotene were determined by dividing the concentration of the pigment by the concentration of biomass in the sample. The initial and final samples were compared for change in pigment per amount biomass and change in pigment per volume culture.

Light Intensity Experiments

Each species of microalgae was first tested under intense light conditions (sunlight). Preliminary PAM readings and pH measurements were taken before exposure to light. Flasks with 200 ml of culture were placed in an outdoor water bath at 25°C in full sunlight for a period up to 5 or 8 hours. Light intensity was monitored by roof top solar panels. Each hour, PAM readings were first taken in ambient sunlight and again in darkness. Flasks were swirled, and the pH was monitored hourly. In addition, 45-50 ml samples were collected for pigment extraction from each sample and 175 ml of culture was used for dried biomass analysis of the initial and final flasks. Samples were collected in duplicate. Pigments were extracted using 5 ml of dimethyl sulfoxide (DMSO), and re-extracted with 2 ml DMSO until the extract color was very pale. The pigments were analyzed by High Pressure Liquid Chromatography (HPLC) using the method described by Zapata et al. (2000). Spectrophotometry was also conducted on the extracts, after further dilution in DMSO.

Irradiance readings from roof top solar panels recorded the sunlight intensity on the dates when the light intensity experiments were conducted (Figure 21). Decreases in intensity represent clouds. PAM data showed that after one hour in the sun, 30% of the reaction centers were functional and remained functional throughout the 5 hour period (Figure 22).

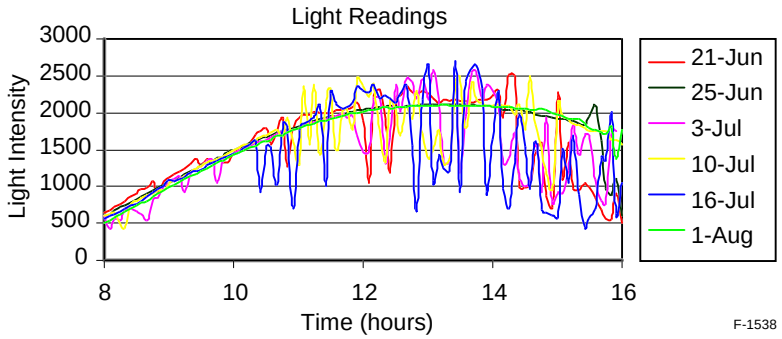

Figure 21. Light intensity (μE m^{-2} s^{-1}) measured outdoors on days when light experiments were carried out with strains AQ0011 (6/21, 7/11), AQ0012 (6/25, 7/11), AQ0052 (7/3, 7/11), AQ0053 (8/1), AQ0033 and AQ0036 (7/16).

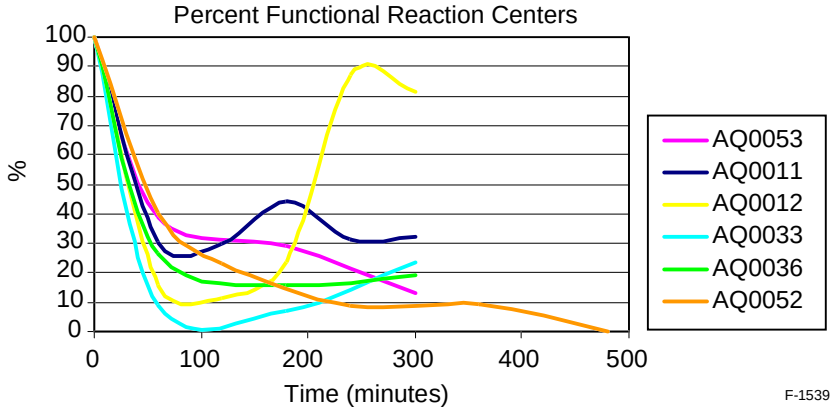

Figure 22. Percent functional reaction centers for each species from initial sample to final calculated with PAM Fv/Fm reading.

The unknown chlorophyte AQ0011 did not increase in biomass during the 5 hour period (Figure 23). HPLC confirmed the presence of large amounts of lutein present throughout the experiment, as percent lutein per dried biomass increased from 0.25% (initial) to 0.28% (5 hour). Initially, no zeaxanthin was detected by HPLC, but after five hours, the percent zeaxanthin per ml dried biomass had increased to 0.12%. Lutein and Zeaxanthin increased per volume as well (Figure 24). In addition, a small amount of β-β carotene was present in varying levels throughout the experiment. Examples of HPLC chromatograms are shown in Figures 25 through 28. The absorbance/ml was determined volumetrically by the spectrophotometer (Figure 29). The difference spectra are shown in Figure 30.

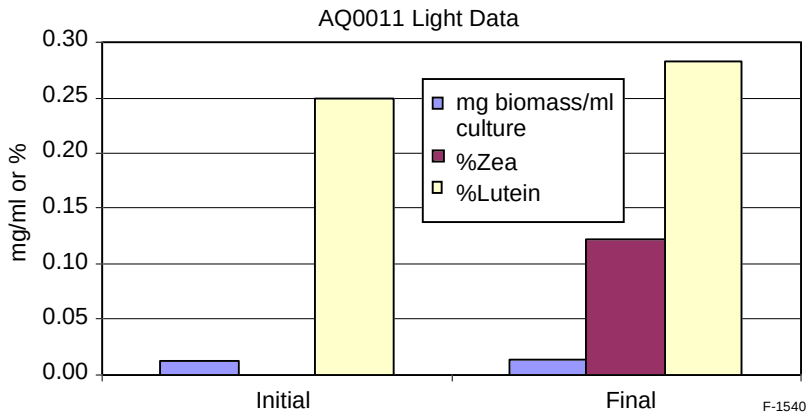

Figure 23. Biomass and % carotenoids from initial (0 hr) to final (5 hr) after intense light exposure.

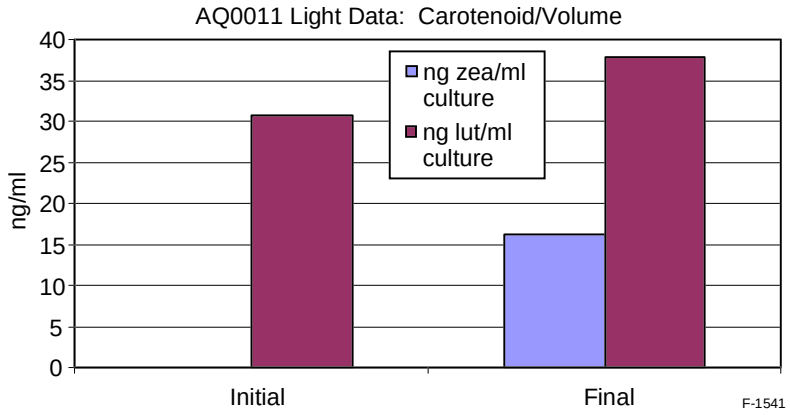

Figure 24. Carotenoid amount per culture volume initially and after 5 hr of intense sunlight.

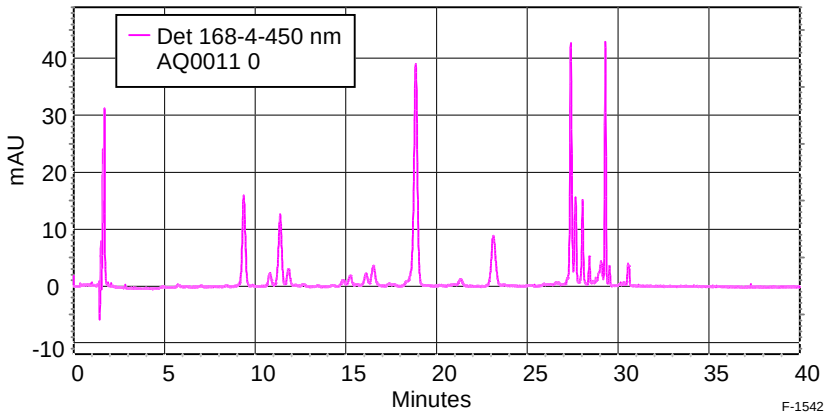

Figure 25. HPLC chromatogram for strain AQ0011, 0 hr sample.

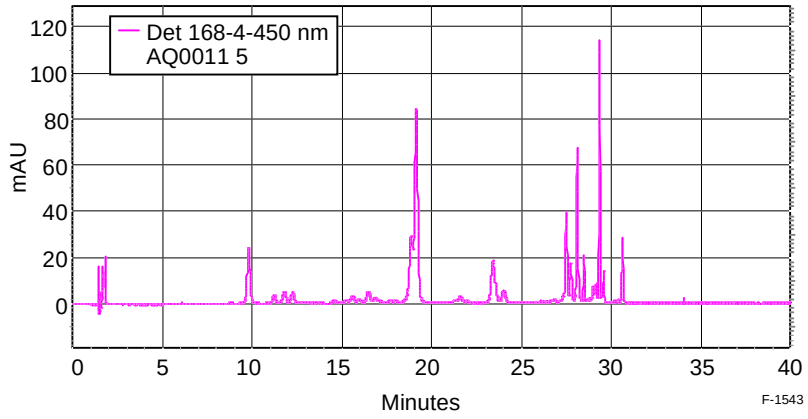

Figure 26. HPLC chromatogram for strain AQ0011, 5 hr sample.

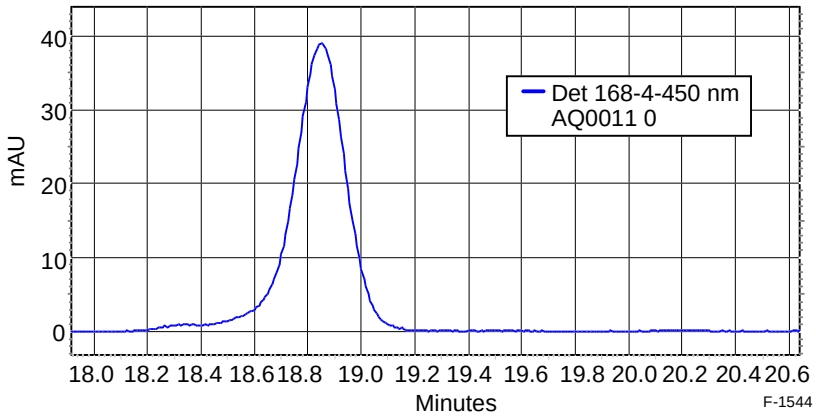

Figure 27. AQ0011 HPLC chromatogram showing the lutein peak at 0 hr. No zeaxanthin present.

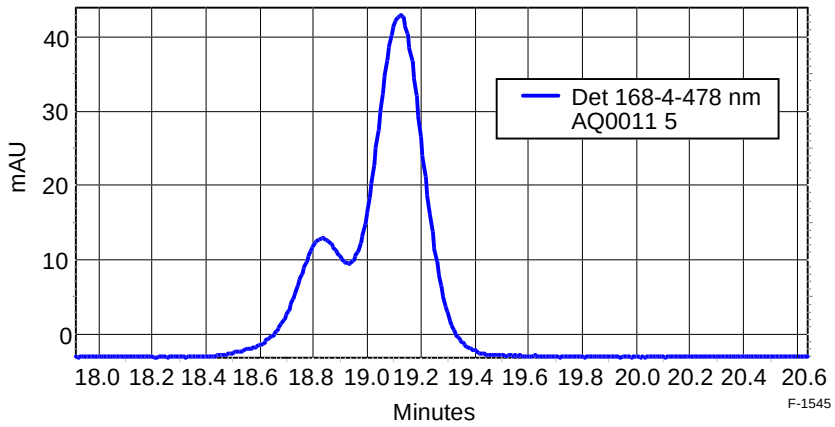

Figure 28. AQ0011 HPLC chromatogram of the 5 hr sample. Zeaxanthin peak present at base of the lutein peak.

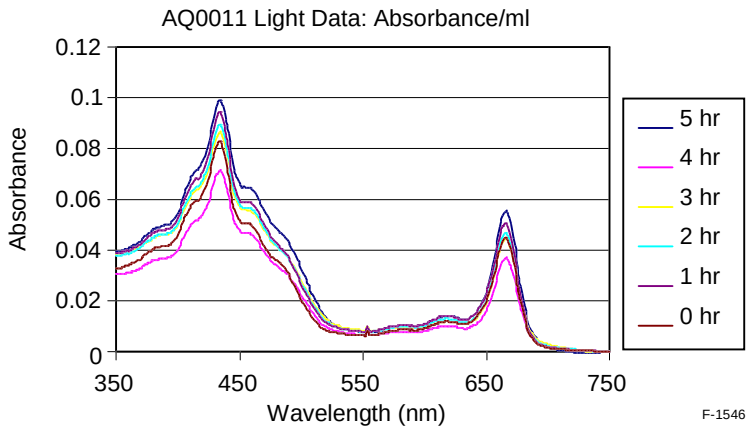

Figure 29. Absorbance per volume determined spectrophotometrically over a 5 hour period of intense sunlight.

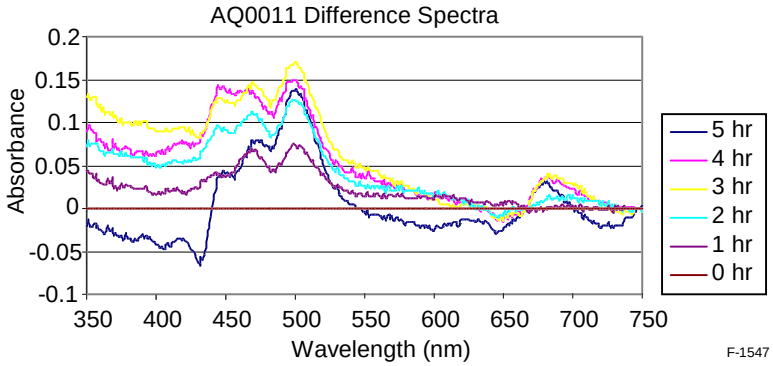

Figure 30. Spectral differences over a 5 hr period of intense sunlight.

The biomass of AQ0012, an unknown strain of cyanobacteria, increased through time. After one hour of light exposure, the biomass in the flask was floating at the top of the liquid in a tight clump. It is likely that this is morphological defense mechanism of the microalgae to increase shading of the cells. Data collected with the Pulse Amplitude Modulator (PAM) in the light show that after 2 hours of intense light exposure, only one-tenth of the initial reaction centers are functioning (Figure 22). Photosynthetic capacity of the cells is very low after five hours. HPLC analysis revealed the initial percent of zeaxanthin per dried biomass to be 0.15% and final percentage was 0.14% (Figure 31). The amount of zeaxanthin per volume increases proportionately with the increasing biomass (Figure 32). It was also noted that AQ0012 produced β-β carotene, but the amount was small and did not change significantly with time.

Dunaliella strain AQ0052 was exposed to intense sunlight for a period of 8 hours to determine if extended light exposure would induce additional zeaxanthin production. After two hours of sunlight, 22% of reaction centers were operating, and this percentage continued to decrease until no reaction centers were functional at 8 hours (Figure 6). The biomass increased slightly, and the zeaxanthin increased from 0% to 0.05% per dried biomass (Figures 33 and 34).

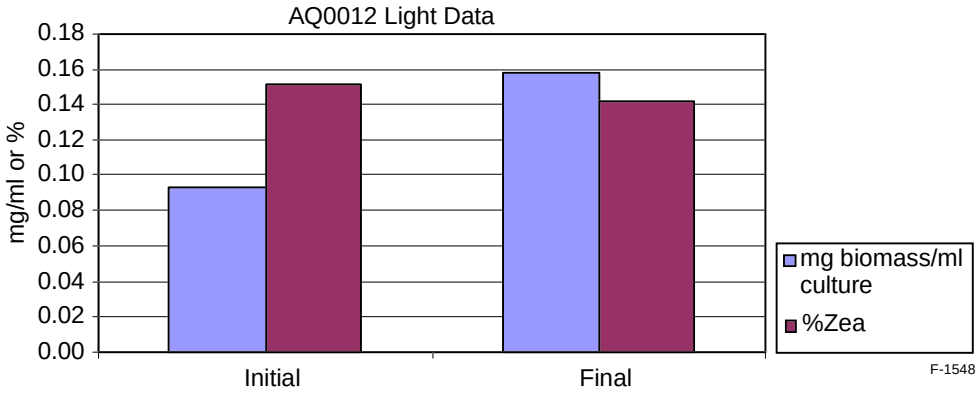

Figure 31. Biomass and % zeaxanthin from initial (0 hr) to final sample (5 hr).

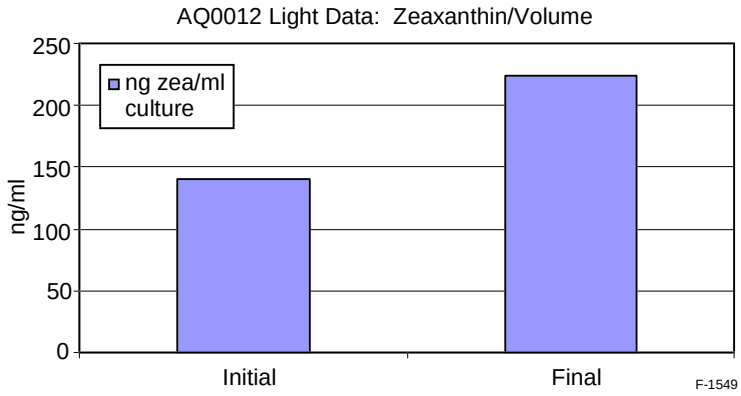

Figure 32. Zeaxanthin measured per culture volume from initial (0 hr) to final (5 hr).

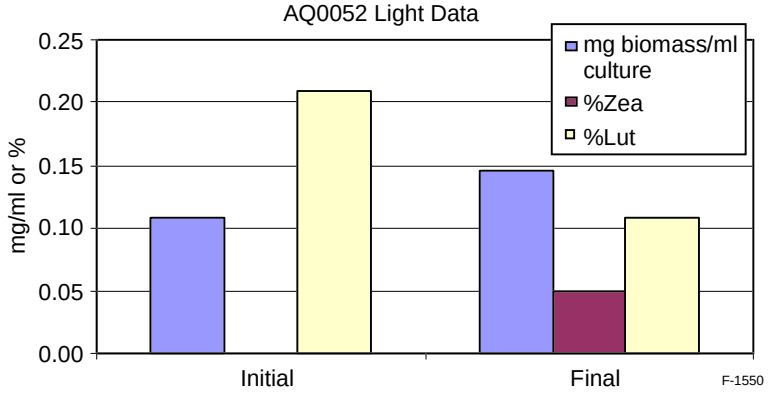

Figure 33. Biomass and % carotenoids from initial sample (0 hr) to final sample (8 hr).

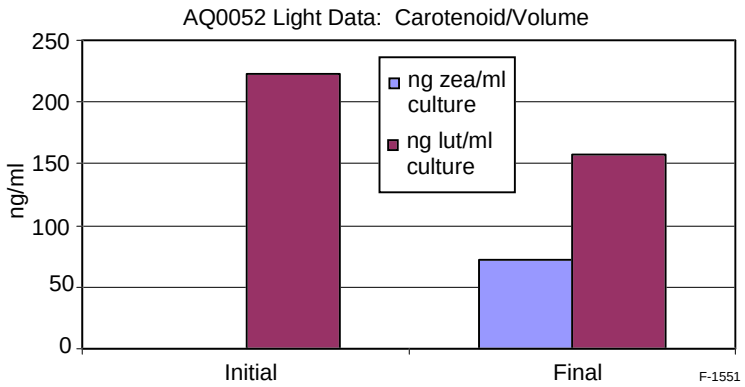

Figure 34. Carotenoid per volume of culture from initial (0 hr) to final sample (8 hr of intense sunlight).

AQ0052 also contained lutein, which decreased during the light exposure from 0.2% to 0.11% per ml dried biomass. Chlorophyll a decreased dramatically throughout the experiment, and was not detectable in the 8 hour sample by HPLC.

Dunaliella strain AQ0053 was exposed to intense light conditions for 5 hours and PAM data showed that after 5 hours of intense light exposure, 12% of reaction centers were functioning (Figure 22). The biomass began to settle to the bottom center of the 1000 mL flask during the experiment, and some small clumps of cells were visible at the end of the time period. Biomass increased from initial to final sample (Figure 35). HPLC data showed that the % lutein increased from 0.31% to 0.35% per dried biomass (Figure 36). Lutein also increased on a volumetric basis. Strain AQ0033 was exposed to intense light conditions for 5 hours, and the biomass decreased slightly. Similar to AQ0012, the biomass clustered together in the flask, but formed a loose mass rather than a tight clump. PAM data showed that only 7% of reaction centers were functional after 3 hours of sunlight (Figure 22). HPLC data confirmed that the 0 hour sample contained 0.2% zeaxanthin per dried biomass, a value higher than any percent zeaxanthin obtained (Figure 37). However, after intense light exposure, this amount decreased to 0.1%. Zeaxanthin decreased on a per volume basis as well (Figure 38). The reasons for this

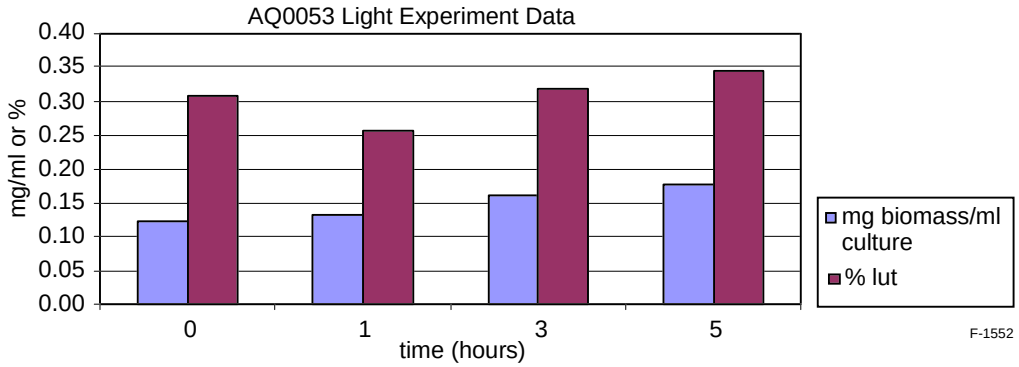

Figure 35. Biomass and % lutein after 0, 1, 3, and 5 hours of intense light.

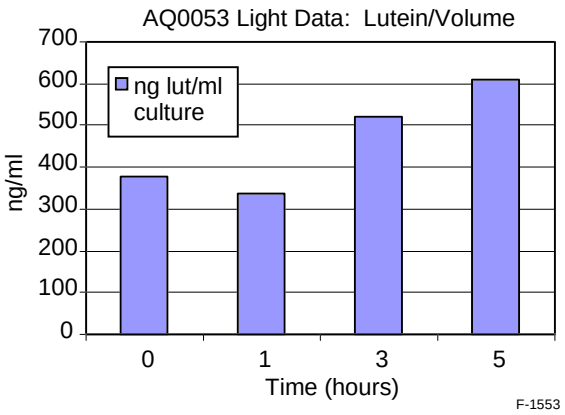

Figure 36. Lutein per culture volume over period of 5 hours.

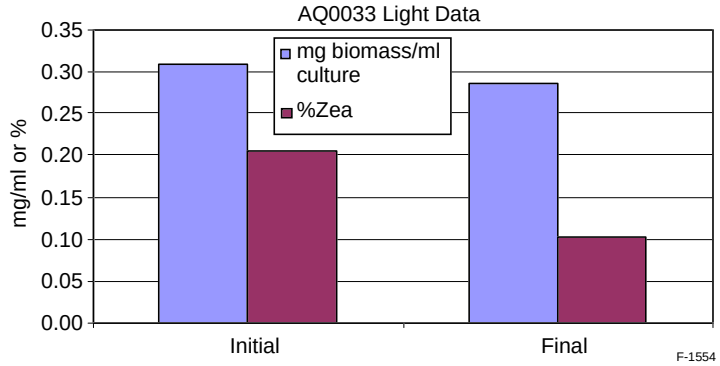

Figure 37. Biomass and zeaxanthin from initial (0 hr) to final sample (5 hr).

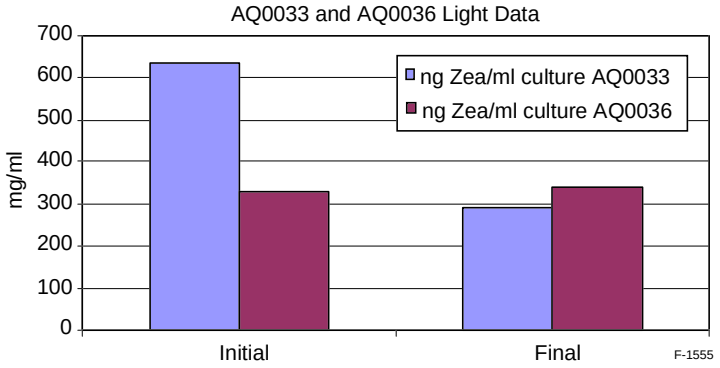

Figure 38. Zeaxanthin per culture volume from initial (0 hr) to final sample (5 hr).

decrease are unknown and are still under investigation. It is possible that because *Porphyridium* was originally a soil algae (Lee, 1989), these strains do not have the ability to efficiently adapt under intense light.

The biomass of *Porphyridium* strain AQ0036 significantly increased during the 5 hour experiment. PAM data showed that after one hour of light exposure, 25% of the reaction centers that harvest light for photosynthesis were operating (Figure 22). This number remained fairly constant throughout the experiment. The amount of zeaxanthin per dried biomass also decreased from 0.13% to 0.05%, levels that are still higher than those of AQ0052 (Figures 33 and 39). Zeaxanthin per volume also decreased for AQ0036 (Figure 38).

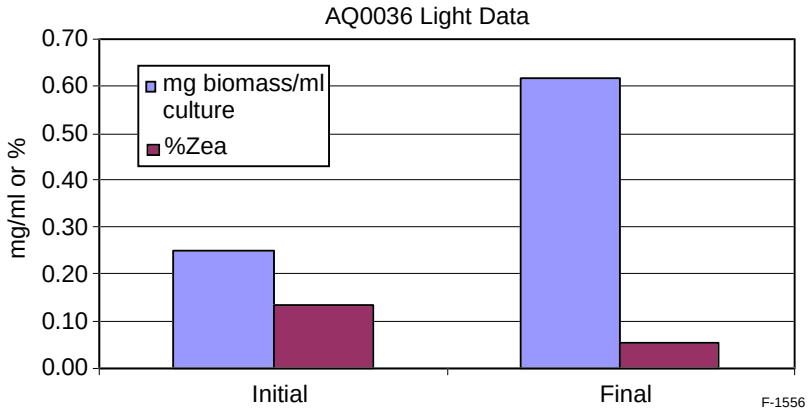

Figure 39. Biomass and % zeaxanthin from initial (0 hr) to final sample (5 hr).

Nitrate Deprivation Experiments

Nitrate deprivation experiments were conducted with AQ0033, AQ0036, AQ0011, and AQ0012. Two hundred ml of each culture was collected from the chemostat and inoculated in 800 ml of 413 media without nitrate. Freshwater media was prepared for AQ0011 and AQ0012, while AQ0033 and AQ0036 were grown in 9 ppt salt media. The cultures were grown in 2800 ml Fernbach flasks in a 25°C water bath on a 14:10 light:dark cycle, with lights measuring an intensity of 60 $\mu E\ m^{-2}\ s^{-1}$. The flasks were mixed by air agitation, and it is probable that ambient CO_2 contributed slightly as a source of carbon. PAM readings were taken daily and pH was monitored. Two additional light banks were added on day 6 of the experiment to increase photosynthesis and expedite the nutrient deprivation effects. The average light intensity was measured to be 175 $\mu E\ m^{-2}\ s^{-1}$. After 10 days, pigments were extracted from 50 ml of each culture and dried biomass analysis was conducted using 350 ml of culture.

Daily PAM readings showed that the Fv/Fm values varied greatly for each strain tested. In Figure 40, the slope of the line for AQ0033 was –0.0218, representing the rate of decrease in Fv/Fm. A flask of AQ0033 was broken on day 9 of the experiment, but data until this point was included in the analysis. For AQ0036, the linear regression line was nearly flat, with a slope of -0.0039 (Figure 41). The slope for AQ0011 also decreased, but at a rate of –0.0167 (Figure 42). In addition, the line for AQ0012 had a negative value of -0.0019, which represents that the cells were experiencing only slight stress after ten days of nitrate deprivation (Figure 43).

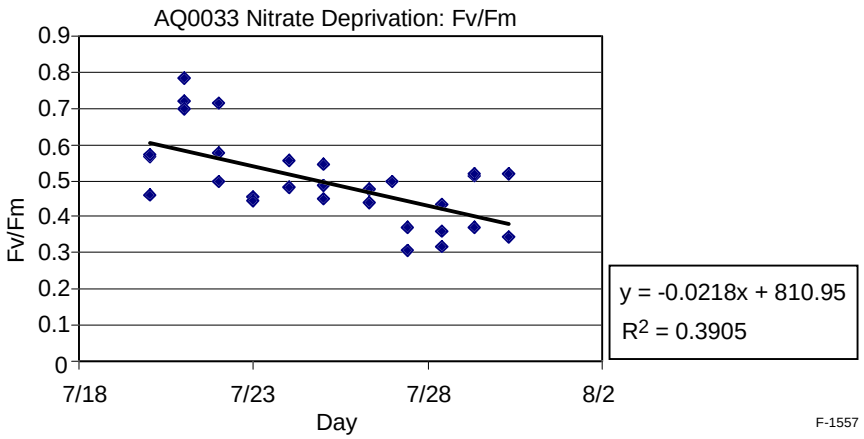

Figure 40. AQ0033 Fv/Fm readings from PAM data over 10 day nitrate deprivation experiment with linear regression analysis.

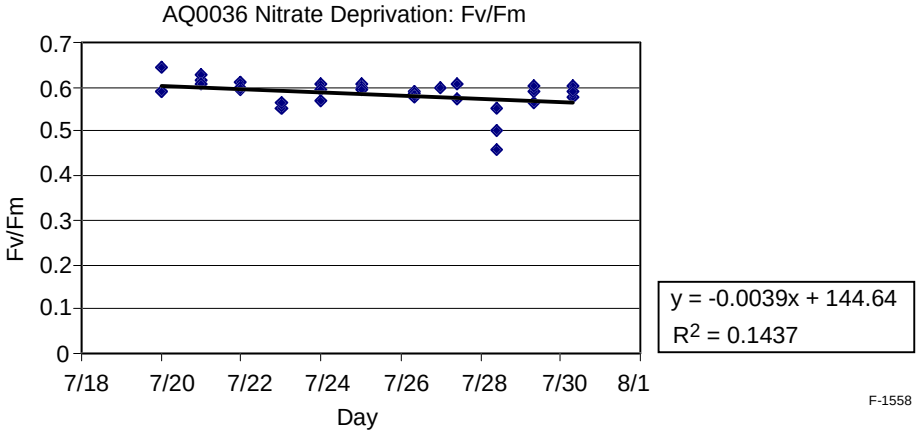

Figure 41. AQ0036 Fv/Fm readings from PAM data over 10 day nitrate deprivation experiment with linear regression analysis.

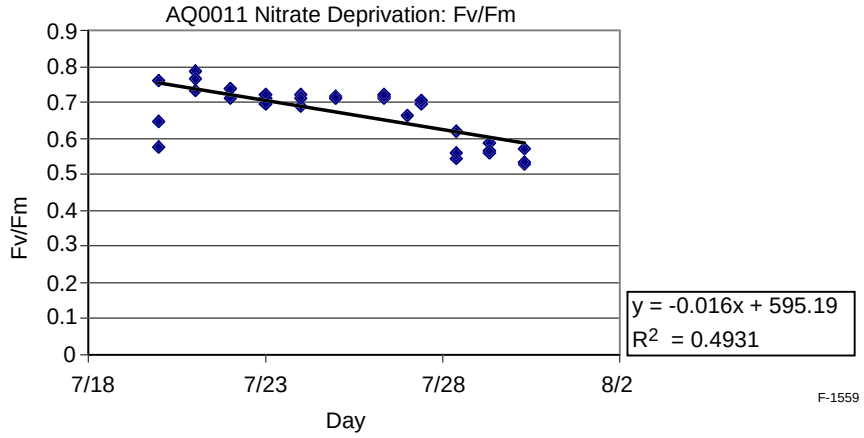

Figure 42. AQ0011 Fv/Fm readings from PAM data over 10 day nitrate deprivation experiment with linear regression analysis.

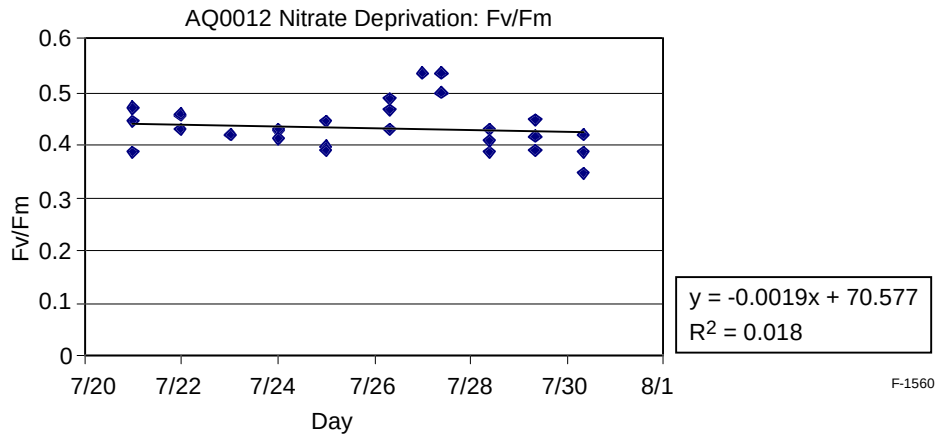

Figure 43. AQ0012 Fv/Fm readings from PAM data over 10 day nitrate deprivation experiment with linear regression analysis.

The percent carotenoid per dried biomass decreased for AQ0011, AQ0033, and AQ0036, but remained constant for AQ0012 (Figure 44). AQ0011 produced only lutein during this experiment, unlike the light intensity experiment where it showed zeaxanthin production after one hour. AQ0012, AQ0033, and AQ0036 all produced zeaxanthin. Both AQ0011 and AQ0012 increased in biomass per culture volume as seen in Figure 45 while the biomass of AQ0033 decreased and AQ0036 was constant. Although the pigments of AQ0011 and AQ0012 did not increase on a % dried biomass basis, the pigments did increase dramatically on a volumetric basis (Figure 46). Thus, as the culture grew over the experimental period, the absolute amount of pigments in each flask increased for AQ0011 and AQ0012 and decreased for AQ0033 and AQ0036.

Because 200 ml of culture were used to inoculate the flasks, it is possible that this volume contained enough nitrate from the original media to support the cultures for the experimental period. It is possible that using a smaller inoculum volume would cause the cells to experience stress more quickly, and perhaps alter the pigments more dramatically.

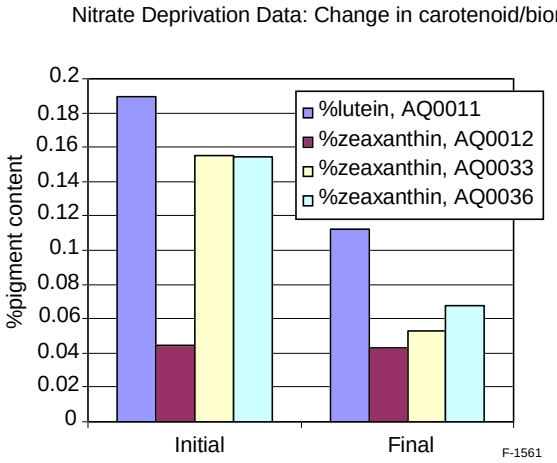

Figure 44. Carotenoid percentages per biomass over 10 day nitrate deprivation experiment.

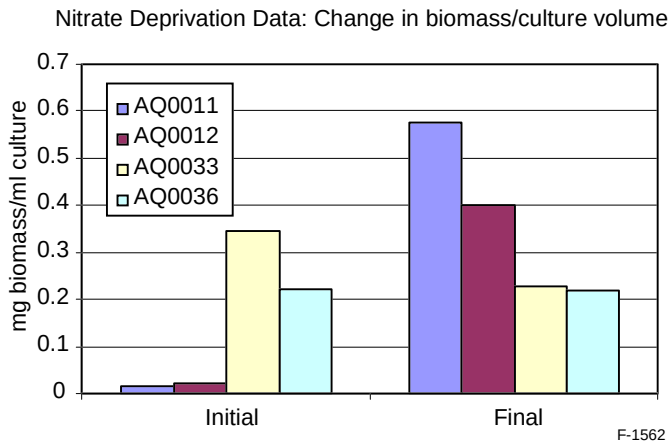

Figure 45. Biomass per culture volume calculated for initial (day 0) and final samples (day 10).

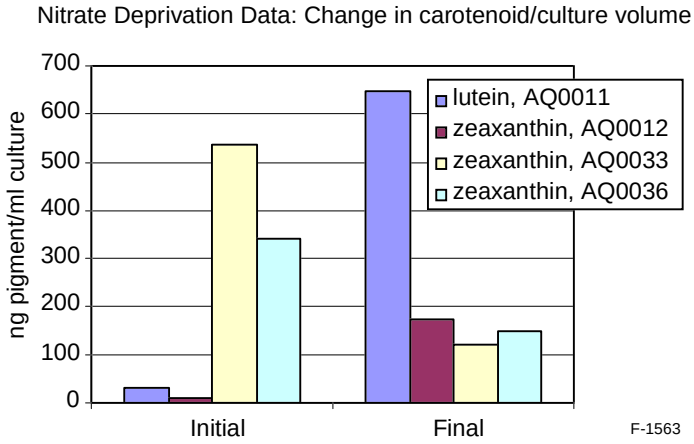

Figure 46. Carotenoid per culture volume for initial (day 0) and final samples (day 10).

Salt/Sodium Acetate Experiments

The third experiment exposed *Dunaliella* species AQ0053 to high sodium chloride and sodium acetate concentrations. Triplicate samples of 200 ml of culture were collected from the chemostat and receiver and grown in batch mode in 250 ml Erlenmeyer flasks. Initial samples were collected for dried biomass (170 ml) and pigment analysis (50 ml). Initial PAM readings were taken of each flask. Sodium chloride was then added to three flasks, creating a 10% salt solution. Sodium acetate was also added to three flasks bringing the concentration of sodium acetate to 1g/l. This additive serves as a source of organic carbon readily taken up by the cells and has been used to increase carotenoid yields. Both sodium chloride and sodium acetate were added to three additional flasks in the previously determined amounts. Flasks were grown in batch mode in a 25°C water bath on a 14:10 light:dark cycle for 3 days. Pigments were extracted from 50 ml of culture, and 150 ml samples were used for dried biomass analysis. HPLC and spectrophotometry were conducted to analyze the pigments.

PAM data showed that the Fv/Fm values of AQ0053 were the same for the initial samples before additions of salt and/or sodium acetate were made compared to the Fv/Fm values immediately after the additions. However, the Fv/Fm ratio plummeted from 0.7 on Day 1 to 0.2-0.3 on Day 2. An example of the Fv/Fm ratios with NaCl is shown in Figure 47. The dramatic decrease was unexpected, and it is possible that the media was contaminated or that the concentrations were higher than calculated.

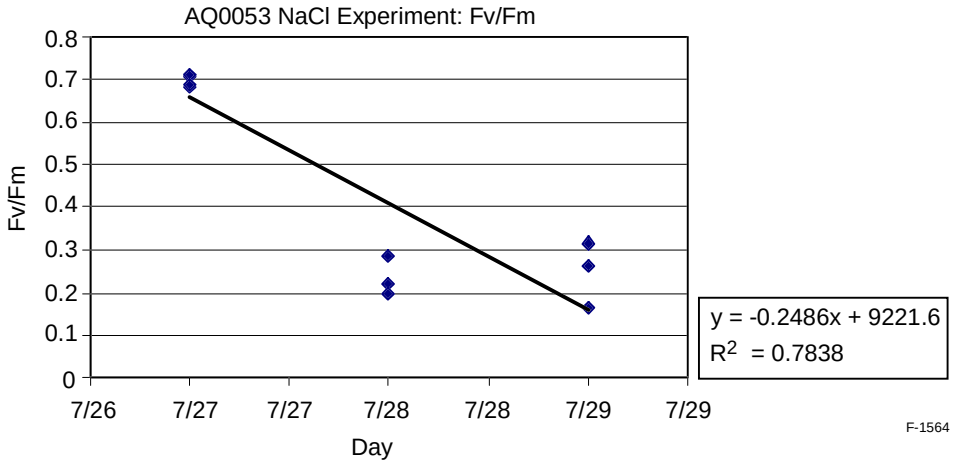

Figure 47. AQ0053 Fv/Fm values from PAM data with linear regression analysis.

The mg biomass per culture volume increased for all flasks slightly during the 3 day experiment, with the greatest increase seen in the flasks with NaCl and NaAc in combination. AQ0053 produced lutein initially at 0.34% per dried biomass, a level higher than any carotenoid for all strains. The % lut decreased for all flasks from initial to final sample, with the lowest value for the NaCl/NaAc flasks at 0.09% (Figure 48). The amount of lutein decreased for all samples volumetrically as well.

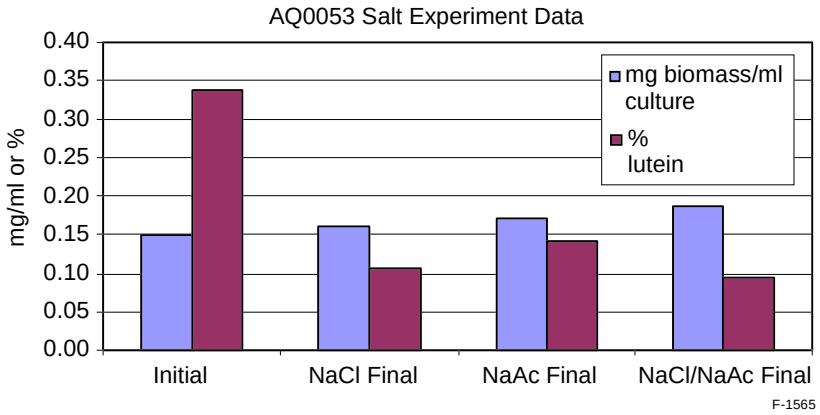

Figure 48. Biomass and % lutein for initial sample (0 day) and samples with additives after 3 days.

Potential for Commercial Production

One goal of these experiments was to determine which strains would be worthwhile to grow at a commercial level to offset the cost associated with microalgal mediated carbon sequestration. The pigment composition of each strain was analyzed before and after exposure to environmental stress to evaluate how the stress affected pigment production. This research was conducted at Aquasearch Inc., where the 25,000 L enclosed outdoor photobioreactors, known as the Aquasearch Growth Modules (AGMs), are producing *Haematococcus pluvialis* at a rate of 9 to 13 g m^{-2} d^{-1} (Olaizola, 2000). Similar growth rates or higher could be expected by growing the tested strains in the AGMs. For AQ0033, AQ0036, AQ0012, and AQ0052 the highest % zea was found in the initial sample before treatment with environmental stress (Table 9). Thus, the most pigment per dried biomass was produced when the cultures were grown in nutrient rich media at low light intensities. On the other hand, AQ0011 and AQ0053 produced the greatest amount of pigments after 5 hours of intense light exposure. AQ0052 produced the most lutein without treatment, but produced a small amount of zeaxanthin after 8 hours of intense sunlight. The ability of AQ0011 to produce both lutein and zeaxanthin makes it a highly attractive strain to grow in the AGM. AQ0053 could be expected to produce 0.04487 g m^{-2} d^{-1} lutein after 5 hours of intense light exposure, which is the highest value found of any carotenoid of any strain in this study. The values in Table 9 most likely represent the minimal amounts of carotenoids that can be obtained from these strains, as yields will increase with optimization of mass cultures. During the Year 2 of this project we will begin to scale up the promising strains to commercial levels and to optimize the conditions under which these strains will produce the most pigment.

Table 9. Highest Percent Carotenoids per Dried Biomass Obtained in Experiments and Predicted Pigment Production Rates at a Production Rate of 13 g Dry Biomass m^{-2} d^{-1}, a Typical Rate of Aquasearch Growth Modules

Strain	Treatment Which Gave Highest % Pigment	Pigment	% Pigment	Production at Growth Rate of 13 g m^{-2} d^{-1}
AQ0011	5 hours sunlight	Lutein	0.28	0.037 g m^{-2} d^{-1}
AQ0011	5 hours sunlight	Zeaxanthin	0.12	0.016 g m^{-2} d^{-1}
AQ0012	No treatment	Zeaxanthin	0.15	0.020 g m^{-2} d^{-1}
AQ0033	No treatment	Zeaxanthin	0.21	0.027 g m^{-2} d^{-1}
AQ0036	No treatment	Zeaxanthin	0.13	0.017 g m^{-2} d^{-1}
AQ0052	No treatment	Lutein	0.21	0.027 g m^{-2} d^{-1}
AQ0052	8 hours sunlight	Zeaxanthin	0.05	0.006 g m^{-2} d^{-1}
AQ0053	5 hours sunlight	Lutein	0.35	0.049 g m^{-2} d^{-1}

3.2.2.3 Carbon Sequestration into Carbonate Minerals Utilizing Microalgae

One of the goals of this project is to identify under what conditions microalgal cultures can be induced to precipitate $CaCO_3$. This would represent a stable, long term, sink of atmospheric CO_2, a goal of the US Department of Energy.

Initially, we proposed to carry out this research by growing microalgal species known to produce cellular structures out of $CaCO_3$. While we still intend to work with such organisms we have decided to take the concept a step further. We intend to describe culture conditions that will induce the precipitation of carbon into $CaCO_3$ via photosynthetically mediated changes in medium pH. As cells photosynthetise and take up CO_2 from the culture medium, the pH of the medium raises. This change in pH produces an increase in the concentration of CO_3^{2-} ions in the medium. In the presence of sufficient amounts of Ca^{2+} $CaCO_3$ is expected to precipitate out of solution. Because the photosynthetically mediated change in pH is not specific to species that produce cellular carbonate structures, in principle, any species of microalgae could be used for this process.

Methods

These experiments were conducted using three different strains of microalgae and one species of cyanobacteria. The species of microalgae will be referred to as AQ0008, AQ0011, and AQ0053, where AQ0008 is *Haematococcus pluvialis*, AQ0053 is a *Duneliella sp.* obtained from the Hawaii Culture Collection, and AQ0011 is an unidentified locally isolated chlorophyte. AQ0012 is an unidentified species of filamentous cyanobacteria also isolated locally. All experiments were conducted using a 14:10 light:dark cycle with a light intensity of 60 $\mu E\ m^{-2}\ s^{-1}$. The source of the culture material for these experiments was our chemostat system.

Our standard growth medium (413) was enriched in Ca^{2+} by the addition of $CaSO_4*2H_2O$ (gypsum) for these experiments. Changes in the concentration of dissolved inorganic carbon species (CO_2, HCO_3^-, CO_3^{2-}) were determined using a standard titration method (Clesceri et al., 1995). Production of $CaCO_3$ was determined by observing the formation of a white precipitate. The precipitate was collected by filtration or centrifugation, dried. A few drops of hydrochloric acid were mixed with the powder thus obtained. A positive reaction (bubbling caused by CO_2 effervescence) was interpreted to indicate the presence of $CaCO_3$.

The first experiment was conducted with species AQ0011. Two types of media were prepared for the experiment. 413 media was prepared for flasks 1 and 3, and 413 media without bicarbonate was prepared for flasks 2 and 4. Each 250 ml flask was filled with 200 ml of its respective media. Flasks 3 and 4 were enriched with 6.16×10^{-4} moles of Ca^{2+}. Four 50 ml samples of AQ0011 were centrifuged and the pellets were used to inoculate each flask. Initial pH and alkalinity was measured and recorded. All flasks were placed in a 25°C water bath under the above mentioned growth conditions. The pH of each flask was monitored periodically. Fluorescence measurements were also measured throughout the five day experiment using a Pulse Amplitude Modulated Flourometer (PAM). After the cultures had grown for 5 days, final pH and alkalinity measurements were taken from each flask. The contents of each flask were gravity filtered using Whatman 15.0 cm filter paper. The filtrate was then tested for the presence of $CaCO_3$ by adding concentrated HCl and observing whether or not a reaction occurred. Bubbling of the filtrate indicated that $CaCO_3$ was present. This test was used throughout all of the experiments.

A second experiment was performed with microalgae species AQ0011, this time on a larger scale. A volume of 2500 ml of culture and media were removed from the receiver. The

sample was divided into two 1600 ml volumes, one of which was enriched with 2.09 x 10^{-2} M Ca^{2+} and stirred until dissolved. Alkalinity and pH measurements were taken from 40 ml of both the Ca^{2+} and non-Ca^{2+} enriched mediums. Four 1 L flasks were used and 780 ml of non-calcium culture was added to both flasks 1 and 2. A volume of 780 ml of Ca^{2+}-enriched culture was added to both flasks 3 and 4. All flasks were grown as previously described. After the pH in each flask reached 9.0 or higher, the contents of each was centrifuged and the pellet dried. The concentrated HCl bubble test was used on the dried pellets to determine if $CaCO_3$ precipitation had occurred.

Another experiment examined cyanobacteria species AQ0012. Approximately 800 ml of culture in medium was removed from the receiver. This volume was divided in half, and 5.60×10^{-3} M Ca^{2+} was dissolved in to one half. It was necessary to add an additional 20 ml of deionized water while stirring the sample in order to dissolve all of the Ca^{2+}. Two flasks were filled with 200 ml of culture each, and two were filled with culture enriched with calcium. Alkalinity and pH measurements were taken initially from each flask. All flasks were then placed in a 25°C water bath and grown as mentioned. Alkalinity and pH measurements were taken periodically. After the flasks had reached a pH of 9.0 or higher, the contents of each were examined under a microscope for $CaCO_3$ precipitates. Also, the contents of each flask was filtered and tested for $CaCO_3$ precipitation using the HCl bubble test.

A second experiment was conducted with AQ0012 on a larger scale using greater volumes and more biomass. Approximately 2 L of culture was removed from the receiver. Initial pH and alkalinity measurements were taken from 50 ml of this sample. Flasks 1 and 2 were filled with 975 ml each of the culture. Again, approximately 2 L of culture was removed from the receiver and was enriched with 2.80×10^{-2} M of Ca^{2+}. Initial pH and alkalinity measurements were taken from 50 ml of this sample. Flasks 3 and 4 were filled with 975 ml of the sample. All flasks were grown under the same conditions as the previous experiments and pH and alkalinity measurements were taken periodically. After the pH of each flask reached 9.0 or higher, the contents of each flask was centrifuged, filtered, and dried in an oven overnight. The HCl bubble test was conducted on the dried samples to determine if $CaCO_3$ was present.

A similar experiment was done with microalgae species AQ0052. One liter of culture and medium was removed from the receiver. Initial pH and alkalinity measurements were taken and 200 ml were added to flasks 1 and 2. A volume of 500 ml of the culture was enriched with 6.39×10^{-3} M of Ca^{2+} and stirred until dissolved. Flasks 3 and 4 were filled with 200 ml of this solution and the remaining culture was used for initial pH and alkalinity measurements. Flasks were grown under the same conditions and pH and alkalinity measurements were taken periodically.

Next, a chemostat system was established with a culture of cyanobacteria AQ0012. The chemostat was inoculated with AQ0012 and allowed to grow in FW 413 media between a pH of 7.4 and 7.6. Media for the chemostat was made by adding 0.134 moles Ca^{2+} to 8.5 L of filtered freshwater and sterilized. Alkalinity and pH measurements were taken from the calcium enriched media, and the chemostat. Once the culture had grown for 4 days, addition of media and removal of the culture from the chemostat began at a flow rate of 1.97 ml min^{-1}. The pH of the chemostat was then set to a range of 8.4 to 8.6. No pH control was given to the receiver that

accumulated the culture. Alkalinity and pH measurements were taken daily from both the chemostat and receiver cultures.

A small experiment was also done to attempt to induce the precipitation of $CaCO_3$ by exceeding the saturation point of CO_3^{-2} in a medium. A flask with 155 ml of deionized water was enriched with 2.10×10^{-3} moles of Ca^{2+}. The medium was then bubbled for approximately ten minutes with CO_2 and was visually examined for precipitate formation. Initial and final pH measurements were also taken.

An experiment was conducted to observe how ion concentrations change with increases in pH and with the addition of CO_2 to the medium. A solution of $NaHCO_3$ was made by adding 3.57 M of $NaHCO_3$ to 8 l of filtered fresh water. Alkalinity and pH measurements were then taken from the solution. Also, a Ca^{2+} solution was prepared by adding 4.10×10^{-2} M of Ca^{2+} to 3.1 l of filtered fresh water. Three large flasks were filled with 2 l of $NaHCO_3$ solution and .8 l of Ca_2+ solution. A 170 ml sample was taken after the solution was well mixed. With a pH probe submerged in each flask, a solution of NaOH was added to the flasks while stirring to raise the pH to 9.0. After the pH of each flask reached 9.0, a 170 ml sample was taken. Next, CO_2 was bubbled into the solution while stirring. When the pH of the flasks reached 8.5, 8.0, and 7.5, 170 ml samples were taken. The pH of flask 1 was decreased to 7.2 and a 170 ml sample was also taken. The samples were centrifuged and the pellets dried on pre-weighed aluminum weigh boats. From this data, the weight of the solid $CaCO_3$ was determined. The supernatant of each centrifuged sample was used for pH and alkalinity measurements.

This experiment was repeated in the same manner using only two flasks. During this experiment, the visible $CaCO_3$ precipitate was removed before the addition of CO_2. Alkalinity and pH measurements were taken from samples collected at each pH (9.0, 8.5, 8.0, and 7.5).

This experiment was repeated again, but standard freshwater 413 media was used instead of filtered freshwater enriched with $NaHCO_3$. Two flasks were filled with 2 L of 413 media and 0.8 l of a calcium solution made by adding 0.112 M of Ca^{2+} to 9.0 l of freshwater 413 media. The initial pH and alkalinity of each flask was measured before and after the addition of Ca^{2+}. NaOH was added to each flask until a pH of 9.0 was reached and a 170 ml sample was taken. The precipitate was not removed from the flasks. CO_2 was bubbled into the solution while stirring and 170 ml samples were taken at pH levels of 8.5, 8.0, 7.5, and 7.0. The samples were centrifuged and the pellets were dried on pre-weighed aluminum weigh boats to determine the amount of $CaCO_3$ precipitate. The supernatant of each centrifuged sample was used for pH and alkalinity measurements.

Another series of experiments were conducted similar to the above method using AQ0008 and AQ0012 cultures to increase the pH of the medium instead of the addition of NaOH. Two large flasks were filled with 2 L of either AQ0008 or AQ0012 culture. The AQ0008 culture was obtained from an outdoor commercial photobioreactor (Olaizola, 2000), where the AQ0012 culture was again obtained from the chemostat system. A solution of FW 413 and Ca2+ was made by adding 1.16×10^{-2} M of Ca^{2+} to 1 L of freshwater 413, and 500 ml of the solution was added to each flask. Alkalinity and pH measurements were taken of each culture before and after the addition of the Ca^{2+} solution. The flasks were then exposed to light

for 14 hours in order for photosynthesis to increase the pH. Samples were taken after the pH of each flask reached 9.0 or higher. CO_2 was then bubbled into the culture while stirring and two 170 ml samples were taken at a pH of 9.0, 8.5, 7.5, and 6.5. The samples were centrifuged and the pellets were dried on pre-weighed aluminum weigh boats. The supernatant of each centrifuged sample was used for pH and alkalinity measurements.

Results

Initial experimentation with species AQ0011 gave no visual indication that $CaCO_3$ precipitation via algal mediation could occur under the conditions tested with these species. Flasks lacking bicarbonate did not increase in biomass and did not produce data indicative of $CaCO_3$ formation (Figures 49 and 50). This was possibly due to the intolerance of algae to the low pH of the 413 media caused by lack of HCO_3^-. After examining the ion concentrations of the media enriched with bicarbonate, it was apparent that a portion of carbon was missing from the calcium-enriched medium (Figures 51 and 52). A greater decrease in total inorganic carbon concentration, along with a decreased amount of dissolved carbonate ions in the calcium-enriched flask with bicarbonate indicates the possible formation of $CaCO_3$ (Figure 52). However, this was not visually confirmed through identification of $CaCO_3$ particles or through a reaction of the filtrate with concentrated HCl. A second experiment with AQ0011 demonstrated similar ion concentrations, although the second experiment displays a clearer depiction of differences in ion concentrations in control and experimental flasks (Figures 53 and 54). The solid was identified as $CaCO_3$ due to the identification of a reaction occurring after the addition of concentrated HCl. Results from the second experiment with AQ0011 were more conclusive because of the method of testing for $CaCO_3$ precipitate. In the initial experiment, the contents of each flask were filtered and exposed to HCl while still damp. Centrifuging and drying of the pellets from each flask better prepared the samples for the "bubble test" with concentrated HCl. In both experiments, it can be recognized that as the pH of the medium increases, the carbon species shift towards CO_3^{-2}. In flasks with Ca, the CO_3^{-2} concentrations are significantly lower than those not enriched with calcium, indicating the binding of CO_3^{-2} ions with the Ca^{2+} ions in solution and ultimately the formation and precipitation of $CaCO_3$. The precipitate was not

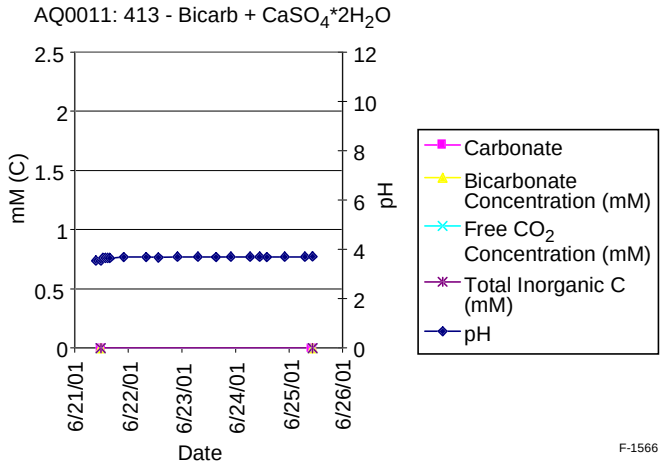

Figure 49. pH and dissolved inorganic carbon species in AQ0011 without HCO_3^- and with Ca.

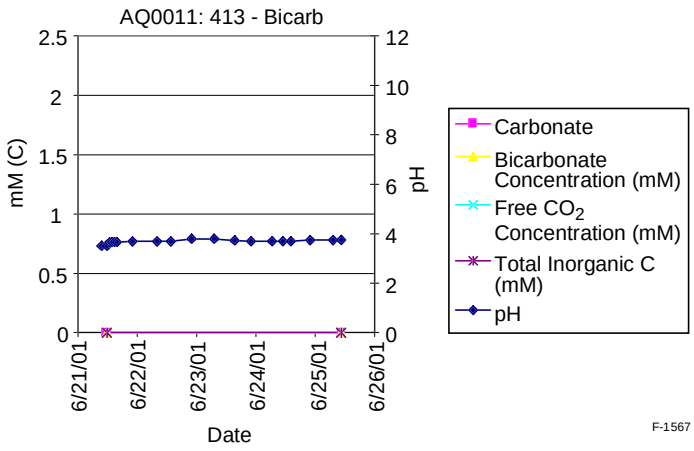

Figure 50. pH and dissolved inorganic carbon species in AQ0011 without HCO_3^-.

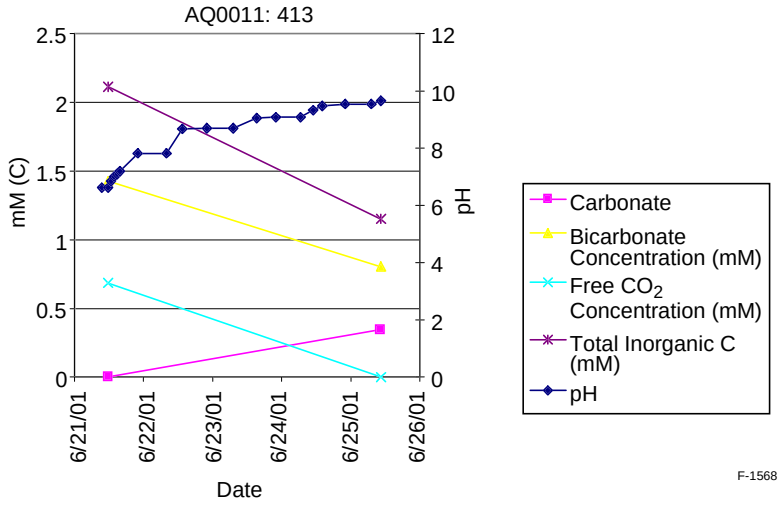

Figure 51. pH and dissolved inorganic carbon species concentrations in AQ0011 with FW413.

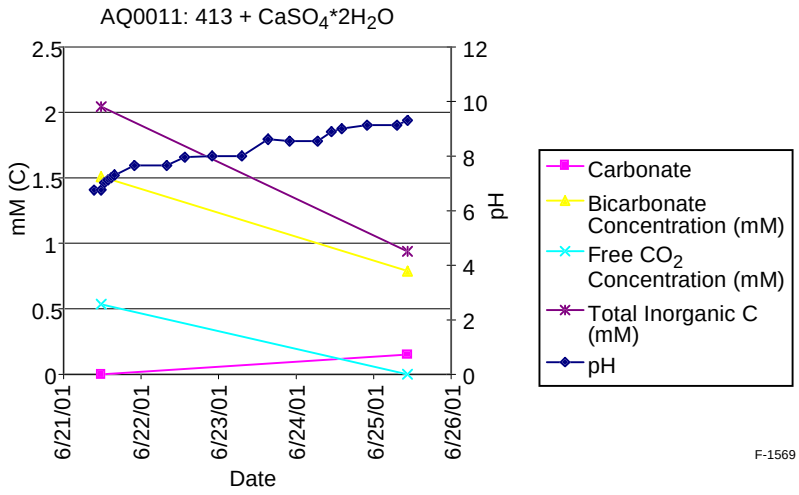

Figure 52. pH and dissolved inorganic carbon species concentrations in AQ0011 in FW 413 + Ca.

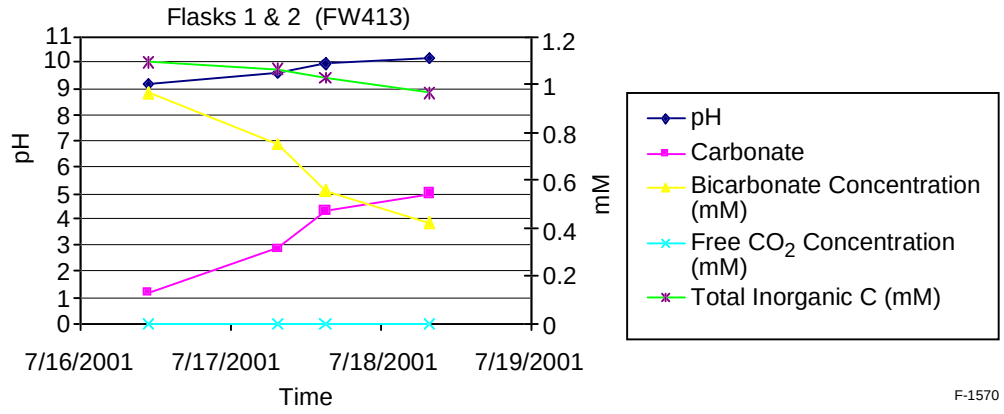

Figure 53. pH and dissolved inorganic carbon species concentrations in AQ0011 exp. 2 in FW 413, average of two flasks.

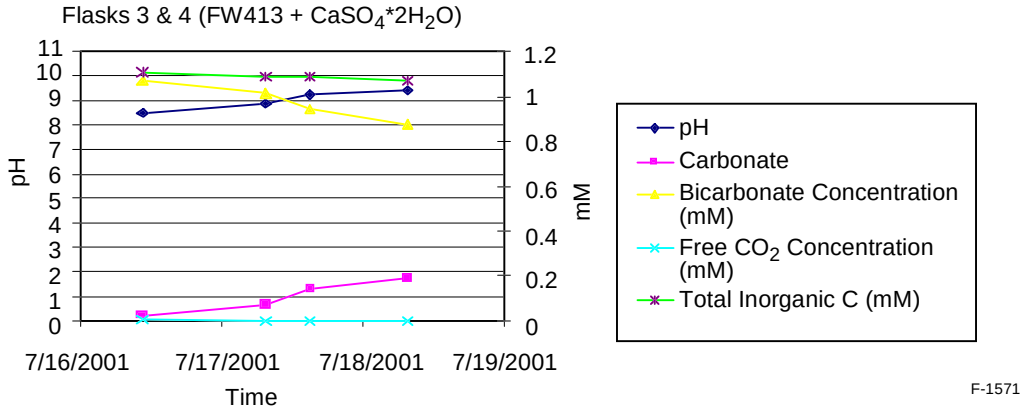

Figure 54. pH and dissolved inorganic carbon species concentrations in AQ0011 exp. 2 in FW 413 + Ca, average of two flasks.

visually apparent due to the biomass of algae in the flasks and the small particle size of the $CaCO_3$ crystals. This dust-like form of $CaCO_3$ is similar to that identified as the source of Bahamas whiting incidents where biologically induced precipitates cloud surface waters (Robbins and Yates 2001).

The microalgae AQ0052 did not increase significantly in biomass from the beginning to the end of experiment. The culture did not photosynthesize enough to raise the pH of the medium to a level where $CaCO_3$ could possibly precipitate. Also, the ion concentrations did not differ between experimental and control flasks (Figures 55 and 56) indicating that carbon had not been removed from the system. It has not been determined why AQ0052 did not increase in biomass, but a low initial biomass may have been the cause for the lack of rapid growth.

Experimentation with cyanobacteria species AQ0012 also yielded promising results. The initial experiment resulted in white particles observed in suspension among the biomass. Dissolved carbon concentrations were found to decrease throughout the experiment in the

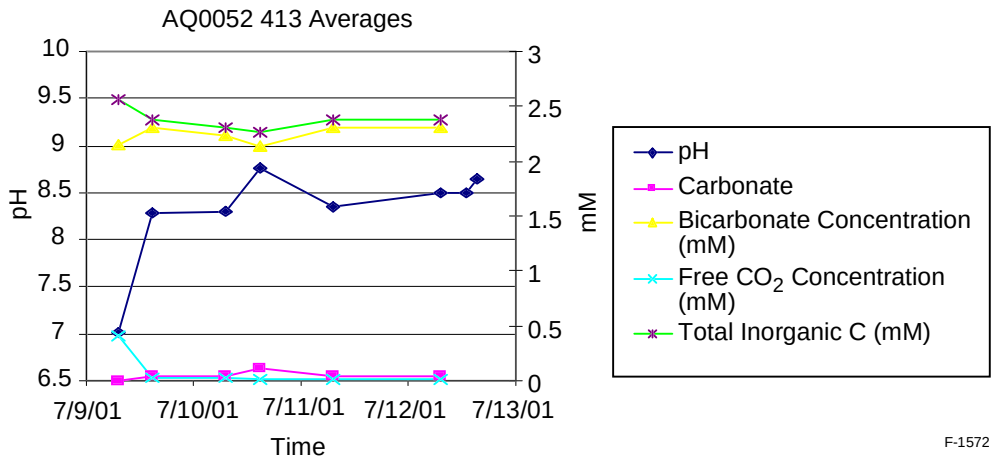

Figure 55. pH and dissolved inorganic carbon species concentrations in AQ0052 in FW 413, average of two flasks.

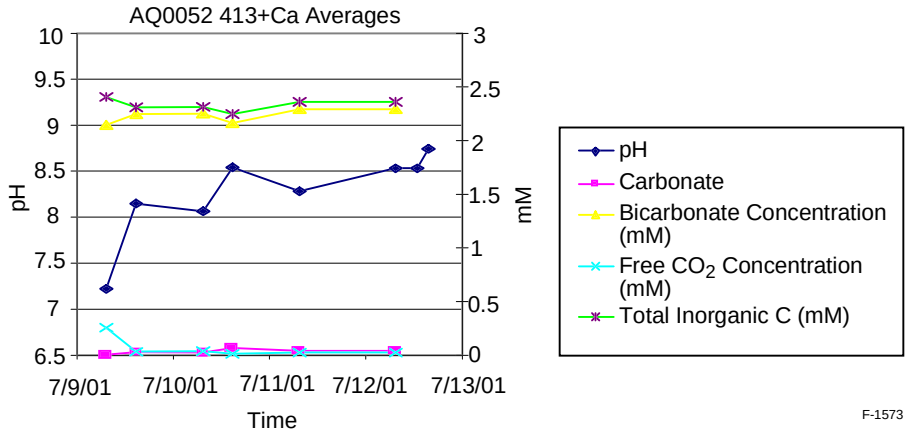

Figure 56. pH and dissolved inorganic carbon species concentrations in AQ0052 in FW 413 + Ca, average of two flasks

experimental flasks containing calcium (Figures 57 and 58). In addition, the total dissolved inorganic carbon at the end of the experiment was lower in the experimental flasks (Figures 57 and 58). This indicates that carbon has been successfully removed from the system, once again suggesting the formation of solid $CaCO_3$. Data from the first experiment using species AQ0012 demonstrated a difference in initial bicarbonate ion concentration of the medium. The experiment was therefore repeated to ensure equal initial ion concentrations. A greater biomass was used to ensure a more rapid increase in pH in order to quickly induce the precipitation of $CaCO_3$. Ion concentrations from the second AQ0012 experiment demonstrate decreased total inorganic carbon, HCO_3^-, and CO_3^{-2} concentrations at the end of the experiment compared to the control flasks (Figures 59 and 60). The white amorphous particles found within the culture of both experiments were determined to be calcium carbonate after being tested for a reaction with concentrated HCl. It is not known why larger particulate $CaCO_3$ was formed in experiments using a cyanobacteria.

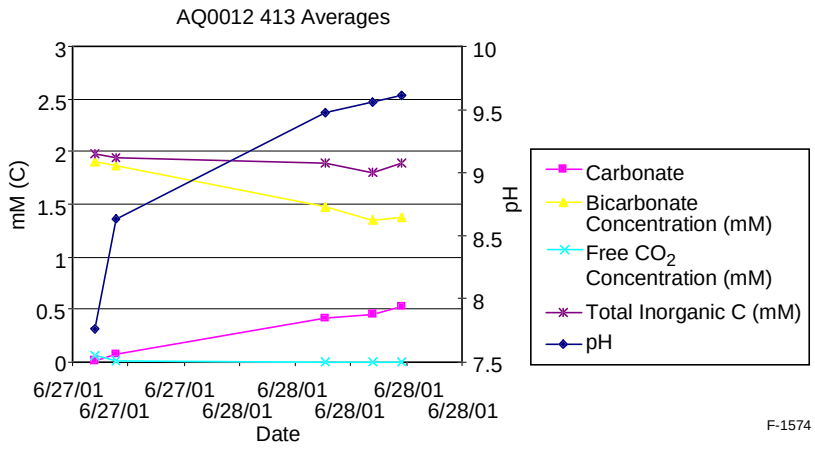

Figure 57. pH and dissolved inorganic carbon species concentrations in AQ0012 in FW 413 + Ca, average of two flasks.

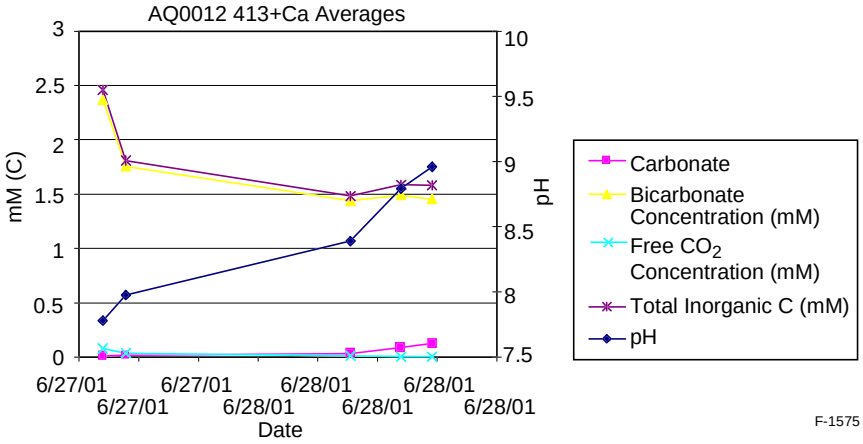

Figure 58. pH and dissolved inorganic carbon species concentrations in AQ0012 in FW 413 + Ca, average of two flasks.

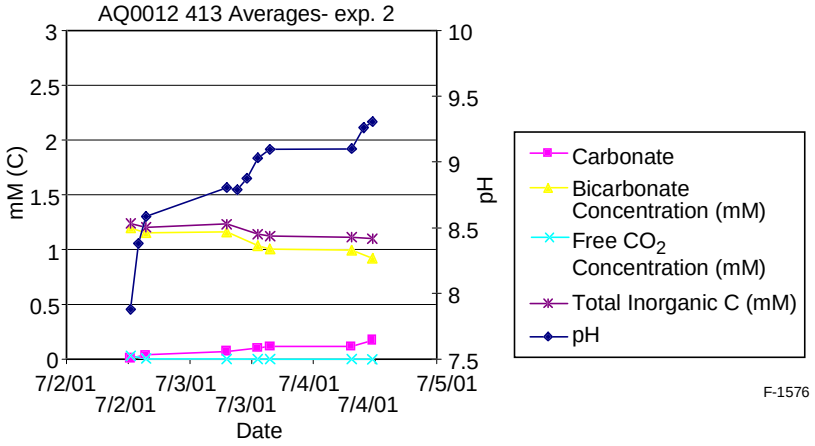

Figure 59. pH and dissolved inorganic carbon species concentrations in AQ0012 2nd exp. FW 413 + Ca, average of two flasks.

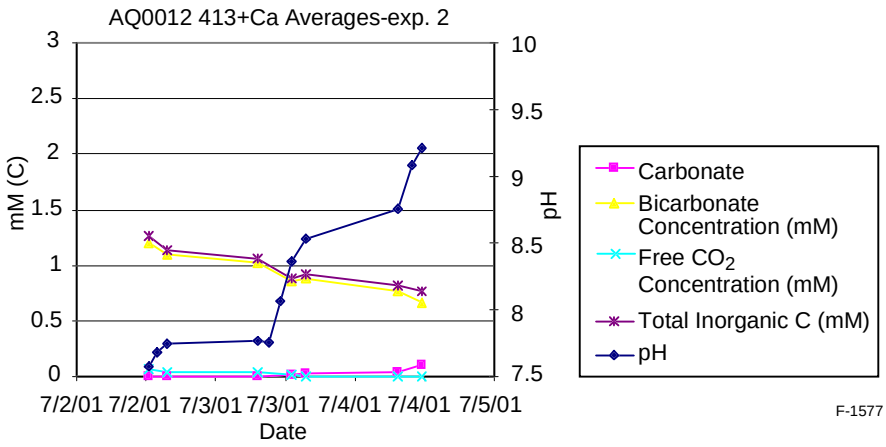

Figure 60. pH and dissolved inorganic carbon species concentrations in AQ0012 2nd exp. FW 413 + Ca, average of two flasks.

Prior examination of calcification in cyanobacteria by Merz-Preiss (2000) shows that under certain conditions, filaments of the organism can become encrusted with $CaCO_3$. However, upon examination of the culture, particulate $CaCO_3$ was not encrusted on the cells of the organism (Figure 61), however were abundant in close proximity with clumps of the algal filaments.

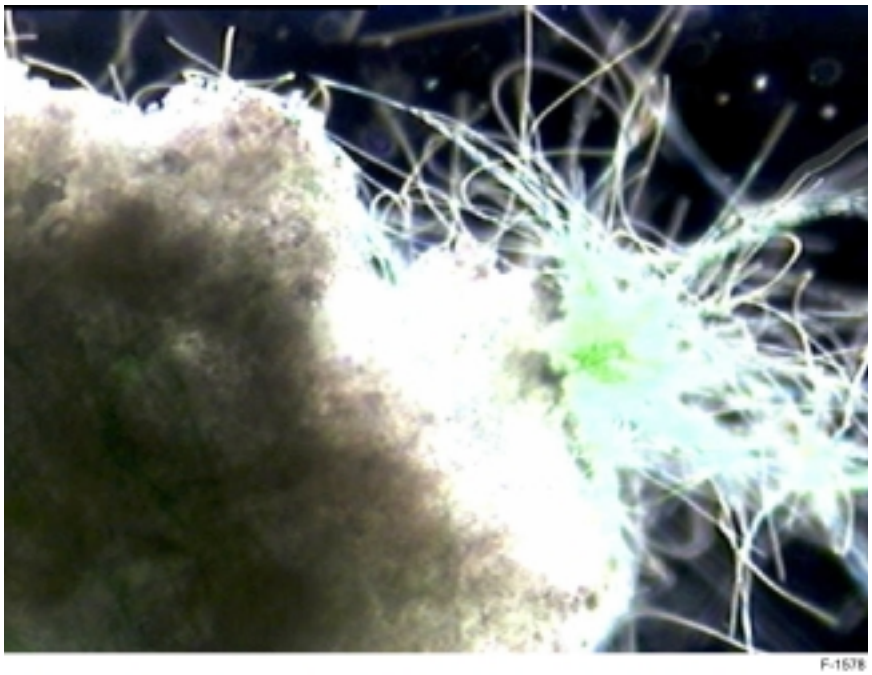

Figure 61. Photomicrograph of a clump of AQ0012 culture. The green filaments are the alga itself. The large white mass is precipitated $CaCO_3$. Although the $CaCO_3$ mass is closely associated with the algal filaments it doesn't seem to crust the filaments.

No significant data could be obtained from the small-scale experiment where CO_2 was dissolved into a solution of deionized, calcium-enriched water. No precipitate was formed after the pH of the solution had been decreased from 6.07 to 4.17.

Experimentation with the chemical precipitation of $CaCO_3$ demonstrated that a medium could precipitate $CaCO_3$ after the addition of Ca to the solution, which had an initial pH above 8.0. Increasing the pH of the medium may have also increased $CaCO_3$ production however the system may have been Ca limited due to characteristics of the Ca species used. This precipitation would occur as a series of reactions are driven by the increase in pH through removal of H^+ ions. Through these reactions, HCO_3^- ions are driven to CO_3^{-2} ions (Figure 62). In the presence of high calcium concentration, $CaCO_3$ can then be produced. Also, it was determined that adding CO_2 to the system drives the reactions to produce more HCO_3^- ions, essentially replenishing the medium and allowing for the eventual production of more $CaCO_3$. These findings are significant because they demonstrate that CO_2 added to the system is captured through the formation of $CaCO_3$. By comparing the results of the experiment where solid precipitate has been removed (Figure 63) with the initial findings (Figure 62), it has been

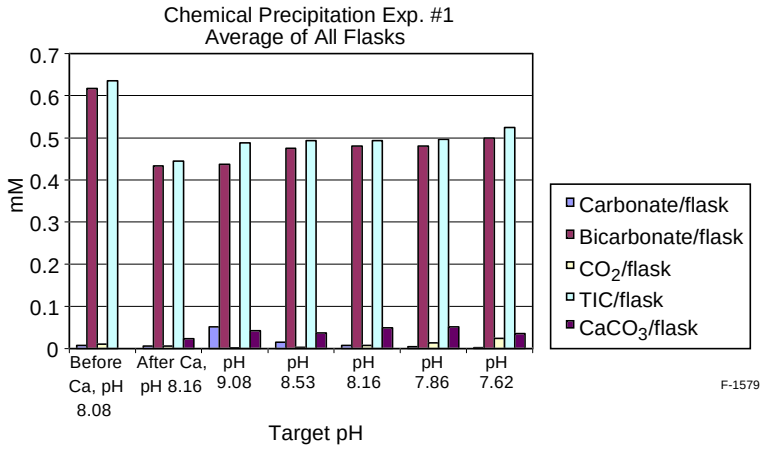

Figure 62. pH and dissolved inorganic carbon species concentrations.

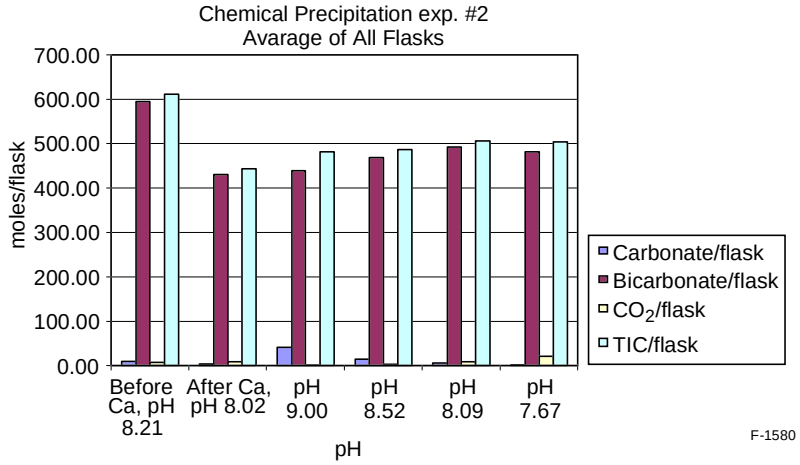

Figure 63. pH and dissolved inorganic carbon species concentrations after solid $CaCO_3$ is removed.

determined that the addition of CO_2 to the pH levels tested does not cause the re-dissolution of $CaCO_3$, indicating that this process can be used to continuously and permanently sequester CO_2 added to the system. In addition, the experiment using fresh water 413 media produced results similar to the first chemical precipitation experiment. However, amounts of each ion in solution were greatly decreased due to the initial concentrations of the ions in the media (Figure 64).

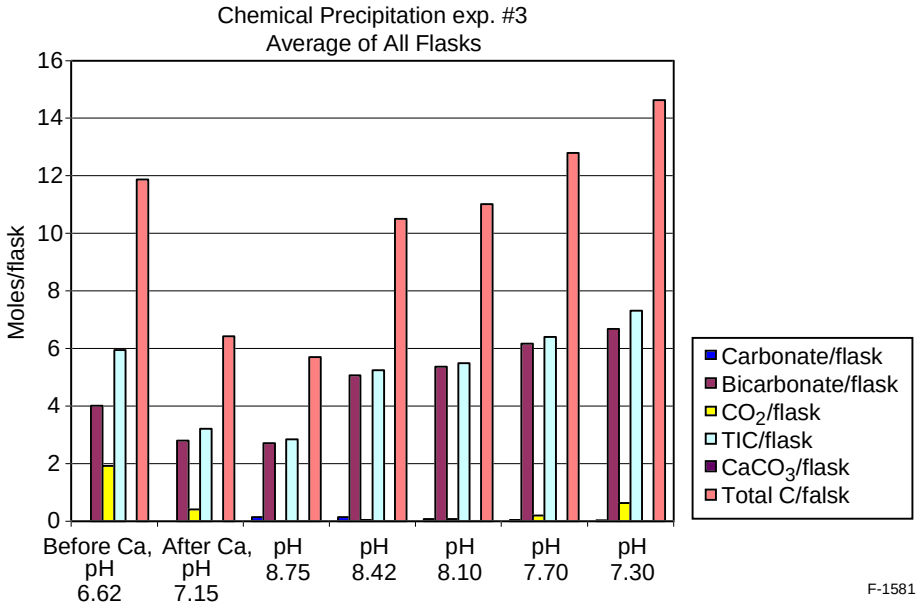

Figure 64. pH and dissolved inorganic carbon species in FW 413 media + Ca.

The experiments conducted using both AQ0012 and AQ0008 to increase the pH of the medium yielded similar trends. The initial ion and total inorganic carbon concentrations of the AQ0008 culture were greater than those found in the AQ0012 culture media. Regardless of the initial difference, however, both cultures displayed a decrease in HCO_3^- and an increase in CO_3^{-2} concentrations as the pH of the media was biologically increased (Figures 65 and 66). Likewise, both culture mediums were replenished with HCO_3^- ions after the addition of CO_2 to each flask. According to Libes (1992) HCO_3^- ions are still dominant when compared to CO_3^{-2} at a pH of approximately 9.0. It is not until an approximate pH of 10.0 is reached when the majority of HCO_3^- ions have been converted to CO_3^{-2}. Further experimentation will examine the chemistry of the medium when the pH is biologically driven to levels exceeding 9.5 to 10.0. This will determine if more CO_3^{-2} ions can be produced, resulting in an eventual increase in the quantities of $CaCO_3$ produced assuming a constant supply of calcium ions.

The chemostat experiment yielded results similar to the flask experiments in that it produced visible particulate $CaCO_3$ in both the chemostat and the receiver at pH values above approximately 8.3. In addition, examination of the ion concentrations in the receiver, which received no pH control via CO_2 addition, reveals that once again HCO_3^- concentrations decreased and CO_3^{-2} increased as the pH increased (Figures 67 and 68). The increase in CO_3^{-2} ion concentration allowed for the production of $CaCO_3$ in the both the chemostat and receiver, but higher concentrations in the receiver explain why more precipitate was formed in this vessel.

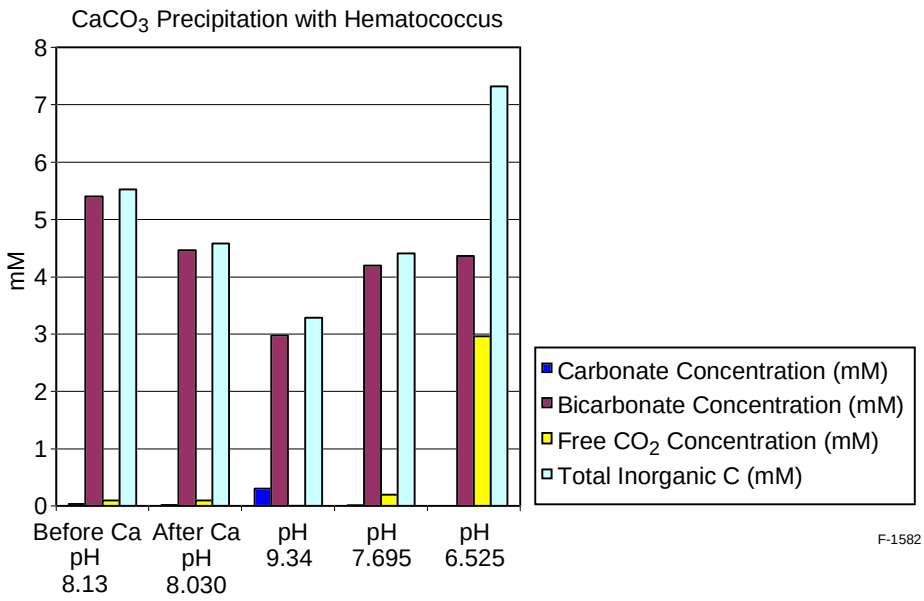

Figure 65. pH and dissolved inorganic carbon species with AQ0008 culture + Ca^{2+}.

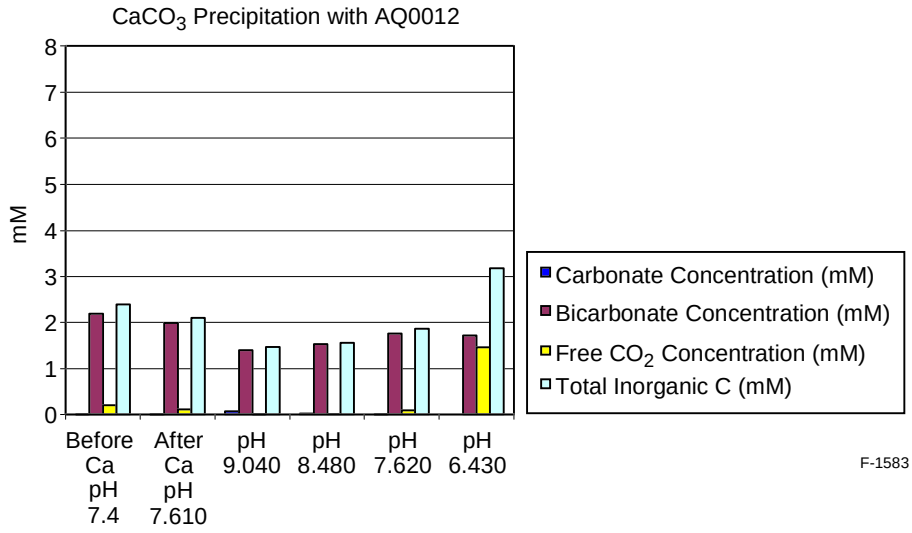

Figure 66. pH and dissolved inorganic carbon species with AQ0012 culture + Ca^{2+}.

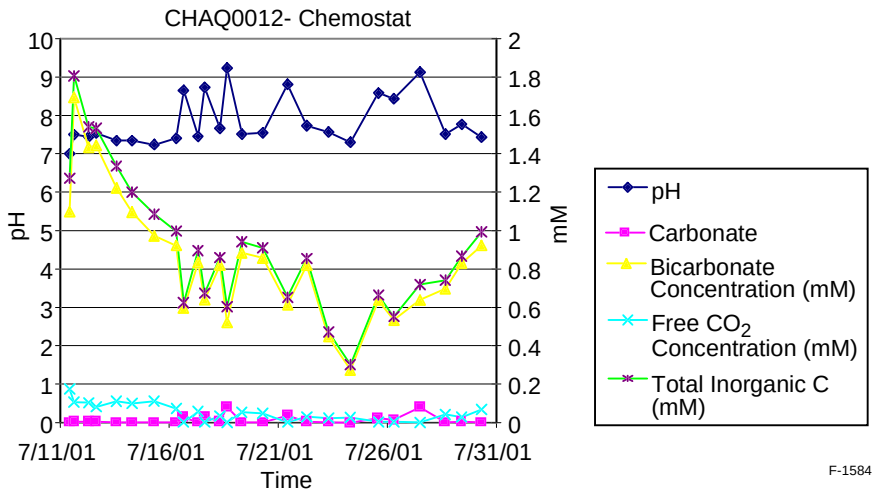

Figure 67. pH and dissolved inorganic carbon species with AQ0012 culture + Ca^{2+} in chemostat.

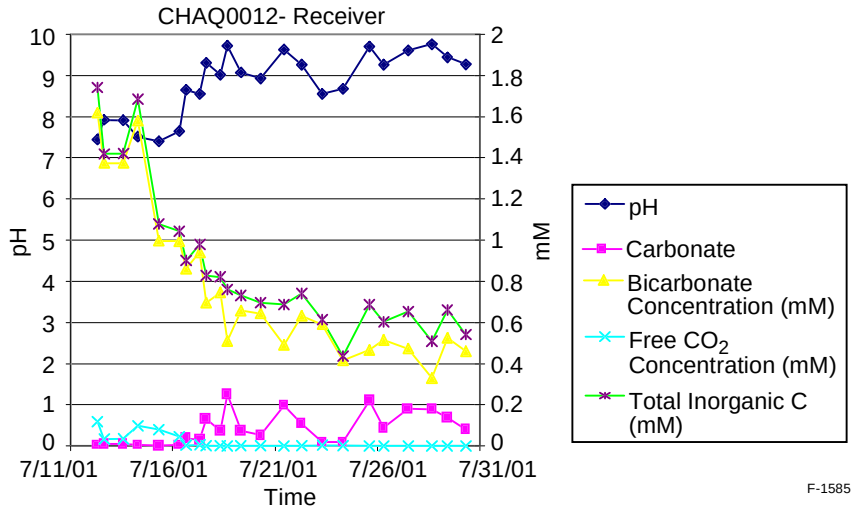

Figure 68. pH and dissolved inorganic carbon species with AQ0012 culture + Ca^{2+} in receiver vessel.

This data demonstrates that it is possible to have a continuous system where CO_2 is bubbled and replenishes the medium with HCO_3^- and a constant supply of Ca^{2+} is available to bind with CO_3^{-2} ions when the pH increases to a point where CO_3^{-2} is dominant.

3.2.2.4 Significance of the Results

From an industrial perspective, this process has the possibility of decreasing carbon emissions that lead to global warming. However, this process must be cost effective in order to promote the energy production industry to utilize its potential. In the past few decades, microalgae have been grown for the production of valuable byproducts of certain physiological characteristics. Some carotenoid pigments produced by algae have been identified as valuable

antioxidants and present many health benefits (see section on high value products). Some are presently utilized in the nutraceutical industry. This byproduct of microalgal growth will help to offset the cost of implementing the algal mediated sequestration of carbon. As the sequestration method requires a calcium supply, a relatively inexpensive source is $CaSO_4*2H_2O$, or gypsum. Deposits of this mineral are abundant throughout the world and it is readily available for use in agriculture as well as other venues. The preceding experiments were all conducted using gypsum as the calcium source, and this mineral has proven successful in its ability to supply calcium to an algal medium. The use of this mineral does have limited potential, however, due to its relatively low solubility. $CaSO_4*2H_2O$ is less soluble than other species of Ca, and therefore limits the number of moles of Ca available for binding with free CO_3^{-2} ions in the experiments. Another Ca source could be used to provide more Ca^{2+} ions to a medium, however some more reactive and soluble species require energy to produce. This in essence defeats the purpose when viewed on a global perspective because CO_2 is released during energy production. Another species of Ca, more soluble than $CaSO_4*2H_2O$ that requires no energy to produce would be a better alternative, however more research must be done to determine the most suitable Ca species.

In conclusion, microalgae and cyanobacteria can be used to induce the precipitation of $CaCO_3$ from a Ca-enriched medium. This process can be used to reduce the amounts of CO_2 degassed from industrial fossil fuel combustion, reducing the large amounts of anthropogenic CO_2 contributed to the global carbon cycle each year. More information is necessary to successfully establish an industrial scale carbon sequestration system, but the research presented demonstrates the feasibility of this method. In conjunction with high value product generation, this process can prove to be affordable to industry and environmentally beneficial.

3.3 Task 4: Carbon Sequestration System Design

To evaluate the potential for application of photosynthetic sequestration of CO_2 to industrial- scale combustion systems, we will conduct a system-level design study. The purposes of this study are as follows:

(1) Identify design concepts for components and the integrated system of the proposed concept

(2) Optimize and evaluate performance of the components and the system

(3) Develop deployment methodologies

(4) Identify key technology issues for further development.

This task consists of two sub-tasks: Task 4.1-Component Design and Development; and Task 4.2-System Integration. Process simulations will be performed for conventional coal-fired and gas turbine power stations and natural gas boilers.

3.3.1 Task 4.1: Component Design and Development

In this subtask we will develop design concepts for each of the key components of the industrial scale photosynthetic sequestration of CO_2. Key components to be designed include: CO_2 removal process; CO_2 injection device; photobioreactor; product algae separation process; and process control devices. As the proposed system depends on the solar energy to photosynthetically convert CO_2 to products compounds, optimization of the photobioreactor is an important part of this task.

In the reporting period, initial work on Task 4.1 has begun. PSI believes that a key to successful CO_2 sequestration is efficient use of solar energy. The area required for photosynthetic process by microalgae is a key cost driving factor. We need to develop a photobioreactor design which makes efficient use of solar light.

Photobioreactor Design Concept

Microalgae utilize solar radiation to convert CO_2 into organic substances and oxygen. This photosynthetic reaction requires solar spectra typically between 400 nm and 700 nm. This is called photosynthetically active radiation (PAR). Solar spectra outside of the PAR wavelength regime are not utilized by microalgae. Figure 69 shows solar spectral data for AM1.5, a typical terrestrial condition in the United States. The portion of the spectra used by microalgae is indicated in the figure. The solar spectral energy between 400 nm and 700 nm is 424 W/m^2, which is 44% of the total solar spectral energy of 962 W/m^2. It is important to note that only a fraction of the solar energy, less than half of the solar energy, is within the spectral range for photosynthetic processing by microalgae.

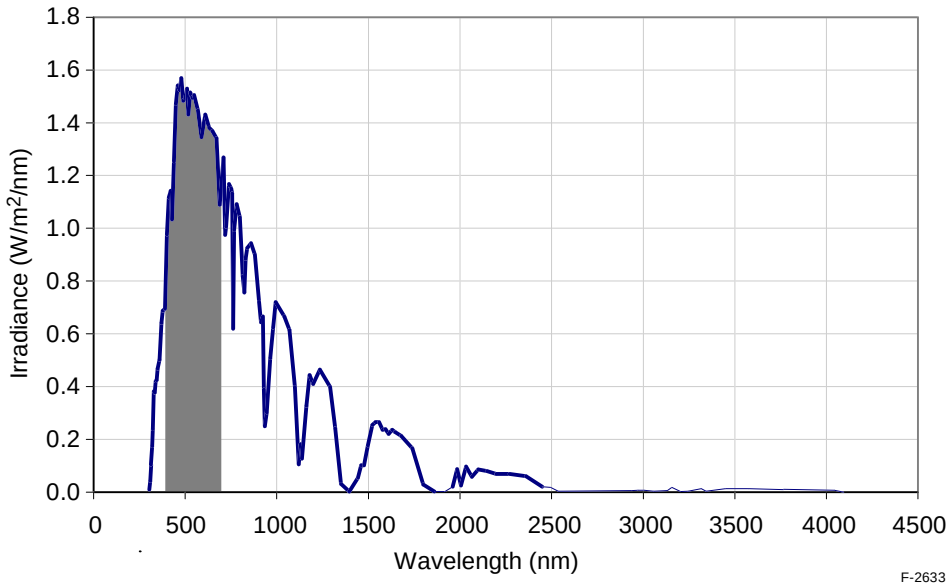

Figure 69. Solar spectral irradiance.

Our strategy for developing an efficient photobioreactor is as follows: (a) design the photobioreactor which maximizes availability of the PAR spectra for microalgae; and (b) develop innovative ways to utilize the solar radiation outside of PAR spectra for generating products that potentially offset the sequestration cost.

Item (a) is the standard method, and researchers have tackled this problem. We are aware that (b) has been discussed in literature (NEDO, 2000) but has not been practiced in the past. PSI has been working on this very issue in the last several months for a program supported by NASA/KSC (Nakamura, 2001). In this program we have demonstrated separation of PAR from the solar spectra and directed it to a location 10 m away from the solar collector, while the longer wavelength spectra outside of the PAR was converted to electrical power by low-bandgap Photovoltaic cells. Figure 70 shows a schematic of the concept. In this concept, the solar radiation from the concentrator is directed to a selective spectral reflector which reflects only the PAR spectra while the longer wavelength components are transmitted to the PV cells.

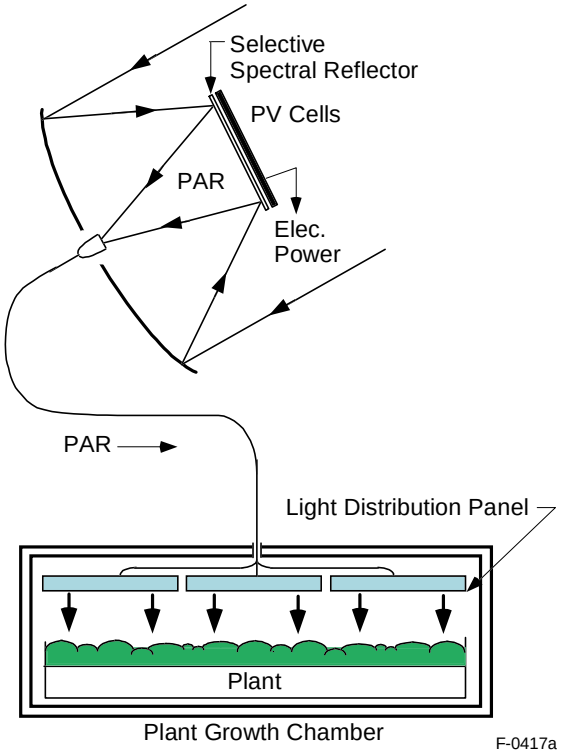

Figure 70. Concept for utilizing solar spectra not used for photosynthetic process.

In the last several months, PSI has been conducting a series of experiments for electrical power generation utilizing the GaSb cell, one of the low-bandgap PV cells. The project has been conducted with PSI's IRAD fund and with NASA/KSC's SBIR fund. The objective of the test project is to demonstrate, for the first time, the potential of using solar IR spectra that would not be utilized in space-based solar plant lighting. The test results showed that it is possible to convert the solar IR spectra into electric power at efficiencies theoretically predicted, e.g., 15.5%

for the GaSb cell, while the PAR spectra are transmitted to the plant growth facility. Figure 71 shows a photograph of the experimental facility. As shown in the photo, a 20-in. parabolic mirror reflects the solar radiation to the PV cell module near the focal point of the mirror. The cold mirror (Coherent 35-6907) installed at the PV cell module reflects the PAR to the aperture of a 10-m lightguide which transmits the light to the inside of the building. Emission of the PAR from the other end of the lightguide in the building is visible.

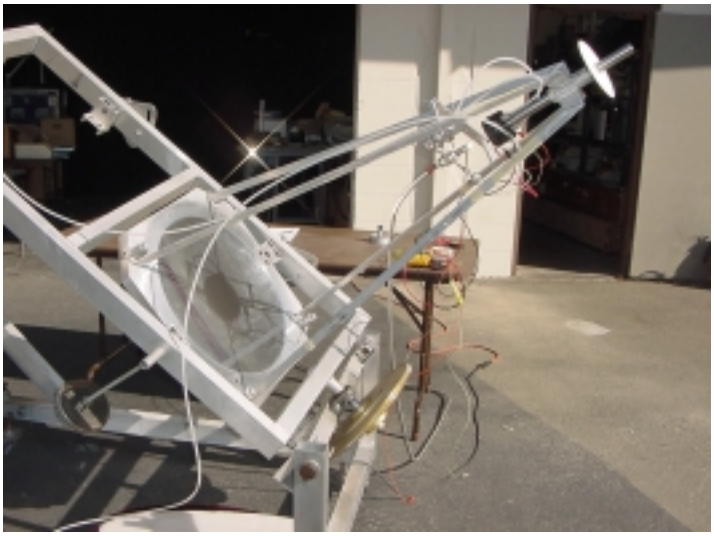

Figure 71. Experimental facility for GaSb cell performance tests with the IR solar spectra.

The experimental results reviewed above demonstrated that full utilizations of solar spectra is possible for two distinct purposes: CO_2 sequestration; and elctric power generation. We consider this result is potentially very important in reducing the cost of CO_2 sequestration. Note that the electric power is generated at no penalty to photosynthesis of microalgae. During the reporting period we have begun our study to assess feasibility of implementing the concept of simultaneous production of sequestered carbon and electric power. We plant to work on design concept development during the second year.

3.3.2 Task 4.2: System Integration

The technical results reported in this Section relate to Task 4.2: System Integration in the Statement of Work.

Using results from Tasks 1 through 4.1, a process model is being developed. This model simulates an integrated CO_2 biological uptake and sequestration system. Parametric studies will be conducted with this model to gain quantitative insight into process performance, identify potential problems and limitations of the system, address scale-up issues, and optimize the system. The process model and applicable property and performance databases are being integrated under the ASPEN PLUS (2000) process simulation software.

Process simulations are being performed for fuel oil, coal, and natural gas-fired boiler and gas-turbine power stations. These scenarios represent a broad range of gas compositions from the standpoints of CO_2 and trace combustion species. Flue gas production rates (which scale with electricity generating capacity) are being varied over an order of magnitude. The concentrations of particulates and gas phase contaminants also are being varied within the limits established under Task 1. Accomplishment in integrating CO_2 supply, separation, and biological uptake during Year 1 of this project is discussed below.

3.3.2.1 Carbon Dioxide Supply, Separation, and Biological Uptake System

A preliminary process model for CO_2 supply, separation, and biological uptake using microalgae has been laid-out to identify critical experimental and other data that need to be collected, and to evaluate alternative photobioreactor designs and carbon sequestration options. Figure 72 presents a skeleton ASPEN flowsheet for the preliminary model presently being simulation tested.

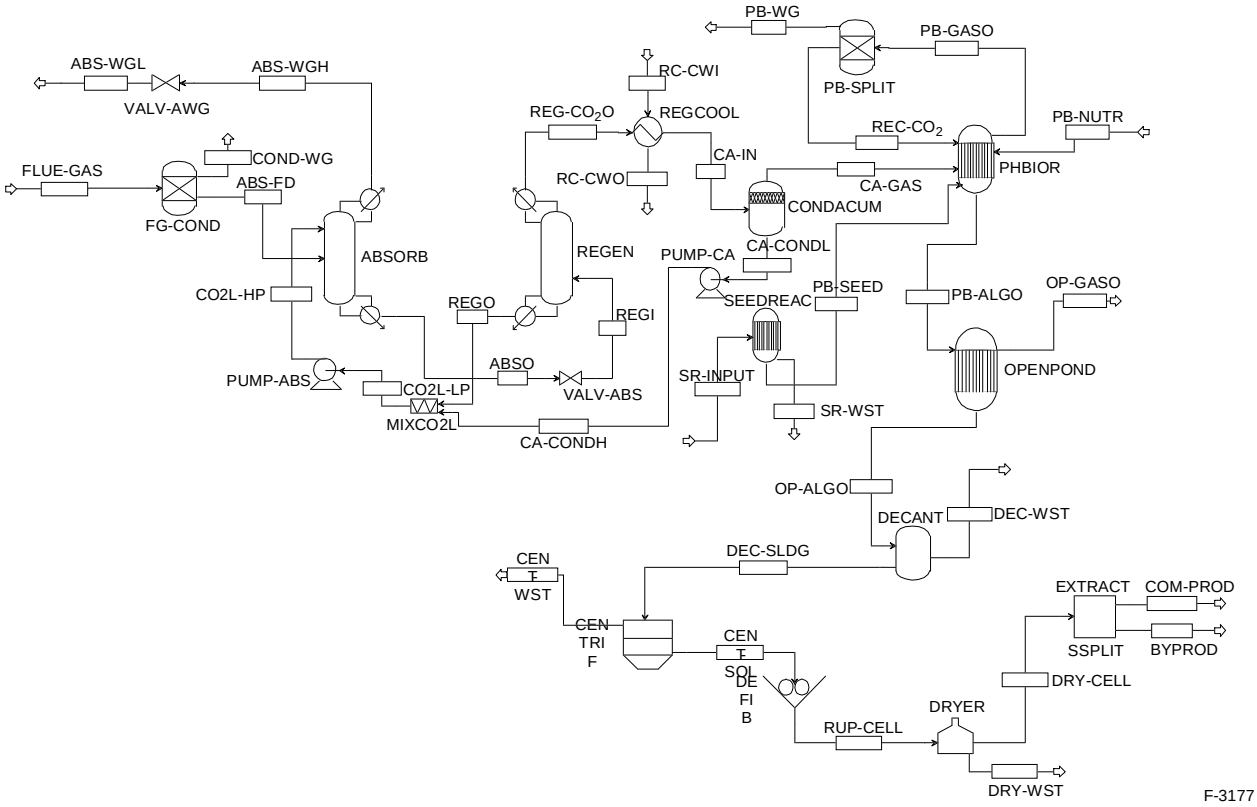

Figure 72. ASPEN flowsheet of CO_2 supply, separation, and biological uptake system.

Flue gas from a power station (FLUE-GAS), with flow rate and composition to be specified by PSI, is preconditioned (in FG-COND) before entering a CO_2 separation and conditioning subsystem (also to be specified by PSI). The CO_2 separation subsystem shown in Figure 72, one of several options under consideration, is an alkaline salt solution CO_2 separation process (in this particular case, hot potassium carbonate), consisting of an absorption column (ABSORB), a regeneration column (REGEN), and associated equipment.

Cooled CO_2-rich gas (CA-GAS) exits the CO_2 separation system into the algae production subsystem for photosynthetic uptake and sequestration. Depending on the commercial product(s) being generated by the industrial entity, the algae production subsystem might utilize closed, open, or both types of photobioreactors. In the preliminary model shown in Figure 72, the algae production subsystem is modeled as a staged process, with closed and open photobioreactors. The primary closed photobioreactor module (PHBIOR) is seeded by small-scale bioreactors (SEEDREAC) (consisting of a sequence of petri cultures, flasks, chemostats, and carboys, which is being modeled as a single block) and is fed appropriate nutrients (PB-NUTR). Because the single-pass CO_2 utilization efficiency of the bioreactors is relatively low, the gas released from the photobioreactors (PB-GASO) might need to be recycled as shown in Figure 72.

Presently, Aquasearch's primary commercial product calls for the algae to be transferred from closed photobioreactors (PB-ALGO) to open raceways (OPENPOND) for additional growth and stressing. The product from the open ponds is partially dewatered in place before undergoing additional dewatering in a mechanical decanter (DECANT). The sludge from the decanter is concentrated further by centrifugation (in CENTRIF) before the cells are ruptured (in DEFIB) and dried (in DRYER). Carotenoid is extracted from the dried, ruptured algae (in EXTRACT). A commercial product (COM-PROD) is produced along with byproducts (BYPROD). Details on the bioreactor and downstream processing subsystems are being provided by Aquasearch.

Table 10 summarizes the main blocks and streams in Figure 72. The first column (Stream/Block) provides a key to the blocks and streams in the ASPEN flowsheet. The process blocks are preliminary selections and are evolving as simulations are processed. The second column (Description) provides a brief description of the particular stream or block. The third column (ASPEN Attributes) summarizes the proposed ASPEN library models (in quotations), data being specified or outputs from ASPEN.

Many of the mechanical power blocks and some of the waste streams in the process model are not shown in Figure 72 or in Table 10; they are being inserted as the model evolves and related data are collected.

The preliminary model described in Figure 72 and Table 10 has been shared with PSI and Aquasearch for review and comment.

3.3.2.2 Biomass Production

The amount of biomass needed (and, in turn, the size of the photoproduction system required) depends on the output of the electric power generation plant, the type of fuel used for generating electricity, and the yield of biomass. Emission factors (i.e., kg of CO_2 released per kWh of electricity generated) reported in the literature (Walsh, 1996) for fuel oil, coal, and natural gas are being used to estimate the amounts of biomass and land required for sequestering CO_2. For fuel-oil-based electricity, it is estimated that roughly 5,000 tonnes of microalgae dry matter would need to be grown annually to capture the CO_2 released from every 1 MW of power generated.

Table 10. Summary of Streams and Blocks in ASPEN Flowsheet

Stream/Block	Description	ASPEN Attributes
FLUE-GAS	Flue gas from power plant into FG-COND	Specify flow rate, composition, properties
FG-COND	Flue gas conditioner	"Sep"; specify split fractions
COND-WG	Waste gas from FG-COND	Aspen output
ABSORB	Absorption column	"RadFrac"; specify configuration, operating conditions
ABS-FD	Feed gas to absorber (from FG-COND)	Aspen output
ABSO	CO_2 rich solution from ABSORB	Aspen output
CO_2L-HP	CO_2 lean solution to ABSORB	Aspen output
ABS-WGH	Pressurized waste gas from ABSORB	Aspen output
VALV-AWG	Pressure let down valve for waste gas from ABSORB	"Valve"; specify outlet pressure
ABS-WGL	Depressurized waste gas from ABSORB	Aspen output
VALV-ABS	Pressure let down valve for solution from ABSORB	"Valve"; specify outlet pressure
REGEN	Regeneration column	"RadFrac"; specify configuration (including reboiler), operating conditions
REGI	CO_2 rich solution to REGEN	Aspen output
REG-CO2O	CO_2 gas from REGEN (into REGCOOL)	Aspen output
REGO	CO_2 lean solution from REGEN	Aspen output
PUMP-ABS	Pump for CO_2 lean solution to ABSORB	"Pump"; specify pressure
CO2L-LP	CO_2 lean solution into PUMP-ABS	Aspen output
REGCOOL	Cooler for CO_2 from REGEN	"HeatX"; specify outlet temperature
RC-CWI	Cooling water into REGCOOL	Specify conditions
RC-CWO	Cooling water from REGCOOL	Specify temperature
CONDACUM	Regenerator condensate accumulator	"Flash2"; specify operating conditions
CA-IN	Cooled gas into CONDACUM (from REGCOOL)	Aspen output
CA-GAS	Gas from CONDACUM (entering PHBIOR)	Aspen output
CA-CONDL	Condensate from CONDACUM	Aspen output
PUMP-CA	Pump for condensate from CONDACUM	"Pump"; Specify outlet pressure, efficiency
MIXCO2L	Mixer for CO_2 lean streams	"Mixer"; specify pressure drop

Table 11. (Continued) Summary of Streams and Blocks in ASPEN Flowsheet

Stream/Block	Description	ASPEN Attributes
SEEDREAC	Bioreactors for seed production (staged)	"Rstoic"; specify reactions
SR-INPUT	Input to SEEDREAC	Specify composition, properties
SR-WST	Waste stream from SEEDREAC	Aspen output
PHBIOR	Photobioreactor (staged)	"RStoic"; specify reactions
PB-SEED	Seed to PHBIOR (outuput from SEEDREAC)	Specify composition
PB-NUTR	Nutrients into PHBIOR	Specify composition, amount
PB-GASO	Gas exiting PHBIOR	Specify composition, amount
PB-ALGO	Algae exiting PHBIOR (entering OPENPOND)	Specify composition, amount
PB-SPLIT	Gas separator for recycle stream from PHBIOR	"Sep"; specify split fractions
PB-WG	Waste gas from PB-SPLIT (exiting photobioreactor system)	Aspen output
REC-CO2	Recycled CO_2 to PHBIOR	Aspen output
OPENPOND	Open pond reactor	"RStoic"; specify reactions
OP-GASO	Gas exiting OPENPOND	Aspen output
OP-ALGO	Algae exiting OPENPOND	Specify composition, amount
DECANT	Decanter	"Decanter"; specify operating conditions
DEC-WST	Waste from DECANT	Aspen output
DEC-SLDG	Algae sludge from DECANT (entering CENTRIG)	Specify composition
CENTRIF	Centrifuge	"CFuge"; specify operating conditions
CENT-WST	Waste from CENTRIF	Aspen output
CENT-SOL	Algae solids from CENTRIF	Aspen output
DEFIB	Defiberator for rupturing algae cells	"Crusher"; specify operating conditions
RUP-CELL	Ruptured algae	Aspen output
DRYER	Dryer for ruptured algae	"Heater"; specify operating conditions
DRY-CELL	Dried algae exiting DRYER	Specify composition
DRY-WST	Waste from DRYER	Aspen output
EXTRACT	Extraction process to separate commercial product	"SSplit"; specify split fractions
COM-PROD	Commercial product	Specify composition
BYPROD	Byproduct (or waste product)	Aspen output

Microalgae presently is being cultivated commercially to generate high valued products, not maximum amounts of biomass; thus, the yield that might be commercially attainable if maximum photosynthesis were an objective is not known. Recent studies (Kinoshita *et al.*, 2002) project that fast growing herbaceous crops such as banagrass (*Pennisetum purpureum* Schumach) can generate commercial yields of 48 tonnes of dry matter per hectare per year in Hawaii. Assuming that microalgae grown in Hawaii would yield comparably (~50 tonnes per hectare per year), a 100 hectare microalgae farm would be needed to sequester the CO_2 released from a 1 MW fuel-oil power generation facility.

4. SUMMARY AND FUTURE PLANS

4.1 Task 1: Supply of CO_2 from Power Plant Flue Gas to Photobioreactor

During the first year of this program we have characterized power plant exhaust. Summary of our study is given below.

- Two-thirds of the capacity in the utility power generation sector in the United States is based on fossil fuel combustion.
- Coal and natural gas are the primary fuels for power generation; fuel oil is important in specific regions.
- All fossil fuels amount to 71% of the electricity generating capacity.
- Fossil fuels represent an even larger segment of the non-utility power generation market (approximately 90%, if the use of biomass is included).
- Sequestration of CO_2 using the photobioreactor needs to be located in an area with higher solar flux and warmer temperatures. The capacity represents about half of the total US capacity.
- Non-utility electricity generators using fossil fuels may be attractive for application of a photobioreactor because the average size of such plants is smaller than that of utility plants (28 MW versus 71 MW).
- The CO_2 content of flue gas from boilers (as opposed to gas turbine combustors) has low amounts of excess oxygen (typically 6 vol%) and CO_2 concentrations on the order of 12-15 vol%. Gas turbine combustors have much lower CO_2 and higher excess oxygen.
- Future efforts to aid CO_2 capture from combustion sources may include modifications to the combustion system that result in much higher concentrations of CO_2 in the exhaust.
- The most likely options currently available for CO_2 separation from combustion flue gas include: gas adsorption (both physical and chemical), cryogenic separation, and membrane separation.
- Physical adsorption processes are more suitable for mixed gas streams that are under high pressure because the solubility of CO_2 increases with increasing gas pressure.
- Chemical solvents (for example, monoethanolamine (MEA), dimethanolamine (DEA), ammonia, or hot potassium carbonate) form an intermediate compound that can be broken down by heating to give the original solvent and CO_2. These processes

can be used at low partial pressure of CO_2, but the flue gas must be free of SO_2, hydrocarbons, and particulate matter.

- Pressure-swing adsorption (PSA) or temperature-swing adsorption (TSA) are used in chemical process streams and have also been proposed for removal of CO_2 from flue gas.

- Gas adsorption or gas separation membranes have the potential to remove CO_2 from flue gas. Gas separation membranes employ a membrane that is selective for transport of CO_2 and high pressure on the flue gas side to concentrate CO_2 on the low pressure side of the membrane.

- Application of these carbon dioxide separation processes to flue gas depends on the concentration of CO_2 in the stream, on the presence of impurities in the gas, and on the pressure of the flue gas stream.

- Chemical adsorption using MEA is the most mature technology and looks to be the most economically viable in the near future. A unit sized for a 25 MWe plant burning a bituminous coal would process 235,000 lb/hr of flue gas and produce 42,000 lb/hr of CO_2. The total major equipment cost is approximately $5M (1999 dollars). The total capital cost is on the order of $11M.

- The cost of these technologies is too high for the reduction of greenhouse gases. The hope is that in the near future, less costly options including membranes, novel gas-liquid contactors, solid sorbents, and the formation of CO_2/water hydrates, will be available for fossil fuel-fired combustion sources.

- We began a theoretical investigation to explore the limits of the mass transfer and the dependence of mass transfer on operating parameters, in preparation for a more detailed experimental and theoretical investigation.

- A more detailed theoretical investigation in the Second Year will address specific questions as:

    - Given the circulation rate of the liquid in the AGM and the flow rate of the flue gas being injected, what is the increase in dissolved CO_2 as a result of injection?

    - If complete dissolution of the flue gas bubbles would not be expected; how much oxygen is stripped from the liquid by the flue gas?

    - Some of the trace acid gases (SO_2, HCl, NO_2) are soluble in water; what are the dissolution rates of these species and how does this affect the pH of the liquid?

    - How much CO_2 and O_2 are removed from the liquid by injection of the transport air?

4.2 Task 2: Selection of Microalgae

Up to this point in time we have

- Tested 50 different strains of microalgae for growth at five different temperatures (15, 20, 25, 30 and 35 °C) and 4 strains at three temperatures (15, 20, and 25 °C),
- Tested 10 different strains for pH shift tolerance in chemostat cultures,
- Analyzed 34 different strains for high value pigments,
- Tested 17 strains at the chemostat level for growth and carbon uptake rate,
- Tested 3 different strains for carbon sequestration potential into carbonates for long-term storage of carbon and we have,
- Designed and built a gas distribution and control system to test the tolerance of microalgae to mixtures of gases representing different flue gases, and
- Started testing the tolerance of microalgae to simulated flue gases.

Our preliminary results indicate that

- Out of 54 strains tested two did not grow at 15°C, one did not grow at 15 and 20°C, nine did not grow at 35°C, and one did not grow at 30 and 35°C,
- Out of 10 strains tested so far for pH tolerance only 2 strains, both Cyanobacteria, appear to lower their ability to photosynthesize as the pH increases,
- Out of 10 strains tested at chemostat scale 4 maintained a higher biomass level at 6.5 pH than 7.5 pH but nine strains maintained lower biomass at 8.5 pH than 7.5 pH,
- Out of 34 strains analyzed for high value pigment content we have identified possible good sources of zeaxanthin, lutein, fucoxanthin, phycocyanin, and phycoerythrin,
- Estimates of carbon uptake based on pH changes of the culture medium for our chemostat system match very closely the estimates of carbon uptake by cultures grown in commercial outdoor photobioreactors,
- Changes in culture pH caused by microalgal photosynthesis appear to be conducive to the precipitation of $CaCO_3$ from the growth medium, and
- Based on preliminary analysis of our first chemostat-grown cultures, the estimated efficiency of CO_2 captured by the chemostat culture systems is several fold higher than our benchmark, a commercial microalgal facility, indicating a large potential for optimization of gas capture by industrial size outdoor photobioreactors.

Within the next quarter we expect to

- Continue to carry out carbon sequestration experiments in chemostat cultures,
- Carry out simulated flue gas experiments in chemostats, and
- Start scale up of promising strains to the 3000 L outdoor photobioreactor scale.

4.3 Task 4: Carbon Sequestration System Design

In the reporting period, initial work on Task 4 has begun. Summary of the results in this task is as follows:

- We have begun initial work on designing key components including: CO_2 removal process; CO_2 injection device; photobioreactor; product algae separation process; and process control devices.

- A key to successful CO_2 sequestration is efficient use of solar energy. The area required for photosynthetic process by microalgae is a key cost driving factor.

- Photosynthetic reaction requires solar spectra typically between 400 nm and 700 nm as called photosynthetically active radiation (PAR). Solar spectra outside of the PAR wavelength regime are not utilized by microalgae.

- The energy within PAR is $424W/m^2$, which is only 44% of the total solar spectral energy of $962W/m^2$.

- Our strategy for developing an efficient photobioreactor is: (a) design the photobioreactor which maximizes availability of the PAR spectra for microalgae; and (b) develop innovative ways to utilize the solar radiation outside of PAR spectra for generating products that potentially offset the sequestration cost.

- PSI has demonstrated separation of PAR from the entire solar spectra and directed it to a location 10 m away from the solar collector, while the longer wavelength spectra outside of the PAR was converted to electrical power by low-bandgap Photovoltaic cells at an efficiency about 15.5%,

- The test results showed that full utilizations of solar spectra is possible for two distinct purposes: CO_2 sequestration; and electric power generation.

- We plant to work on design concept for photobioreactor incorporating concept for full utilization of solar energy.

- A preliminary process model for CO_2 supply, separation, and biological uptake using microalgae has been laid-out. A skeleton ASPEN flowsheet for the preliminary model is presently being simulation tested.

- The ASPEN model incorporates:
  - the CO_2 separation subsystems including an alkaline salt solution CO_2 separation process
  - the algae production subsystem utilizing closed, open, or both types of photobioreactors
  - the product processing subsystems.

- The model has the ability to perform parametric studies to identify critical experimental and other data that need to be collected, and to evaluate alternative photobioreactor designs and carbon sequestration options.

- The ASPEN model has been shared with PSI and Aquasearch for their review and comment.

5. REFERENCES

ASPEN PLUS, Part Number: Aspen Engineering Suite 10.2, Aspen Technology, Inc., Cambridge, Massachusetts, February 2000.

Clesceri, L.S., Eaton, A.D., Greenberg, A.E., Standard Methods for the Examination of Water and Wastewater, United Book Press, Baltimore, Maryland, 1995.

Jeffrey, S.W., Mantoura, R.R.C., Wright, S.W., Phytoplankton Pigments in Oceanography, UNESCO Publishing, France, 1997.

Kim, J.M., Araki, S., Kim, D.J., Park, C.B., Takasuka, N., Baba-Toriyama, H., Ota, T., Nir, Z., Khachik, F., Shimidzu, N., Tanaka, Y., Osawa, T., Uraji, T., Murakoshi, M., Nishino, H., Tsuda, H., "Chemopreventive effects of carotenoids and curcumin on mouse colon carcinogenesis after 1,2-dimethylhydrazine initiation," *Carcinogenesis* **19**(1), 81-5, 1998.

Kinoshita, C.M., Turn, S.Q., Jakeway, L.A., Osgood, R.V., and Dudley, N.S., "Banagrass-For-Energy Scale-up Trial," to be submitted, 2002.

Lee, R.E., Phycology, Cambridge University Press, New York, 1989.

Libes, S.M., An Introduction to Marine Biogeochemistry, Wiley & Sons Inc., New York, p. 242-261, 1992.

McCabe, W.L. and Smith, J.C., Unit Operations of Chemical Engineering, McGraw-Hill, New York, pp. 697-700, 1976.

Merz-Preiss, M., "*Calcification in cyanobacteria*," in Microbial Sediments, Awramik, S.M., Riding, R.E., Eds., Springer-Verlag: Berlin, Germany, p: 50-56, 2000.

Nakamura, T., "Optical Components for Space Based Plant Lighting", NASA SBIR Contract NAS10-01056, NASA/KSC, November 2001.

NEDO Report, "Sequestration and Utilization of CO_2 by Bacteria and Microalgae", March 2000.

Nyholm, N., Peterson, H.G., "*Laboratory bioassays with microalgae,"* in Plants for Environmental Studies,Wang, W., Gersuch, J.W., and Hughes, J.S., editors, CRC Press, Florida, 1997.

Olaizola, M., "Commercial production of astaxanthin from Haematococcus pluvialis using 25,000-liter outdoor photobioreactors," *J Appl. Phycol*. **12**, 499-506, 2000.

Perry, R.H. and Chilton, C.H., Chemical Engineer's Handbook, McGraw-Hill, New York, 1973.

Robbins, L.L., Yates, K.K., "*Microbial lime-mud production and its relation to climatic change,"* in Geological Perspectives of Global Climate Change, Gerhard, L.C., Harrison, W.E., Hanson, B.M., Eds., p. 267-283, 2001.

Schreiber, U., Schliwa, U., Bilger, W., "Continuous recording of photochemical and non-photochemical chlorophyll fluorescence quenching with a new type of modulation fluorometer," *Photosynth. Res*. **10**, 51-62, 1986.

Walsh, J.H., "A Simple Spreadsheet for the Assessment of Options for the Mitigation of World Carbon Dioxide Emissions," *Energy Conversion and Management* , Vol. 37, No. 6-8, pp. 709-716, 1996.

Yamamoto, H.Y., Kamite, L., "The effects of dithiothreitol on violaxanthin de-epoxidation and absorbance changes in the 500-nm region," *Biochim Biophys. Acta* **267**, 538-543, 1972.

Zapata, M., Rodriguez, F., Garrido, J.L., "Separation of chlorophylls and carotenoids from marine phytoplankton: a new HPLC method using a reversed phase C_8 column and pyridine-containing mobile phase," *Mar Eco Prog Ser*. **195**, 29-45, 2000.